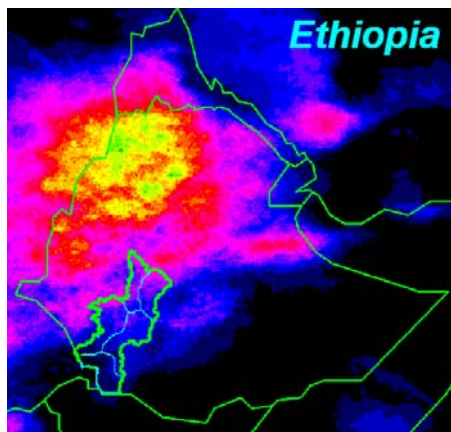


Addis Ababa  
University  
(Since 1950)



Satellite-Based Rainfall Estimation: Evaluation and Characterization  
(A Case Study Over Omo-Gibe River Basin)



**A THESIS  
SUBMITTED TO THE SCHOOL OF GRADUATE STUDIES OF  
ADDIS ABABA UNIVERSITY**

In partial Fulfillment of the requirements for the Degree of  
Master of Science in GIS and Remote Sensing

**BY  
DEREJE MEKONNEN ASFAW  
JULY 2007**



Satellite-Based Rainfall Estimation: Evaluation and Characterization  
(A Case Study Over Omo-Gibe River Basin)

BY  
Dereje Mekonnen Asfaw

A THESIS  
SUBMITTED TO THE SCHOOL OF GRADUATE STUDIES OF  
ADDIS ABABA UNIVERSITY

M.Sc. In GIS and Remote Sensing Program  
Department of Earth Science

APPROVED BY EXAMINING BOARD:

SIGNATURE

Balemwal Atnafu (PhD)

Chairman, Department Graduate Committee

K.S.R.Murty (PhD)

Advisor

Dagnachew Legesse (PhD)

Examiner I

KV.Suryabhagavan(Phd)

Examiner II

\_\_\_\_\_  
\_\_\_\_\_  
\_\_\_\_\_  
\_\_\_\_\_

## Acknowledgement

It is a great pleasure for me to express my heart felt indebtedness to all individuals and organizations that helped me in the completion of this paper

I am very particularly grateful to my essay Supervisor Dr. K.S. R Murthy for his invaluable support in all aspects of my work through out this paper.

I would like to express my gratitude to my employer the National meteorological Agency (NMA) for permitting me to continue this study .Thanks also go to Addis Ababa University for making it possible for me to take up this study.

I also want to thank to all those NMA staffs that have contributed through providing me technical advice and study materials.To mention a few: Ato Muluegeta Malede, Ato Kassa Fekadu, Ato Dejena Mola (Head of Bahir Dar Meteorological Branch Office), W/t Yitaktu Tesfatsion, for giving me the important hints and technical support at the very start of this study.Thanks also to Ato Mamuye Belihu and Ato Messfine Kassa who were strongly supported me in preparing this thesis and giving encouraging moral support during my study period.

Especial thanks also goes to the staffs of the computer and GIS service of the ministry of water resource , for all the moral and material support you have provided me to make this study a success.

Thanks also to my course mates for the friendliness and the group work.

I extend my thanks to my mother, brothers and sisters for all the loving and encouraging support. In particular I would like to thank my old brother Ato Befekadu Thilahun for his unlimited support and encouragement during my stay in this study

Finally, I am very grateful to extend my thanks to my wife Yebechaye(Yebu), and my sons: Luel(Kon-chhu) and Dagmawi(Tomi), whom are source of my strength throughout the study year and for their immeasurable love and concern shown for me.

# Table of Contents

|  |          |
|--|----------|
| Acknowledgement  |          |
| Table of Content.....                                    | IV       |
| List of Figure.....                                      | VII      |
| List of Table.....                                       | VIII     |
| Acronyms.....  | X        |
| Abstract.....  | XI       |
| <br>   |          |
| <b>CHAPTER ONE.....</b>                                  | <b>1</b> |
| <b>Introduction.....</b>                                 | <b>1</b> |
| 1.1 Background.....                                      | 1        |
| 1.2 Problem of the Statements.....                       | 4        |
| 1.3 Objectives of the Research.....                      | 5        |
| 1.3.1 General Objectives.....                            | 5        |
| 1.3.2 Specific Objectives.....                           | 5        |
| 1.4 Limitation and Scope of the Study.....               | 6        |
| 1.5 Benefits and Beneficiaries from Expected Output..... | 6        |
| 1.6 Structure of the Dissertation.....                   | 8        |
| <br>   |          |
| <b>CHAPTER TWO.....</b>                                  | <b>9</b> |
| <b>Review of Literature.....</b>                         | <b>9</b> |
| 2.1 Theoretical Background.....                          | 9        |
| 2.1.1 Rainfall and Raingauge.....                        | 9        |
| 2.1.2 Satellite Remote Sensing.....                      | 11       |
| 2.1.2.1 Remote Sensing.....                              | 11       |
| 2.1.2.2 Satellite.....                                   | 12       |
| 2.2 Rainfall and Satellite–Based Measurements.....       | 15       |
| 2.2.1 Meteorological Satellite–METOSAT.....              | 15       |
| 2.2.2 Characteristics of METOSAT Satellite.....          | 21       |

|   |  |           |
|---|--|-----------|
| 2.3   | Rainfall Estimation Techniques.....                | 23        |
| 2.3.1   | TAMSAT Rainfall Estimation System (TRES).....      | 27        |
| 2.4   | Previous Research Works.....                       | 28        |
| <br><b>CHAPTER THREE.....</b>                     |  | <b>32</b> |
| <b>General Description of the Study Area.....</b> |  | <b>32</b> |
| 3.1   | Overview.....                                      | 32        |
| 3.2   | Location.....                                      | 35        |
| 3.3   | Topography and Drainage.....                       | 36        |
| 3.4   | Climatic Features.....                             | 38        |
| 3.5   | Socio-economic and Population Profile.....         | 39        |
| <br><b>CHAPTER FOUR.....</b>                      |  | <b>42</b> |
| <b>Materials and Methods.....</b>                 |  | <b>42</b> |
| 4.1   | Data Type and Source.....                          | 42        |
| 4.2   | Methodology.....                                   | 44        |
| 4.2.1   | Schematic Flow-Chart.....                          | 47        |
| <br><b>CHAPTER FIVE.....</b>                      |  | <b>49</b> |
| <b>Data Processing and Analysis.....</b>          |  | <b>49</b> |
| 5.1   | Data Processing.....                               | 49        |
| 5.1.1   | Input Dataset Format.....                          | 49        |
| 5.1.2   | Extent of Data Records.....                        | 50        |
| 5.1.3   | Homogeneous Rainfall Regions (HRR).....            | 51        |
| 5.1.3.1   | Selection and Delineation.....                     | 51        |
| 5.1.4   | Processing of Gauge Rainfall Data.....             | 54        |
| 5.1.5   | Building RFE Image from MetoSat -TIR raw DATA..... | 55        |
| 5.1.6   | RFE Image and Value Extraction Process.....        | 57        |

|   |           |
|---|-----------|
| <b>CHAPTER SIX.....</b>   | <b>65</b> |
| <b>Results and Discussion.....</b>  | <b>65</b> |
| 6.1 Evaluation and Interpretations.....   | 65        |
| 6.1.1 Performance of Value Extracted from RFE.....                                      | 65        |
| 6.1.2 Validation and Accuracy.....  | 66        |
| 6.1.2.1 Bias indicator.....   | 66        |
| 6.1.2.2 Validation using Correlation and Quartile Deviation.....                        | 70        |
| 6.1.2.3 Rainfall Surface Map (filled contour pattern).....                              | 74        |
| 6.2 Climatological Characterization of RFE Vs Gauge Values.....                         | 75        |
| 6.2.1 Rainfall Regime of Omo-Gibe Basin.....  | 75        |
| 6.2.2 Results from Temporal Characterization.....                                       | 77        |
| 6.2.2.1 Decadal Pattern and Trend of Rainfall.....                                      | 77        |
| 6.2.2.2 Monthly and Seasonal Profile.....   | 78        |
| 6.2.2.3 Maximum Rainfall Profile.....   | 79        |
| 6.2.2.4 Rainfall Surface Map on Temporal Overview.....                                  | 80        |
| 6.2.3 Results From Spatial Characterization.....  | 82        |
| 6.2.3.1 Seasonal Profile of Spatial Pattern of RFE value.....                           | 82        |
| 6.2.3.2 Rainfall Surface Map on Spatial Overview.....                                   | 85        |
| 6.2 Advantage and Disadvantage of Using Satellite Data for<br>Rainfall Estimations..... | 87        |
| <b>CHAPTER SEVEN.....</b>   | <b>90</b> |
| <b>Conclusion and Recommendations.....</b>  | <b>90</b> |
| 7.1 Conclusion.....   | 90        |
| 7.2 Recommendations for Future Studies.....   | 93        |
| <b>References.....</b>  | <b>95</b> |
| <b>ANNEXES.....</b>   | <b>99</b> |

## List of Figures

|            |   |    |
|------------|---|----|
| Figure 2.1 | The Electromagnetic Spectrum.....   | 11 |
| Figure 2.2 | Areas viewed by geostationary meteorological satellites.....                      | 17 |
| Figure 2.3 | Rain Bearing (Cumulonimbus) Cloud Viewed from the Earth's Surface.....            | 19 |
| Figure 2.4 | The life cycle of Cloud :( grey area indicates rainfall).Sketched.....            | 20 |
| Figure 2.5 | Comparison of actual and estimated 5-year average rainfall.....                   | 32 |
| Figure 3.1 | OMO-GIBE BASIN (Location of the Study Area).....                                  | 35 |
| Figure 3.2 | Physiographic and Land use System of Omo-gibe Basin.....                          | 36 |
| Figure 3.3 | Long Year Mean Annual Rainfall of Omo-Gibe Basin.....                             | 38 |
| Figure 4.1 | Schematic Flow Chart: Steps in the Analysis and the General Study.....            | 48 |
| Figure 5.1 | Homogeneous Rainfall Regions of OMO-Gibe Basin.....                               | 53 |
| Figure 5.2 | Map of Geographic Distribution of Stations.....                                   | 54 |
| Figure 5.3 | Average gauge values against CCD hour at 25 degree square pixel size....          | 56 |
| Figure 5.4 | The Raw MetoSat-TIR CCD and Processed RFE Image.....                              | 58 |
| Figure 5.5 | Steps in the Processing of RFE Value Extraction.....                              | 59 |
| Figure 5.6 | Map of RFE image Average for rainfall 2 <sup>nd</sup> decade of august, 2006..... | 62 |
| Figure 5.7 | Extraction of VERTEX for HRRs (ArcMap: Spat. Analysis Tools).....                 | 63 |
| Figure 5.8 | Sample View of Value extracted at ASCII file from RFE image.....                  | 63 |
| Figure 6.1 | Bias Indicators for 1 <sup>st</sup> Decade August, 2000/2003/2006.....            | 67 |
| Figure 6.2 | Bias Indicators for the Month April, 2000/2003/2006.....                          | 68 |
| Figure 6.3 | Bias Indicator for Kiremet season, 2000/2003/2006.....                            | 69 |
| Figure 6.4 | Plot of RFE Value Against Gauge :(a) 2000,(b) 2003 and (c) 2006.....              | 71 |
| Figure 6.5 | Graph of Validation for estimated and gauge recorded rainfall.....                | 73 |
| Figure 6.6 | Monthly Rainfall Map for March over Omo-Gibe Basin.....                           | 74 |
| Figure 6.7 | Monthly Rainfall Map for August over Omo-Gibe Basin.....                          | 74 |
| Figure 6.8 | Seasonal Rainfall Map for Kiremet in 2003 over Omo-Gibe basin.....                | 75 |
| Figure 6.9 | Rainfall Regimes in Ethiopia.....   | 76 |

|                  |   |    |
|------------------|---|----|
| Figure 6.10      | Plots of Rainfall Pattern and Characterization for RFE value<br>(Using Pattern analysis, decadal in2000/2003/2006)..... | 77 |
| Figure 6.11      | Average Monthly Rainfall Profile.....   | 79 |
| Figure 6.12      | Rainfall Map for Bega Season:2000.....  | 81 |
| Figure 6.13      | Rainfall Map for Belg Season: 2003.....   | 81 |
| Figure 6.14      | Rainfall Map for Kiremet Season: 2006.....  | 82 |
| Figure 6.15.(a). | Plots of Spatial Pattern of RFE Value on Seasonal Basis.....  | 83 |
| Figure 6.15.(b). | Plots of Spatial Pattern of RFE Value on Seasonal Basis.....  | 84 |
| Figure 6.16      | Rainfall Map: Average Annual2000/2003/2006.....   | 86 |



## List of Tables

|           |  |    |
|-----------|--|----|
| Table 1.1 | The GOES radiometer channels (Source: EUMETSAT, 1997).....                                   | 18 |
| Table 2.2 | The METEOSAT radiometer channels.....  | 22 |
| Table 2.3 | Characteristics of MetoSat. From (Kidder and Vonder Haar (1995).....                         | 23 |
| Table 3.1 | Summery of Basin Description.....  | 41 |
| Table 5.1 | Data format generated from different sources for the Analysis.....                           | 49 |
| Table 5.2 | Statistical Summery for Classified HRRs.....   | 51 |
| Table-5.3 | Mean cross-correlation between stations within and with stations<br>in the other region..... | 52 |
| Table 5.4 | Profile of Mean Rainfall Distributions and Annual Variability.....                           | 55 |
| Table 6.1 | Data Table for Quartile of Coefficient for Selected Months.....                              | 72 |
| Table 6.2 | Maximum Rainfall Profile for RFE and Gauge Value.....  | 80 |
| Table 6.3 | Correlation results of average Annual RFE Value Vs Gauge record.....                         | 84 |
| Table 6.4 | Average Annual rainfall of Estimated and Gauge Values.....                                   | 85 |

## ANNEXES

|          |  |     |
|----------|--|-----|
| Annex-A: | List of Meteorological Stations in Omo-Gibe Basin.....                   | 99  |
| Annex-B: | Climatological Mean Annual Rainfall (1974-2004).....                     | 101 |
| Annex-C: | Average Decadal Estimated Rainfall Value & Gauge Records in Years....    | 102 |
| Annex-D  | Estimated Rainfall for HHRs at Decadal Average.....                      | 103 |
| Annex-E  | Average Gauge Record for HHRs at Decadal Average.....                    | 103 |
| Annex-F  | Monthly Average Rainfall for Gauge Records in Years & at HHRs level..    | 104 |
| Annex-G  | Satellite Estimated Monthly Average Rainfall in years at HRRS Level..... | 105 |
|          | Photograph Taken During Field Visit.....                                 | 106 |

## **ACRONYMY**

|          |   |
|----------|---|
| AVHRR    | Advanced Very High Resolution Radiometer                                |
| ASCII    | American Standard Code for Information Interchange                      |
| BNA      | Block Numbering Area  |
| CCD      | Cold Cloud Duration   |
| EUMETSAT | European Organization for the Exploitation of Meteorological Satellites |
| HRRs     | Homogenous Rainfall Regions   |
| ITCZ     | Inter Tropical Convergence Zone   |
| GIS      | Geographic Information system   |
| GOES     | Geostationary Operational Environmental Satellite                       |
| GPS      | Satellite Positioning System  |
| MM       | Millimeter  |
| WMO      | World Meteorological Organization                                       |
| NMA      | National Meteorological Agency  |
| RFE      | Rainfall Estimates  |
| Rms      | Root mean square  |
| SEDI     | Satellite Enhanced Data interpolation                                   |
| TAMSAT   | Tropical Application of Meteorological Satellite                        |
| TIR      | Thermal Infrared  |
| WMO      | World Meteorological Service Agency                                     |

## Abstract

*Rainfall is a key climatic element considered as the most important factor that influencing the Ethiopian agriculture and it is also principal cause of droughts and flood triggered by the fluctuation and excess of rainfall extreme events respectively. It is known that the pattern and distribution of rainfall in Ethiopia is highly variable. Therefore, the understanding of such situations and integration of this knowledge into planning and decision making process is not doubtful. At present, the great amount of available rainfall data does not allow to a direct access by human user to the whole content of information. As D.Grimes, professor of reading university in UK, cited in the proceeding of meteorological satellite data users conference in 1997, the past 30 years there has been concern about decreasing rainfall in Africa and weather this is linked to climate change. He stressed that the problem of accurately assessing the situation are exacerbated by the sparseness of the raingauge network, which has meant difficult to determine it with out satellite applications. The development of remote sensing technology and application which are now able to manage the Satellite –based rainfall estimates by giving answer for specific complain such as - stations do not adequately reflect the various climatic zones of the country, unevenly distribution of Gauge Networking system, establishing dense network is not economically viable, accuracy and missing of gauge readings and records, and so on. Therefore, this problem can be alleviated only through the application of satellite data. The fact that satellite derived data is continuous in space and could be obtained regularly has made it very useful for early warning purposes. Most operational rainfall monitoring system in Africa including our country uses thermal infrared (TIR) imagery from MetoSat satellite. This is because of high repetitions rate of MetoSat images and the link between the rainfall and its convective source of clouds which is sensitive to TIR data. Half-hourly digital data from European Meteorological Satellite METEOSAT has been receiving at the National Meteorological Service agency since 1990. The study presented in this paper took place to investigate and show methods and practical application of satellite based rainfall estimates of TAMSAT methodology developed at the University of Reading, UK for tropical Africa. The data used are two types, dekadal MetoSat-TIR CCD image and ground gauge measurements represented the study area of Omo-Gibe basin. The CCD images are converted into RFE image through automated image processing module and values are extracted at delineated homogeneous rainfall region (HRR). The extracted rainfall values obtained are further processed and characterized quantitatively using statistical and GIS Geostatistical tools, indicated that reasonable agreement and in small extent variability between the satellite estimate and gauge value.*

# CHAPTER ONE

## 1. Introduction

### 1.2 Background

The main climatic features that help to explain Ethiopian climatic resources are spatial and temporal distribution of mainly rainfall, temperature and other derived indices. Rainfall measured at a single location such as a raingauge, bucket, or similar collecting device is known as “Point Rainfall.” Rainfall estimated over a large area is termed “Areal Rainfall.”

The country, found within tropics, and has also great geographical diversity, with high and rugged mountainous, flat-topped plateaus, deep gorges, etc. The Great Rift Valley divides the country into two parts forming the eastern and western highlands. Its altitudinal range lies between 120m below sea level and 4600m above sea level. (Admasu, 1989) The differences in altitude and relief create a large variation in climate in various regions of the country (Workneh, 1987). In most cases the greater the annual rainfall in amount the lesser is the annual variability. Semi arid regions receive very small, irregular, and unreliable annual rainfall. The annual cycle of the climatology of the rainfall over tropical Africa and in particular over Ethiopia, strongly determined by the position of the ITCZ, which is a primary feature of the meridional Hadley Circulation and the walker Zonal circulation (Griffiths C.G, 1971).

Due to Ethiopian economy is mainly dependent on rain-fed agriculture and subjected to vagaries of weather and climate system, many investigations have shown that fluctuations of rainfall have always been the natural curse of agriculture and caused droughts and floorings. Moreover, rainfall risk assessments, warning and response systems are not yet to be well functioning integrated with vulnerability and risk management. Conventionally, rainfall is measured using rain gauges, which provide the measurement of the amount of rain in the surrounding area. The distributions of rainfall stations are also very sparse and non-evenly distributed and most of which are located along the main roads. It is so that, further improvement of data availability and accuracy should be vital. The devastating effect of river and flash flood is now recurring event that cause the loss of life, properties and

evacuations of settlements. Particularly, at higher rainfall values, problems may arise in early warning and preparedness system if such data are unavailable. Specifically, the availability of water in the river basin is also determined by rainfall in order to design, operation and management of water resources projects such as water supply, sewerage disposal, irrigation, and hydropower in that watershed. Distribution of water in Ethiopia exhibits an abundance of rainfall over the north and north western zones contrasted by extensive and extreme aridity of the Ogaden in the northern and the lowland areas in the south, and south eastern direction. Between these extremes, there are many place to be characterized as a semi-arid zones, where rainfall shows wide fluctuation from year to year and even with in seasons in the year. The rainfall ranges from less than 200mm along the northern and eastern low lands to more than 2000 mm in the western part of the country. (Bekele,1993)

The knowledge about the characteristics of the rainfall over an area such as the source, quantity, distribution and the frequency of rainfall is essential in all of the experimental and implication in utilization and associated problems with its natural events. Therefore, rainfall monitoring in the country is of vital importance. Rainfall is the most critical and key variable both in atmospheric and hydrological cycle. To understand present condition and forecasting the future trends not only in a single river basin but also overall the country, historical rainfall data should be important used to form a database. Rainfall is also one of the most variable meteorological parameters that can be characterized and mapped in time and space. The standard surface measurement network provides much localized information about the seasonality, pattern of its distribution and variability. The maps of rainfall with additional geographical data and administrative boundaries are necessarily assists in providing information for the agriculture, weather forecasting, water management and other activities.

This study aimed at application of modern IT tools like remote sensing for acquisition of rainfall estimation from satellite, and characterizing the rainfall statistics, integrating with spatial and attribute data from in a specific format developed for the purpose. These integrated rainfall-estimation systems are embedded within a GIS, Spatial and Geostatistical analyst and database. The rainfall in Ethiopia is mainly convective and thus it

is more localized and it's spatial and temporal distribution as well as the intensity of rainfall is highly variable. Therefore, it is essential to measure area rainfall on real time as accurately as possible. Traditional terrestrial telecommunication, particularly in remote areas of disaster-prone countries, the remote sensing, GPS and GIS applications have the capability to improve risk assessment, disaster preparedness, early warning and relief operations dramatically. In doing this, it can be possible to provide objective measures which enable decision makers to follow the spatial and temporal impact of rainfall between years or season in the way very useful for early warning purposes

In general, the satellite based rainfall estimation process can assist mainly to get rainfall data and disseminate to user agencies on a real-time basis via satellite link. Based on more than 20 years of actual experience, the weather satellite particularly has been hand into efficient tools for both observing and communicating weather and rainfall data in timely fashion. As a result of this, the "Best Advantages" that have been practiced are for identifying periods of well- above or below average rainfall rather than trying to estimate actual rainfall amounts for gauging and ungauged stations, provided that a suitable technology and analyzing methods is used. In addition to this, some of the advantages over the conventional techniques are. (a) In combining satellite communication, remote sensing, GIS and GPS in an institutionalized framework with multi-sectoral linkages. (b) in identifying the regions that have the highest amount of risks, emanating from multiple hazards, as well as the safest places, to help policy formulation towards disaster reduction and (c) in using remote sensing for rapid mapping of disaster events and an early warning network by disseminating the information to end-users on a real-time basis. (d) Need for reliable and timely information on rainfall related parameters.

This study is mainly intended to show the practical application of satellite based rainfall estimations using the MetoSat -TIR image data and to validate the results and compare it with the actual rainfall over the hydrological regime, Omo- Gibe river basin. Therefore, of these different measuring devices, satellite is useful and advantageous in providing continuous, large area coverage and real-time estimating of rainfall for operational applications, and in particular helps to monitor and evaluate the basin rainfall characteristics. The use of meteorological satellite data certainly could expand the spatial

and temporal coverage of rainfall estimation and improve the consistence with the nature and development of precipitating systems within the basin in the objective of providing the rainfall information and meteorological service to end users.

## **1.2 Problem of the Statements**

Rainfall is the meteorological parameter-affecting people in the most direct way. Forecasting the spatial and temporal distribution of rain is therefore one of the major challenges for the meteorological services and research purposes. Accordingly, Scarcity of rainfall data for ungauged places and remote area within the basin is one of the major problem and gap for rainfall information users. The distribution of station in the central and extreme lowlands and the border areas have consist only 2.8 percent of the total stations found within the basin. The distribution of raingauge network of stations for point measurements can be made but to derive continuous aerial amounts would still remained inadequate because of an unfeasibly dense network. In the country, it takes months to collect data from the other stations, which are not equipped with radios and telephone service. In Omo-gibe basin only about 4.6 percent of existing stations are equipped with radios and report on real time basis. (UNICA/WMO, 1995).

Besides, the shortage of gauge stations, the management of the existing stations, recording and dissemination system are conventional, and this have its own problem on the need of rainfall data for immediate and future uses in development research program. This is witnessed on that many researcher and research institutes, Master's students are facing to have timely data at least for those few of stations having a gauge records. In addition, the ground rainfall data collection and processing system have been invited to make securitization and statistically proof for its effective application in operational and seasonal forecasting system. In such situation, satellite remote sensing of rainfall could help to solve such problem as long as the technology and methods rainfall estimation is accurate and practical.

As a whole, this study address to investigate the capability of the satellite based rainfall estimates and value extraction method in solving the data requirement less and more badly gauged area in the basin.

## 1.3 Objectives of the Research

### 1.3.2 General Objectives

Due to the stated problems; scarcities of real time meteorological data from ground stations and declining of observations, the objective of this study has focused into two broad objectives. The first main objectives of this paper considered is:-

- ✚ To obtain rainfall from satellite source data and to evaluate and characterized the representation the estimated rainfall value comparing with the corresponding gauge value and rainfall climatology of the study area at temporal and spatial profile.

### 1.3.2 Specific Objectives

- ✚ Delineation of Similar climatic zones (HRR) within the study area based on long year climatologically mean rainfall data.
- ✚ Manipulation of Satellite image processing software
- ✚ To generate ten-daily RFE image derived from the MetoSat (TIR)-CCD data for similar rainfall regions within the basin.
- ✚ To extract quantitative values of the estimated rainfall value fro RFE image for the predefined HRRs.
- ✚ To Validate and compare the satellite rainfall estimates using statistical Analysis with ground raingauge data in time and for HRRs.
- ✚ Characterizing the estimated rainfall value-RFE under different seasons and rainfall peak time within the basin.
- ✚ And to characterize “Satellite” and “Ground” rainfall amounts in spatial dimension using standard Kriging method and to prepare Isohyetal map for the study area.
- ✚ To prepare reports and documents indicating the evaluation and interpretation of the results.



## 1.4 Limitation and Scope of the Study

During the processing and analyzing of an overall input dataset there have been some limitations encountered by the researcher. That includes:

- ✚ Time was a very critical problem to cover all the activities.
- ✚ Financial resources limitations to cover all the necessary required expense for technical assistant and material supply.

Based on the limitations, and with reference to the content of this thesis study, as presented in the following section 2 to 7, the scope of this research is summarized under the following study topics.

- ✚ Review of literature and previous studies. And identify methodologies.
- ✚ Identifying the location, relief and Physiographic features of the study area.
- ✚ Compilation of climatic-rainfall station(gauge) data and Satellite data and
- ✚ Creation of a project database using GIS Script (ILWIS, WinDisp,) ArcGis, Arc Catalogue.
- ✚ Satellite data and gauge data processing and analyzing.
- ✚ Extraction of rainfall from satellite data at homogenous rainfall regimes.
- ✚ Qualitative and quantitative analysis of estimated rainfall value using statistical method and Characterization of the rainfall distribution against the climatology of the study area over a given time and places.
- ✚ Displaying rainfall maps showing temporal and spatial variation of rainfall distributions
- ✚ Conclusions on the results and recommendation for future study

## 1.6 Benefits and Beneficiaries from Expected Output

The expected output of the study will be two types.

- ✚ Digital decadal estimated rainfall value and image averaged over time and places in the basin, so as to put it in use when it is require in the future study. .

- ✚ Guiding reports and documents, with graphs and maps based on the the performance of estimated rainfall particularly for inaccessible area in the basin.
- ✚ As a general understanding, it introduced the efficiency and optimization of data collection through remote sensing technique than field measurements.

The rainfall estimates showing the spatial and temporal characteristics of rainfall have been successfully used to Therefore, there is no doubt that satellite based real time rainfall measurements contribute substantially for sectoral development and research objectives.

*The Benefits of the research here include,*

- ✚ Application of modern approaches for satellite based rainfall estimation which can assist for planning and decision making in research activities and sectoral development strategies.It is also serve in improving operational status of meteorological and hydrological applications in measuring and studying the spatial variability that cannot otherwise be observed.
- ✚ Analysis of images and thematic parameters include various professional integration Including expertise and technical assistance
- ✚ Using automated image processing softwares and GIS as a tool with cost and time maximization

*Beneficiaries of the research project area:*

- ✚ Planners, decision makers, and all interested agencies and individuals above all involved in rainfall forecasting, flood monitoring, and risk assessment both in the basins and throughout the country.
- ✚ It can also increase short-term weather forecast system of NMA, and enhanced rainfall-monitoring network over the upstream parts of river catchments.
- ✚ Efficient communication system in up-to-date and fast rainfall information exchange system, among the stakeholders like researchers and academia institutes, NGOs and other users.

## **1.6 Structure of the Dissertation**

This paper is divided into seven chapters. The First-Chapter is an introduction part that includes the problem and objectives of the study, and benefits and recipient of the result of this study will be elaborated. This is followed by the Second -Chapter of the review literature that describes the concepts or theories and earlier studies on related to the topic under consideration. This chapter describes the basic concept and scientific literature on satellite based data source that is related to the different rainfall estimation approaches.

The Third-Chapter is the general descriptions about the study area with the distribution of existing meteorological distributions are described in the third section. The fourth chapter gets a part described about the nature of the data and methodology.

In the Fifth-Chapter, activities of data preparation, processing and creation of database are briefly discussed. In order to better understand the rainfall estimation process and how the estimated rainfall value is extracted from RFE image over ten daily periods (decadal) base are discussed in this chapter. The explanation of extent and processing of gauge data and other geographic datasets are integrated into GIS ArcMap environment and Geostatistical functions for generating rainfall surface map are also included in this chapter.

The work necessary to validate the estimated rainfall values as well as characterizing it with the coincident climatic condition of the study area is fully described in the Sixth-Chapter. The combination of estimated and gauge records will be statistically verified and analyzed. The chapter mainly dealt on the applicability of the methodology and its results obtained from the analysis output.

Chapter-Seven gives conclusions, limitation of the work and ideas for future investigations. In summary, it is concluded that the TMSAT method of rainfall estimation is a useful technique in provides useful information about the rainfall of the study area both in a given time and place.

## CHAPTER TWO

### 2. Review of Literature

#### 2.1 Theoretical Background

##### 2.1.1 Rainfall and Raingauge

###### (a) Rainfall

Rainfall is one of important climatic control factor in the hydrological cycle .It is the main source of water that is most vital for human life. The spatial and temporal depth of rainfall is necessary for all activities, scientifically, in the earth and atmospheric system. Thus, rainfall studies are essential in order to understand the supply and demand of water. Rainfall varies in its frequency, duration, intensity and spatial distribution and hence requires accurate observations. Tropical rainfall is mainly convective and thus it is more localized and its spatial and temporal distribution as well as the intensity of rainfall is highly variable.

Rain consists of liquid water drops mostly larger than 0.5 mm in diameter .rainfall usually refers to amount of liquid precipitation .in most countries rain is reported in three intensities: these are, light for rates of rainfall up to 2.5mm/hr, moderate-from 2.8 to .6 mm/hr, and heavy over 7.6mm/hr. (WMO, 1988)

###### (b) Raingauge

Ideally the catch of raingauge would represent the point rainfall falling in the surrounding area. The records are mostly subjected to errors because of the standard of the instrument position itself and the wind effect of the surroundings. The rain gauge types are considered in two categories, non-recording and recording gauges. A non recording raingauge is a cylindrical funnel used for collecting and measuring rainfall at a point. The depth of the rainfall caught in a gauge is measured by means of a graduated cylinder. It is widely used standard measuring device. The measurement is read once every day and this gives a total rain fall over a place during 24 hours of time. The Second type is an automatic recording system using rainfall charts. That is, when the rainfall is fed into the top of gauge

compartment and as the level of water rises, the vertical movement of the float connected with the clock-dram is transmitted into the movement of a pen on the chart fixed with the clock-dram. This would help to measure both the amount and duration of the rainfall fallen in the area as a point measurement. The rain gauge has the following advantages and disadvantages:

### **I. Advantages**

- ✚ It is cheap and easy to maintain and read;
- ✚ Gauge data are available for many years and hence it is possible to do climatologically analysis using long period gauge data; and
- ✚ Comparison between gauge data from different region is possible.

### **II. Disadvantages:**

Although gauges are read once every day to get real time information they should be located in places where there is easy access for an observer, but there are remote areas of interest that are difficult to be accessed every day. Therefore, gauge networks can not cover all area of interest to make a real time observation. Source of errors in the reading gauge can also easily be occurred due the following some cases.

- ✚ Airflow( wind direction and speed)
- ✚ Unrepresentative orientation and exposure of the gauge.
- ✚ Protection problem; by local community over the site
- ✚ Human Observation and transmission, error and miscode.
- ✚ and Evaporation from within the cylinder
- ✚ Gauge leaks and overflow. Some times there might be time delay in getting the gauge data due to communication problem between the observer and the main center.

Thus, the above limitations lead to the use of satellite based rainfall estimation that augments the rain gauge data.

## 2.1.2 Satellite Remote Sensing

### 2.1.2.1 Remote Sensing

Because of considerable development of space technology airborne or satellite techniques are now common and most widely applied technology to obtain data on earth phenomena from distance. In simple language, remote sensing meant acquisition of data from a distance without physical contact of the objects. In fact, areal photographs date back quite a way, satellite based remote sensing is a very new technology dating from the launching from the first weather and earth observant satellites in 1960s.( (OECD,1984-88)

Remote sensing, defined as “ – the transport of information from an object with a distance to a receiver (observer) by means of radiation transmitted through the atmosphere” (<http://www.gis.com/whatisrs/dowithgis.html>) offers the possibility of observing rainfall in real or near real time over relatively large areas and of complimenting the conventional precipitation measurements. The basis for all remote sensing is the electro magnetic spectrum (EMS) viewed in Figure 2.1

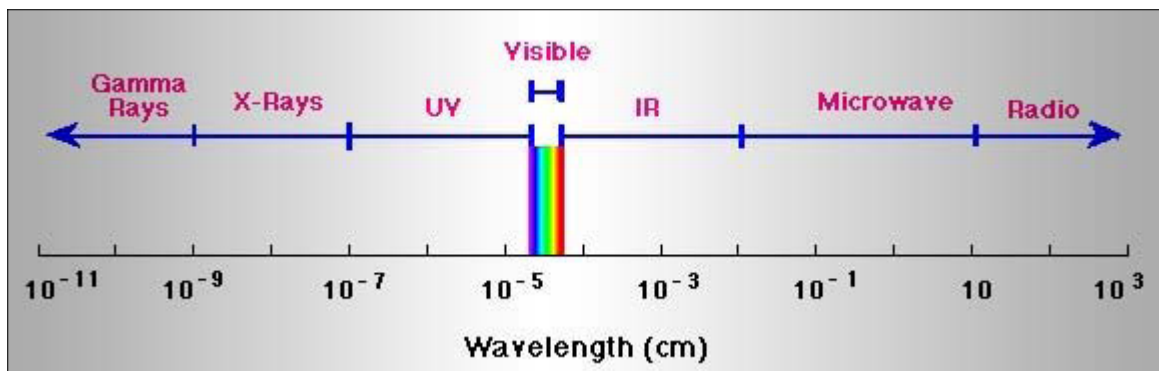


Figure 2.1. The Electromagnetic Spectrum (Source: <http://www.maic.jmu.edu/>)

Remote sensing takes the advantage of unique interactions of radiation from the specific regions in the spectrum (as shown in Figure 2.1) and the earth. There are four basic component of a radiation based remote sensing system, given as follows:

- I. Radiation source (e.g. the sun, radar laser)
- II. Transmission path (atmosphere vegetation canopy, shallow soil surface)

III. Target (e.g. river soil.) and

IV. Sensor (multi-spectral-scanner, thermal sensor, microwave sensor).

Remote sensing is based on interpreting measurable variations in spectral temporal and spatial characteristics of the earth. Spectral characteristics (or signature) of the target are the unique spectral reflectance for specific earth features.(Engman E.T and Gurney.1991) The process of data acquisition remote sensing are the fruit of a complex set of operation using the serious of sophisticated methods. These consists satellite and data reception or processing stations. Remote sensing also classified into three types in respect to the wave length region as shown in figure 2.1.These are:

- I. Visible and reflective infrared remote sensing.(0.4-0.7 $\mu$ m)
- II. Thermal infrared remote sensing.( Greater than 3  $\mu$ m)
- III. Microwave remote sensing. (1mm-1m)

### **2.1.2.2 Satellite**

#### **(a) Overview**

A Satellite is a spacecraft that orbits the earth and returns images of the earth and the atmosphere back to the receiving station on the ground. Satellites are used to estimate rainfall using radiation signals reflected or emitted from the ground and atmosphere and observed by it. Satellite based rainfall estimation is also one part of this technique, and it is a method of deriving qualitative(image) and quantitative(value) using visible and infrared techniques through indirect relationships between solar radiance reflected by clouds, that is, the clouds brightens temperature and rainfall. The detail will be discussed in the coming sections in this study.

There are two basic and important approaches in using satellite for rainfall estimation purposes. These areas:-

- (a) Cloud index and
- (b) Life-history method.

The first type based on the cloud classification and does not require serious consecutive observations of the same cloud system. The second type is makes use of data from the geostationary satellites which produce images usually every half an hour. It has been applied mostly for convective cloud system.

(b) Satellites are divided into two functional Sub-Systems.

I. Surface-Based Sub-system

This system comprises stations of various kinds making observations at or from the surface of the earth and oceans including observation made aboard aircraft and by instruments carried aloft by balloons or rockets. The main component of this system is a network of surface and upper air by members for their own use and as a contribution to international meteorological information exchange system .some of this are for example Ozone stations, World Climate Program (WCP), etc.

II. Space-based sub system

This system comprises Satellite of two types, polar orbiting and geostationary satellite. Both satellites provide qualitative information such as visible and infrared cloud images over wide areas. The next section will be dealt about these satellites.

(c) Satellite Data Receiving System.

The ground segment of the space-based sub-systems of the satellite has two functions.

- I. To provide for reception of signals from satellite containing qualitative and quantitative information, including observations from data collection platforms and others similar systems.
- II. To process, format, display and distribute the information received either directly fro satellites themselves or digital forms received at required standards.



There are also two type of transmissions utilized for dissemination of satellite data. These are:

- Special digital transmission (High Resolution-HR)
- Conventional analogue transmission method

#### (d) Advantage and Disadvantage of Satellite-Based rainfall Estimation

##### I. Advantage

- ✚ Relatively time consuming, and easily for large volume of data acquisition and extraction system.
- ✚ Easy to operate and maintain.
- ✚ It is Tried and Proven, but mainly in tropical zone.
- ✚ In connective rainfall, accurate monthly totals can be obtained

##### II. Disadvantage

- ✚ At night, no visible data are available therefore rainfall estimation are achieved using infrared and, perhaps, microwave data.
- ✚ The techniques for rainfall estimations are based upon assignment of temperature and /or brightness thresholds to rainfall amounts vary in performance with month and seasons.
- ✚ If the satellite sensors fail, there is no possibility of repair until another satellite is launched.

Radar is also a very good devise used to estimate rainfall over a given area by observing the back-scatter of electromagnetic radiation from liquid water drops. Radar has an advantage over raingauge for providing a spatially continuous image. Hear, we don't discuss about radar because it is not the scope of this study.

## **2.2 Rainfall and Satellite–Based Measurements**

### **2.2.1 Meteorological Satellite - METOSAT**

As many references cited, understanding the importance of observing weather from space Verner Sumoi and colleagues at the University of Wisconsin developed the first successful meteorological satellite that was launched on 13 October 1959. This satellite used a Suomi radiometer and returned coarse maps of reflected solar radiation from the earth surface and infrared radiation emitted by the earth (Tucker.M.R.1997). On 1 April 1960 a first satellite completely dedicated to meteorological purpose was launched and TIROS 1 (Television and Infrared Observational Satellite) was the 22<sup>nd</sup> successfully launched satellite. TIROS 1, had a lifetime of 79-day, was the first satellite that returned an image of the earth with its weather systems as a whole. Since then several technological improvements were made in the TIROS series and eventually the present standard TIROS N-series is reached.

Geostationary Operational Environmental Satellite 1 (GOES 1) was the first operational geostationary satellite that was launched in 1975. In the late 70s Japan's Geostationary Meteorological Satellite 1 (GMS 1) and European Space Agency's MetoSat 1 were launched. The MetoSat 1 in addition to the visible and infrared had a third channel of water vapor. Since 1978 one or more passive microwave sensors have been available on polar orbiting satellites, such as the Special Sensor Microwave/Imager (SSM/I) on the Defense Meteorological Satellite Program (DMSP).

The earth's artificial satellite can be classified according to their functions; but the interest of this study lies with the meteorological satellite such as METOSAT, NOHA, Indeed, it was for weather observation that these satellites were used. The first was polar orbited satellite up to until 1966 and geostationary satellite afterwards.

#### **(a) Polar Orbiting Satellites**

Polar orbiting satellites are launched into sun-synchronous orbits at an altitude of about 800km. The sun-synchronous orbit of the polar orbiting satellite enable them to observe the signal at each location with the sun always be in the same place in the sky (Houghton and Taylor, 1973). For example, if the satellite crosses a certain place at midday when it goes

to the northern pole then as it goes to the southern pole it re-crosses the place at midnight. The satellites have a period of about 100 minutes i.e. they take about 100 minutes to complete an orbit and scan the earth's surface in about 24 hours. The METEOR of the former Soviet Union and the US TIROS are polar orbiting satellites and of which the TIROS (NOAA Series) are the most widely used. India also launched two polar orbiters: Bhaskara 1 and Bhaskara 2 in 1979 and 1981, respectively. Polar orbiting satellites are essential to provide global and hemispherical image of the weather (Houghton and Taylor, 1973). However, images from polar orbiting satellite are obtained only once or twice per day, and hence for continuous monitoring of the weather it becomes difficult to rely only on polar orbiting satellites.

On the other hand, because of their low orbits the spatial resolution obtained from polar orbiting is higher than the geostationary one's (i.e. polar orbiters observe a lot of detail information than the geostationary satellites).

### **(b). The Geostationary Satellites**

Geostationary satellites were first launched in the 1970's. Each satellite has a lifetime of approximately 5 years. Satellites have been launched and maintained by NOAA (GOES E+W), and the space agencies of Europe (METEOSAT), Japan (GMS), India (INDSAT), Russia (Elektro) and China (FY-2). The Russian Elektro satellite has not yet produced reliable operational imagery and the Chinese FY2 satellite failed shortly after its launch. This leaves an unfortunate gap in the global coverage in this important part of the world. However, the latest Indian geostationary satellite, INSAT-2B positioned at 93.5<sup>0</sup> E *does* provide useful coverage in Asia. Currently,

METEOSAT 5 is also stationed over the Indian Ocean. The other regions poorly served by geostationary satellites are the Polar Regions, where image distortions occur due to the satellite's position above the equator. The global geostationary satellite coverage is illustrated in Figure 2 below

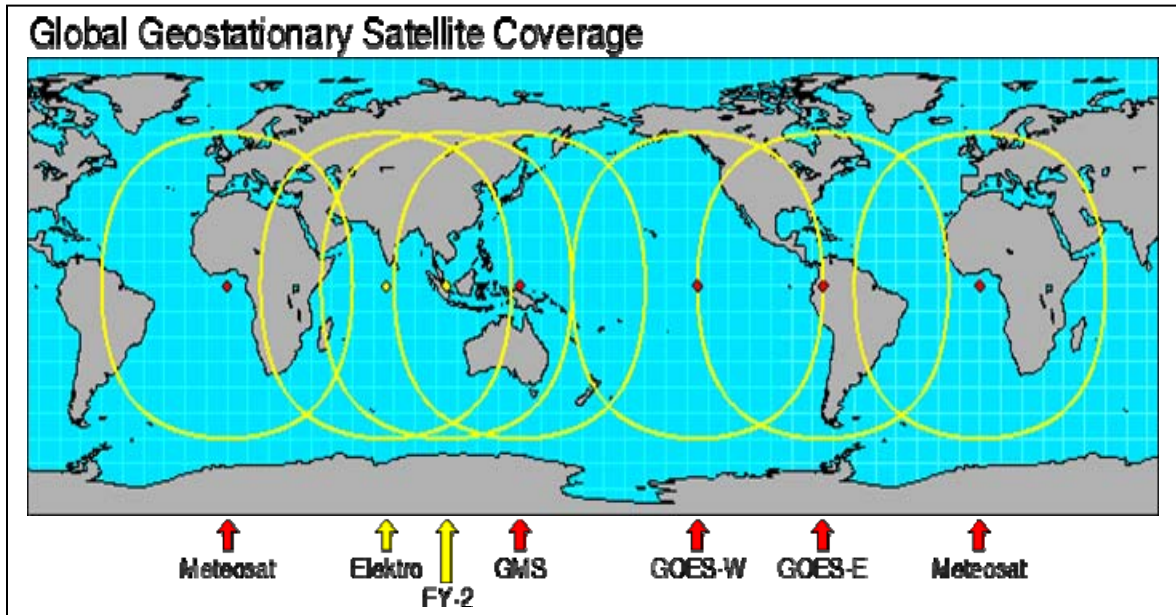


Figure 2.2. Areas viewed by geostationary meteorological satellites.  
 (The solid line shows the extremity)  
 (Source: Source: <http://www.tamsat.red.rsta.uk.edu/> )

According to (Dugdale G.1994), the geostationary satellite orbits eastwards around the equator at an altitude of approximately 36000km. An orbit at this altitude has a period of 24 hours, which means the satellite remains fixed relative to the Earth's surface, hence the name geostationary satellite. The scanning system allows about 42% of the Earth's surface to be viewed from a single satellite, so that a network of five satellites gives global coverage. The geostationary satellite can monitor developments in the field of view continuously and in almost real-time. This allows the user to follow quickly developing weather systems or diurnal variations in the weather. This is of great value to forecasters. However, the large distance of the satellite from the Earth's surface means the resolution is lower than with polar orbiting satellites

NASA launched the first Geostationary Operational Environmental Satellite (GOES) in 1975. Currently GOES numbers 8 and 10 are in orbit, launched in 1997. One satellite is positioned at 75°W (east coast of the US) and the other is positioned at 135°W (west coast of the US). The satellites are named GOES-E and GOES-W respectively. The GOES satellites are equipped with radiometers with five spectral channels.

Table 1.1 The GOES radiometer channels (Source: EUMETSAT, 1997)

| Channel | Wavelengths (microns) |
|---------|-----------------------|
| 1       | 0.55-0.75             |
| 2       | 3.80-4.00             |
| 3       | 6.50-7.00             |
| 4       | 10.20-11.20           |
| 5       | 11.50-12.50           |

With the advent of geostationary weather satellites in the 1960s and 70's, positioned above the equator at 5-6 positions around the globe to provide complete coverage, various techniques have been developed to estimate rainfall from visible and infrared (IR) radiation upwelling from the Earth into space. The higher the cloud albedo, the more droplets and/or ice crystals it contains and the deeper it tends to be, so the more likely rainfall is on the ground. And also the lower the IR brightness temperature, the higher the cloud top, and the more likely the rainfall. A combination of both channels works best. Imagine a fair day with cirrus clouds, for instance. The IR channel may flag this as wet, because of the cold cloud tops; however cirrus is optically thin, so in the visible channel it is dry. The visible/IR rain retrieval algorithms work best at low latitudes, because at higher latitudes the view is more slanted, confusion arises with high-albedo surfaces of snow or ice, and deep-convective precipitation is less common. Another problem is incomplete pixel filling for small cumulonimbus clouds

At night no visible imagery is available. One can then use an empirical relationship between cloud-top temperature (deduced from the outgoing radiation in the 10.7-micron waveband), the simultaneous precipitation rate inferred from surface radar reflectivity, and the humidity profile (derived from radiosonde data). The rainfall rate (R, mm/h) depends on the cloud-top temperature (Temperature Degrees Kelvin) thus  $R = 1.1183 \times 10^{11} \times \exp(-3.6382 \times 10^{-2} \times$

$T^{0.5}$ ). Adjustments are then made according to the perceptible water and surface relative humidity. The rate of change of cloud-top temperature can be used as well. It indicates the speed of cloud growth, and hence the areas of heavy rainfall.

In practice, the procedure allows useful estimates over 6 hour's periods. However, it overestimates rainfalls over 24-hours in the case of slowly moving thunderstorms with a broad anvil, by exaggerating the area of rainfall. On the other hand it underestimates rainfall from warm-top stratus, especially near coastlines and in mountainous terrain. In short, quantitative precipitation estimates from geostationary satellites can yield cumulative rainfall and thus flood warnings, for instance, because of the continuous coverage, but large discrepancies with raingauge data occur.



Figure 2.3 Rain Bearing (Cumulonimbus) Cloud Viewed from the Earth's Surface.

(Source: Source: <http://www.tamsat.red.uq.edu/> )

Cloud towers like the one in Figure 2.3 above are visible from space bubbling up and decaying, particularly in the tropics. Satellites are able to measure the temperature of the cloud tops. The temperature of the atmosphere decreases regularly with height in the

lowest 15 km of the atmosphere. The temperature at the tops of the tallest clouds can be as low as  $-80^{\circ}\text{C}$  and this contrast sharply with the warm ground. We can produce images showing the areas where the cloud-top temperature is below certain threshold temperatures.

Generally, when the cloud top temperature falls below approximately  $-40^{\circ}\text{C}$ , there is some rainfall occurring below. Such Clouds are Cold Clouds. The life cycle of this Cold cloud is also shown in Figure 2.4 below. The time spent by an area with cloud top temperatures below the thresholds is known as cold cloud duration–CCD. The relationship between of CCD and rainfall is discussed in the coming sections in detail.

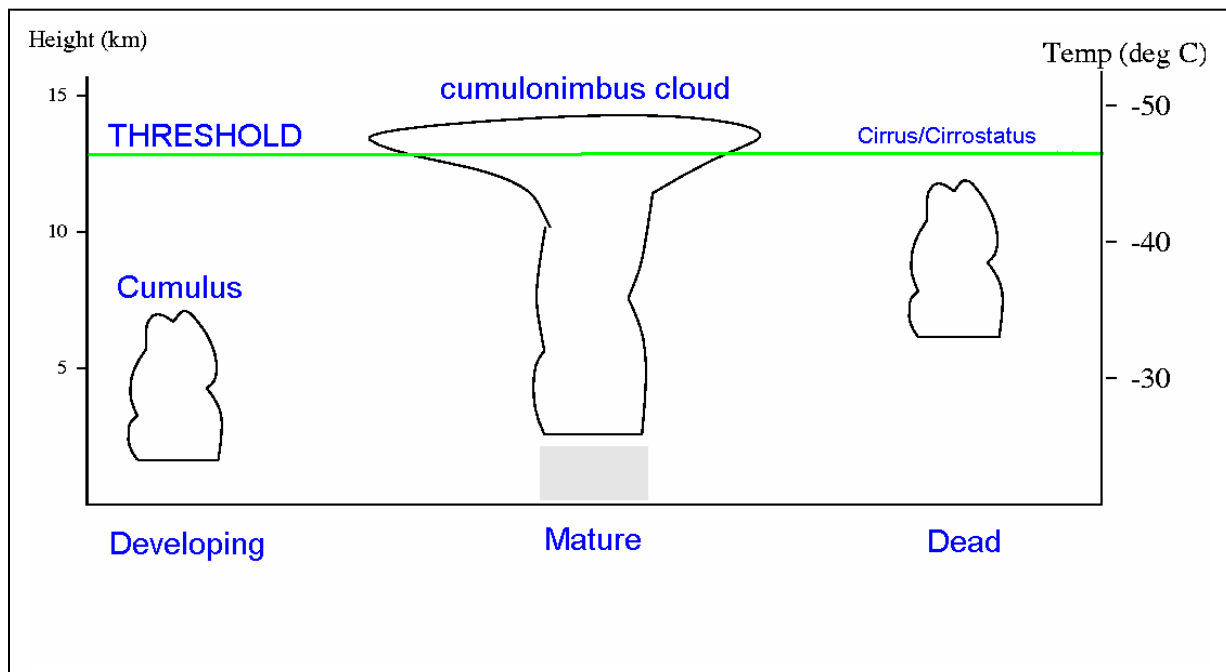


Figure 2.4. The life cycle of Cloud :( grey area indicates rainfall).Sketched.

In the life cycle of the cloud system, the developing stage produces rainfall before the top of the height of the cloud has exceeded the threshold. And then the rain bearing clouds have died down after the convective cloud weakened. The reflectance from the top of cloud at given temperature is a sensitive part to observe by the satellite mechanisms. There are various type of Satellite designed to perform specific tasks. However, there now follows a description of the major geostationary satellites. The scanning and transmission systems of each satellite are broadly similar, so only the METEOSAT system is discussed in detail.

## 2.2.2 Characteristics of METOSAT Satellite

### (a) METEOSAT

European Space Agency launched METEOSAT. The first METEOSAT was launched in 1977 after the success of the American TIROS satellites. Initially 8 European countries financed the project. Today there are thirteen countries working together under the EUMETSAT organization with the aim to "establish, maintain and operate a European system of operational meteorological satellites".

The headquarters of EUMETSAT is in Darmstadt, Germany. The latest, METEOSAT-7 was launched on the 2 September 1997 and became operational on the 3 June 1998. (EUMETSAT, 1997) A previous satellite, METEOSAT 5 was moved to a position above the Indian Ocean (around  $63^{\circ}\text{E}$ ) to support a 2 year experiment in that region. This is described in more detail in EUMETSAT's website. METEOSAT 6 was relocated to the stand-by position at  $10^{\circ}\text{W}$  after METEOSAT took over as the operational satellite

The METEOSAT satellite which is viewed in Figure 2.2, it orbits at an altitude of 36000km above the point  $0^{\circ}\text{N}$ ,  $0^{\circ}\text{E}$  in the Gulf of Guinea. This point vertically below the satellite is called the sub-point. The satellite rotates around an axis which passes lengthwise through the centre of the satellite and is perpendicular to the plane of its orbit, completing 100 revolutions per minute.

A spin Scan Radiometer is the meteorological instrument on MetoSat that enables it to return images of the earth and atmosphere in the Visible ( $0.4\text{-}1.1\ \mu\text{m}$ ) and thermal Infra-red ( $10.5\text{-}12.5\ \mu\text{m}$ ) and Water vapor ( $5.5\text{-}7.1\ \mu\text{m}$ ). East-west optical scanning is achieved by the rotation of the satellite at the rate of 100 rpm, while a scan mirror that moves in 192 mrad steps does the north-south optical scanning. Thus, full-disk hemispherical image is obtained from the east west and north-south optical scanning. This takes a further 5 minutes, so a full image is produced every 30 minutes. (EUMETSAT, 1997)



## (b) Characteristics of METOSAT

### Thermal Infra-Red (TIR) Imagery

MetoSat transmits TIR images every 30 minutes. It is from these CCD images are derived. You need to know the calibration data required to convert each TIR image in a cold cloud counter. You can add these to obtain CCD Images at any desired temporal step above 30 minutes but production is usually restricted to one day and ten day cold cloud duration images, requiring at least 24 and 240 TIR images, respectively.

The METEOSAT radiometer is equipped with a visible channel and two infra-red channels. Their wavelengths are shown in Table 2.2.

Table 2.2: The METEOSAT radiometer channels

| Channel             | Wavelengths (microns) |
|---------------------|-----------------------|
| 1. Visible          | 0.5-0.9               |
| 2. Thermal Infrared | 19.5-12.5             |
| 3. Water vapour     | 5.7-7.1               |

The visible channel scans 5000 lines in each image, with each line consisting of 5000 pixels. The infrared scans 2500 lines and pixels. The sub-point resolution in the visible and infrared channels is 2.5km and 5km respectively. The resolution decreases somewhat towards the edges of the image (4.5km over Europe in the visible) due to the viewing angle of the radiometer.( Source: <http://www.tamsat.red.uk.edu/> )

Currently EUMETSAT are working on the second generation of METEOSAT satellites. The new satellites will be spin-stabilized like the current generation, but with many design improvements including a new radiometer, which will produce images every fifteen minutes, in twelve spectral channels.

Table 2.3 Characteristics of MetoSat. From (Kidder and Vonder Haar (1995)

|                       |                                    | Value                     |                         |
|-----------------------|------------------------------------|---------------------------|-------------------------|
| Parameter             | Visible                            | Infrared                  | Water vapour            |
| Detectors             | 2silicon photodiodes + 2 redundant | 1 Hg Cd Te + 1 redundant  | 1 Hg CdTe + 1 redundant |
| Wavelengths           | 0.4 - 1.1 $\mu\text{m}$            | 10.5 - 12.5 $\mu\text{m}$ | 5.5 - 7.1 $\mu\text{m}$ |
| Digitization          | 8 bits                             | 8 bits                    | 8 bits                  |
| Angular field of view | 65rad                              | 140rad                    | 140rad                  |
| Resolution at nadir   | 2.5km                              | 5km                       | 5km                     |
| Frame size            | 5000x5000                          | 2500x2500                 | 2500x2500               |
| Frame time            | 25 min                             | 25 min                    | 25 min                  |

## 2.3 Rainfall Estimation Techniques

Different methods are available for estimating area rainfall using images of visible (wavelength between 0.4 and 0.7  $\mu\text{m}$ ) and infrared (wavelength between 10.5 and 12.5  $\mu\text{m}$ ) electromagnetic radiation from geostationary satellites. (Turk, F.*et al.*1997).

**The visible channel** measures the short wave radiation backscattered by the atmosphere and the earth. This channel gives the albedo of the reflecting body and high brightness implies a highly reflecting cloud. The high cloud brightness in turn is related to the cloud optical thickness and liquid water content. However, this relation is valid only for cloud thickness less than 700m beyond which the relation saturates and there is little change in the cloud albedo

**The infrared channel** measures thermal radiation emitted by cloud (assumed to be a perfect emitter) and this is related to the temperature of the emitting cloud by the Planck's radiation law. On this approach the height of the cloud is inferred from the temperature of the cloud top that is obtained from satellite infrared observation. Thus, cold cloud is assumed to be deep and rain giving. Therefore, high brightness in the visible channel and low temperature in the infrared channel imply large cloud thickness and high cloud top respectively. These in turn imply greater probability of rain. Therefore, the brightness and or temperature of precipitating cloud are an indirect measure of convective rainfall intensity.

There are different type of methods are found to estimate rainfall from the satellite source. Microwave, CPC, OSTROM and TAMSAT are some of the common methods used by American climate prediction center and reading university in UK. Estimation of rainfall from satellite over Africa is useful in order to augment the rainfall data obtained from relatively sparse raingauge network in the region. Moreover, the real time satellite estimation also solves the delay of information on rainfall that might be caused by ineffective means of communication from out-station to the central body. Some ideas about the Methodology of rainfall estimation are summarize below

#### **(a) Microwave Rainfall Estimation Technique**

Microwave radiation (3 – 300 GHz or 10 – 0.1 cm) may be absorbed, reflected or scattered by water and ice hydrometeors. The strong interaction of the water drops and ice crystals with microwave radiation makes the microwave rainfall estimation technique more direct and physically based than the infrared and visible techniques particularly over ocean surfaces. The technique is based on the fact that microwave radiation at frequencies below 30GHz are absorbed or emitted by liquid raindrops while higher frequencies are scattered by ice crystals and raindrops (Kidder.S.Q.et.al.1997). Microwave radiation from the surface depends on the angle of view, the surface emissivity and the frequency of the radiation being detected. Ocean has a greater reflectivity and thus lower emissivity than land surface. Moreover, the emissivity of ocean surfaces is almost constant while changes in land surface and soil moisture make the emissivity of land surfaces highly variable.

Therefore, microwave rainfall estimation can be carried out over ocean surfaces without problem; however, the estimation is affected over lands surfaces.

### **(b) CPC Rainfall Estimation Technique**

The CPC (Climate Prediction Center) technique is a technique developed for estimating accumulated rainfall using MetoSat satellite data, raingauge data obtained from Global Telecommunication System (GTS), model analysis of wind and relative humidity and Orographic feature (Hallikainen.M.,1984). The technique was developed for drought monitoring purpose by United States Agency for International Development (USAID) Famine Early Warning System (FEWS)

GOES Precipitation Index (GPI) is an algorithm developed to estimate accumulated rainfall for ten-day period from convective cloud using cold cloud tops duration over a region (Herman *et al*, 1997). In the GPI algorithm 3mm of precipitation corresponds for each hour that cloud top temperature are measured to be less than 235K. The raingauge data obtained every six hours from GTS is summed every 24 hours and then every ten-day is compared with the GPI estimated rainfall. A bias adjustment to the GPI estimate is then done empirically using statistical estimation by fitting the GPI estimates to raingauge data. Then this improved GPI algorithm is called CPC (Climate Prediction Center) technique and is used for estimation of convective rainfall. However, the CPC technique still has an overestimate and underestimates biases over some cases (Herman *et al*, 1997). It overestimates rainfall particularly over a region where there is persistence of cirrus cloud (cloud that is cold but not thick enough to precipitate).

The CPC technique is advantageous in that it can estimate precipitation from both cold and warm clouds. In Ethiopia winter rainfall over the south, eastern, and southeaster peripheral areas and the eastern escarpment is mainly from warm cloud. Moreover, during summer warm cloud rainfall occurs over the highlands and eastern escarpment when there is enough moisture and favorable low-level wind flow. Therefore, the CPC technique is also useful for Ethiopia in estimating rainfall from warm cloud. Even Though it is important to calibrate using CPC technique for estimating warm cloud rainfall in the country, the

technique require dense contemporaneous gauge data rather than historical data, therefore for, the number of stations that report raingauge data on ten-day basis are roughly 40 and these may not include all areas of interest and also may not be sufficient in number to do the calibration.

### **(c) ORSTOM Rainfall Estimation Technique**

The ORSTOM technique uses ground surface temperature (Ts) obtained from MetoSat images for estimating rainfall (Hulme. M.,(1992.)). It was developed by the Lannion Centre De Meteorological Spatial (CMS) and tested in West Africa. The approach depends on the relationship between ground surface temperature (Ts) and pluviometer and this is based upon the following two balances (Hulme. M.,(1992.)) (a) Energy balance that links sensible heat flow to evapo-transpiration and water balance that links evaporation to rainfall. (b) The negative linear correlation between the rainfall totals and the mean temperature.

### **(d) TRMM**

Precipitation Measurement (GPM) is an international cooperative program whose objectives are to (a) increase understanding of rainfall processes, and (b) make frequent rainfall measurements on a global basis. The National Aeronautics and Space Administration and the Japanese Aviation Exploration Agency have entered into a cooperative effort for the formulation and development of GPM. This effort represents a continuation of the partnership that developed the highly successful Tropical Rainfall Measuring Mission (TRMM).

The Tropical Rainfall Measuring Mission (TRMM), launched in November 1997, demonstrated both the capability of making rainfall measurements from space, and the value of those measurements to the scientific and meteorological communities. The National Aeronautics and Space Administration (NASA) of the United States and the Japanese Aerospace Exploration Agency (JAXA) are in the process of implementing a successor mission to TRMM called Global Precipitation Measurement. In comparison to TRMM GPM will expand the measurements of rainfall and rainfall processes from the tropical regions to global measurements, increase the frequency with which measurements are made, and provide significant improvements in the measurement parameters. Global

Precipitation Measurement is structured to be an evolution and expansion of the Tropical Rainfall Measuring Mission (TRMM). TRMM is an on-going, joint mission between the United States and Japan that is still taking rainfall measurements after nearly eight years of successful on-orbit operation.

### 2.3.1 TAMSAT Rainfall Estimation System (TRES)

The TAMSAT group in the University of Reading, UK developed the technique from the GOES Precipitation Index (GPI) for estimation of rainfall over Africa, particularly for tropical Africa. Unlike the CPC and ORSTOM or other techniques, TAMSAT technique is entirely pre-calibrated i.e. it is calibrated against historical data rather than contemporaneous gauge data. (Grimes, D.I.F., 1999)

The TAMSAT (**T**ropical **A**pplication of **M**eteorological **S**atellite) rainfall estimation technique uses half-hourly or hourly infrared images from MetoSat satellite. The use of a single infrared sensor made the TAMSAT techniques simpler to automate; otherwise the technique would have been difficult for automatic operational procedures.

The technique has the following assumptions:

- ✚ Convective clouds are the main source of rain;
- ✚ The convective clouds give out rain if and only if they reached a certain threshold height i.e. if they are deep enough;
- ✚ The threshold height, above which the cloud gives out rain and below which it doesn't, corresponds to certain cloud top temperature and thus it is expressed in terms of the cloud top temperature; and
- ✚ The amount of rainfall over a place is directly proportional to the duration of the convective clouds with the top temperature below the threshold temperature. The duration of time is called Cold Cloud Duration (CCD).

Because it is pre-calibrated the TAMSAT technique has lesser accuracy than for example the ORSTOM technique. If the TAMSAT technique were calibrated against contemporaneous gauge data the accuracy would be greater. However, unlike the CPC and ORSTOM techniques in the TAMSAT technique the calibration can be carried out with more historical gauge data because these data are easily available than the real-time data.

In Ethiopia in order to estimate rainfall from cold cloud the use of TAMSAT method is highly recommended. The TAMSAT technique is appropriate because it is entirely pre-calibrated, automated and easy for operational applications. Of many available techniques the TAMSAT, methods developed at the University of Reading in UK for tropical Africa is taken as the major concern of the discussions in this study. Therefore, in the following chapters analysis and discussions are carried out for Ethiopia, a case study over Omo- Gibe hydrological regime using TAMSAT technique.

## 2.4 Previous Research Works

Several studies have been conducted to evaluate satellite based rainfall estimation for different methods mentioned in the above section 2.3. These studies can be classified in terms of two ways.

- I. Depending on the purpose of the studies; for example, some to evaluate just the rainfall over the given area based considering the estimated rainfall value.
- II. To evaluate how the methods themselves works and their accuracy and reliability in estimating the rainfall..

Among those studies globally are the uses of Cold Cloud Duration as Arkin first made a surrogate for rainfall in the 1970's. In 1987, Arkin and Meissner (1987) have showed that rainfall in the tropical Atlantic could be related to the fractional coverage of cold cloud using a threshold temperature of  $-38^{\circ}\text{C}$ . This work led to the development of the TAMSAT group at the University of Reading.

The TAMSAT technique derives a relationship between CCD imagery and historical raingauge data recorded on the ground over 20 years in Africa. The approach takes into account regional differences in rainfall behavior and also seasonal variations. This technique use visible and infrared channels, over Africa are found to be useful in order to augment the rainfall data obtained from relatively sparse raingauge network in the region. The known study carried by this group was in Zambia designed project on Agro-meteorological Information System (AMIS).

The satellite data these methods use is Cold Cloud Duration derived from the Thermal Infrared images (TIR) of the METEOSAT satellite. The generated CCD image from The MetoSat- TIR data was covered most of Zambia and the Vicinity courtiers at 2.5 km satellite resolution. This was an indicator of convective activity and hence the methods are strictly only applicable to convective rainfall.

The methods rely on a calibration between CCD and rainfall on historical data of gauge rainfall and CCD data. Briefly, you use an historical set (we advise 4 years or more) of geographical data samples of gauge rainfall and the values of the satellite data at the pixels containing the gauges to derive statistical relationships

In the study over 15 years raingauge values are related to the CCD values using the following linear relationship:

$$R = a + \text{CCD } b \quad R = 0 \text{ when CCD} = 0$$

Where R is rainfall, CCD is Cold Cloud Duration value and “a” and “b”are constants to be determined by comparison of CCD images with raingauge data.

### **Procedures of the TAMSAT Techniques**

- ✚ Generate CCD images at different temperature thresholds;
- ✚ Determine an optimum threshold temperature for each calibration zones; (Determination of optimum temperature threshold for each calibration zone is done using contingency table)



- ✚ Determine calibration parameters “a” and “b” for each calibration zone; and then
- ✚ Using the CCD / rainfall relationship formula estimate rainfall

The assumption made here is that the raw TIR data are being acquired in real-time using autosat software and the CCD images are being produced using the TAMSAT rainfall estimation System (TRES). To determine the calibration parameters (a and b) and thereby to estimate the rainfall RFE image and value were described into two different Statistical approaches.

#### I. Regression of median gauge against mid-class CCD:

- In this approach days are classified according to CCD value. Regression of median gauge in each class against mid-class CCD is used for the calibration. The approach of using median as a representative rainfall value is to eliminate the influence of outliers on the calibration. Here only non-zero CCD values are used in calculating the calibration parameters “a” and “b”. The approach was useful for drought monitoring purposes.

#### III. Regression of ten- daily (decadal) mean gauge values against decadal mean MetoSat TIR-(CCD) for pixel or for predefined similar climatic zone

- The approach assumes that gauge pixels are representative of the rainfall and CCD relationship for the basin area. This approach was also useful for hydrological purposes.

Of the above approaches, the second one i.e. regression of decadal rainfall against decadal CCD is used in the investigation of this study. The approach is useful for drought monitoring as well as basin water resource assessment purpose, which is relevant to Ethiopia.

One of the main problems identified from the above study is that satellite-based rainfall estimates is no allowance made for the accuracy or otherwise of the raingauge data as

estimators of pixel rainfall. There is an implicit assumption that if we average over sufficient gauges, the discrepancy between the mean gauge value and the true area average will become small. In such a case the study suggested to replace the 'sufficient gauges' Geostatistical techniques such as Kriging is appropriate.

In General, The method puts a quantitative value on the influence each raingauge has on the estimate for each pixel. The influence is determined by distance and also other factors such as orography. In this ways, the method derives the associated error for each pixel estimate.

Another regional study is also carried out for estimating rainfall at ten - daily rainfall totals from MetoSat infrared imagery from the April – June, 1996, which is - long rains- of Kenya's, in an area covering the eastern highlands and the Taba and Athibe river basin. The study also took TAMSAT method because of the advantage it has on pre-calibrated and assigned threshold temperature  $-40^{\circ}\text{C}$  for the zone. The method gave best rainfall estimate by identifying periods with well below or well above average rainfall even in the over the highlands area and was useful for providing food security and early warning system.

In Ethiopia, accordingly, the National Meteorological Agency (NMA) has been utilizing METOSAT since 1991 for estimating ten-daily total rainfall by applying TAMSAT methodology. Apart from striving to increase the number of stations, NMSA has also been trying to use rainfall estimation techniques using satellite data since 1991. Estimates are being validated using data collected from raingauge network. Results found are in good agreement with the observed data. However, the network density of conventional stations does not adequately reflect the various climatic zones of the country. In fact, the raingauge network does not represent some parts of the country.

Tufa Dinku(1994),NMA staff, has been studied making comparism of the gauge data with the estimated rainfall for march to October in 1995 for all country. In his study, the TAMSAT was the method applied based on five years decadal average for the western and north eastern part of the country. As in Figure 5 below, the result of the study shows that the

accuracy for western part of the country is relatively better while the northern part is not good. For the western part the standard deviation (Sd) is less than the estimates. While in the northern part its close to the estimates.

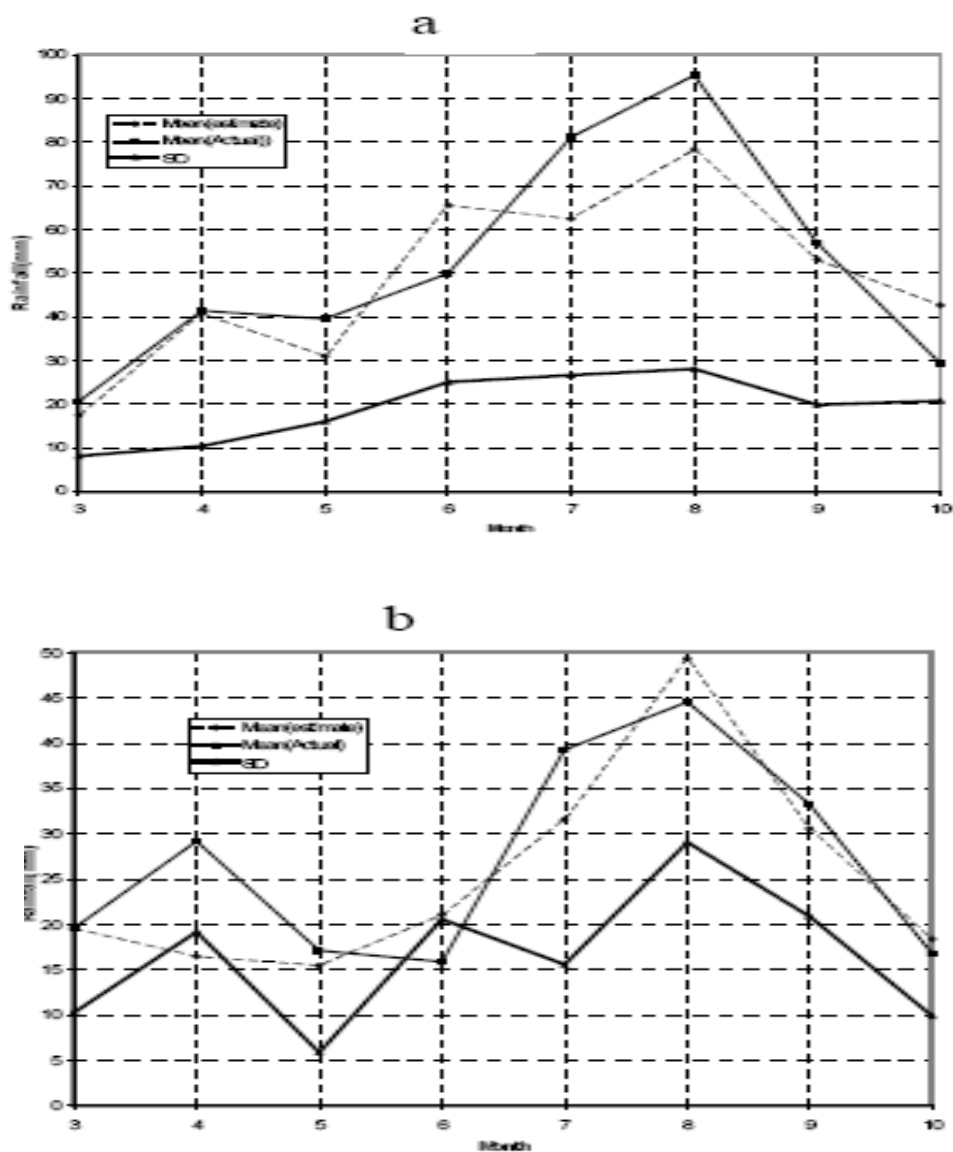


Figure 2.5 Comparison of actual and estimated 5-year average rainfall for (a) Western and (b) Northern part of Ethiopia from March to October. (Tufa dinku, 1994)

Gissila, T.et.al,(2004),made study for the spatial variability in rainfall by grouping the raingauge station into four geographical cluster zones based on the seasonality and cross-correlation rainfall analysis for all Ethiopia. This study also followed the TAMSAT method and argued the satellite estimates were representative for the cluster zones defined both spatially and temporally manner. The study suggested that the estimate of rainfall using the linear regression method may provide the base of an operational seasonal forecasting system for Ethiopia.

Among the works, that addresses the concern of this study, Omo-Gibe River Basin Integrated Development Master plan (December 1996, FDRE, Ministry of water resources) is also a very good document cited that indicate indicating the rainfall characteristics in relation to the basin physical and socio-economical features. This document was the leading materials that provide both the geographical and the rainfall information about the basin.

The use of MSG satellite data certainly could expand the spatial and temporal coverage of rainfall estimation and improve the consistence with the nature and development precipitating systems. However such rainfall measurements systems are generally characterized by uneven distribution, very limited spatial coverage and non uniformity (rain gauges give point and time-cumulated measurements), satellites measurements are spatially limited. It is therefore the comparism of estimated rainfall with the gauge is crucial. The GIS environment application seems to be an optimal and flexible way to perform data comparison and merging, enabling precise geolocations and the management of different data layers such as cloud-coverage, orographic, forecasted fields, etc.

In general, published researches and scientific exercises within the study area could not be found posing a lack in detail and sub-detail information. In those studies have shown some good result, but there is still some work to be done around this Scientific and applied approaches.

## CHAPTER THREE

### 3. General Description of the Study Area

#### 3.2 Overview

Ethiopia has 12 river basins within an area of  $1.129 \times 10^6 \text{ km}^2$  with annual flow of  $122 \text{ Bm}^3$  of water. Eight of these are river basin, one lake and three dry basins four of the river basins, Abbay, Baro-Akobo, Merebe and Tekeze are part of Nile River system, flowing generally in the western direction towards Sudan. Five basins namely, the Omo-Gibe, Awash, Rift Valley lakes, Denakil and Aysha can be categorized the rift valley system as all of them drain their water along in the grate east African Rift valley system. The remaining three, Geneale-Dawa, Wabishebale and Ogaden are part of the eastern part of Ethiopia that generally flows in the southeastern direction towards the Somali and then to Indian Ocean.

A review master plan studies related river basin surveys shows that the aggregate annual runoff from the nine river basins amounts to  $122 \text{ Bm}^3$  excluding ground water. The three largest river basins (Abay, Baro-Akobo, and Omo-Gibe) contribute 76 percent of the total runoff from catchments area, comprising only 32 percent of the total area of the country. (MoWR),1996)

*“A river catchments (also often: watershed or river basin) is an area that topographically appears to contribute all the water that passes through a given cross section of a stream. A river basin is the portion of land drained by a river and its tributaries. It encompasses the entire land surface dissected and drained by many streams and creeks that flow downhill into one another, and eventually into one river” (A.Gebeyehu, 1989)*

Almost 80 percent of the annual rainfall is observed during March to September. Spatial distribution is very irregular, even during years with good quality rainy season. Even though the basin has abundant water resources all of which generated locally, these resources have never adequately contributed to the economic and social goals of the country's well as the local residents and community. Residing in the dominantly dry lowland are

influenced by recurrent vagarious of climate extremes such as drought and flood making it prone to natural disasters, which in most cases have devastating effect on food security, water resources and other socioeconomic needs.

### 3.2 Location

The study area, Omo -Gibe river basin, is geographically bounded between Latitude 4° 30' North to 9° 30' and longitude 35° 00' to 38° 00' East in the south west of Ethiopian river basin system with an areal extent of almost 79 000 km<sup>2</sup>. the location map of the study area is indicated in Figure.3.1

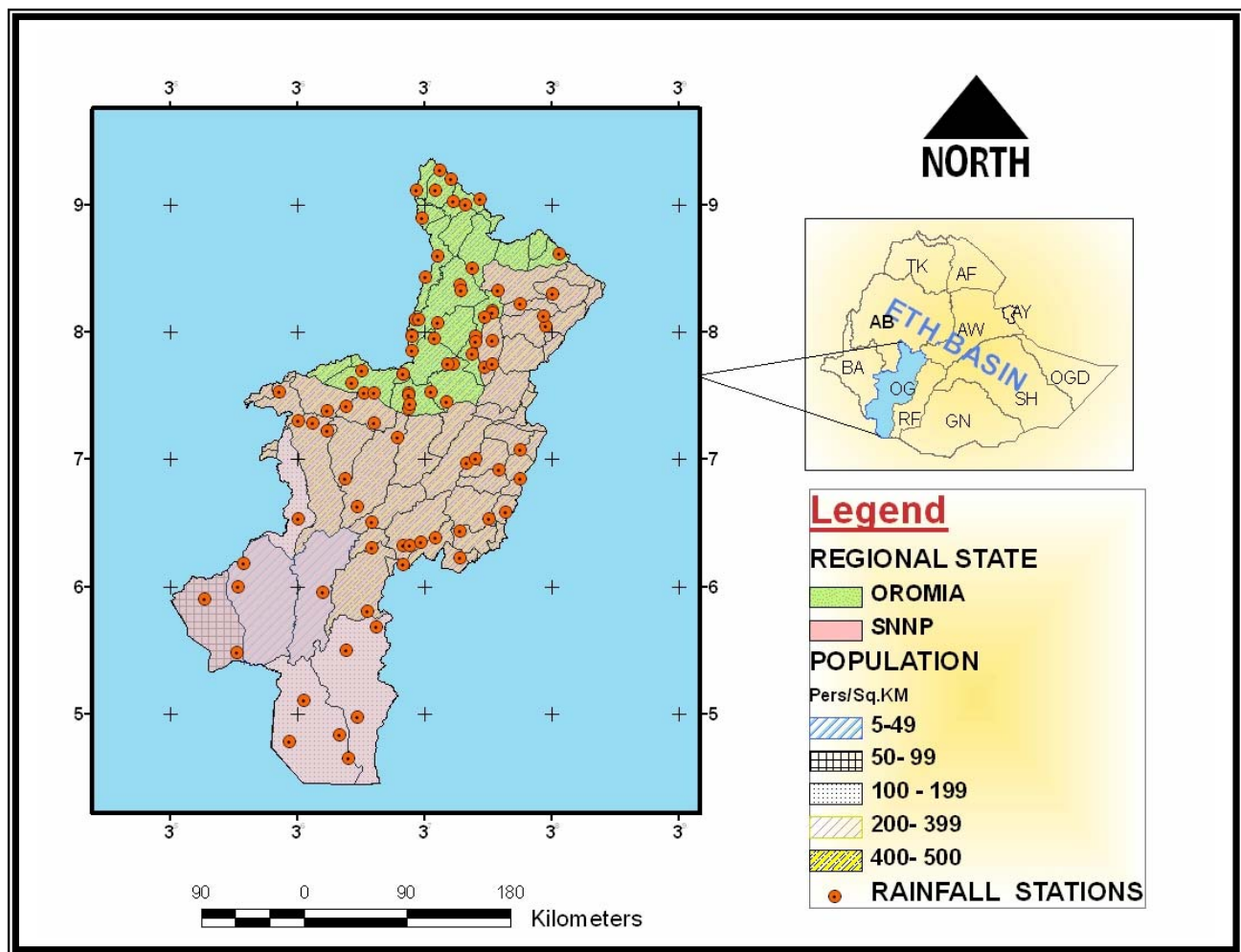


Figure .3.1 OMO-GIBE BASIN (Location of the Study Area)

The basin encompasses parts of the Oromiya National Regional State at the north eastern part of the basin, and the southern nations and nationalities people’s regional state (SNNP)

### 3.3 Topography and Drainage

As cited in the master plan study of the basin topography is a key characteristic of the basin that divides into highlands in the northern half of the area and low land in the southern half.

Because of this, the basin is divided into various altitudinal zones as indicated below:-

- I. Mountainous region:
  - A. above 2500 m                    10002 km<sup>2</sup> (East to West of basin)
  - B. between 1500-2500 m        33015 km<sup>2</sup> (North to South of basin)
- II. Flat region: below 1500m        34796 km<sup>2</sup> (Between Highlands and Lowlands)
- III. Arid region                                -----

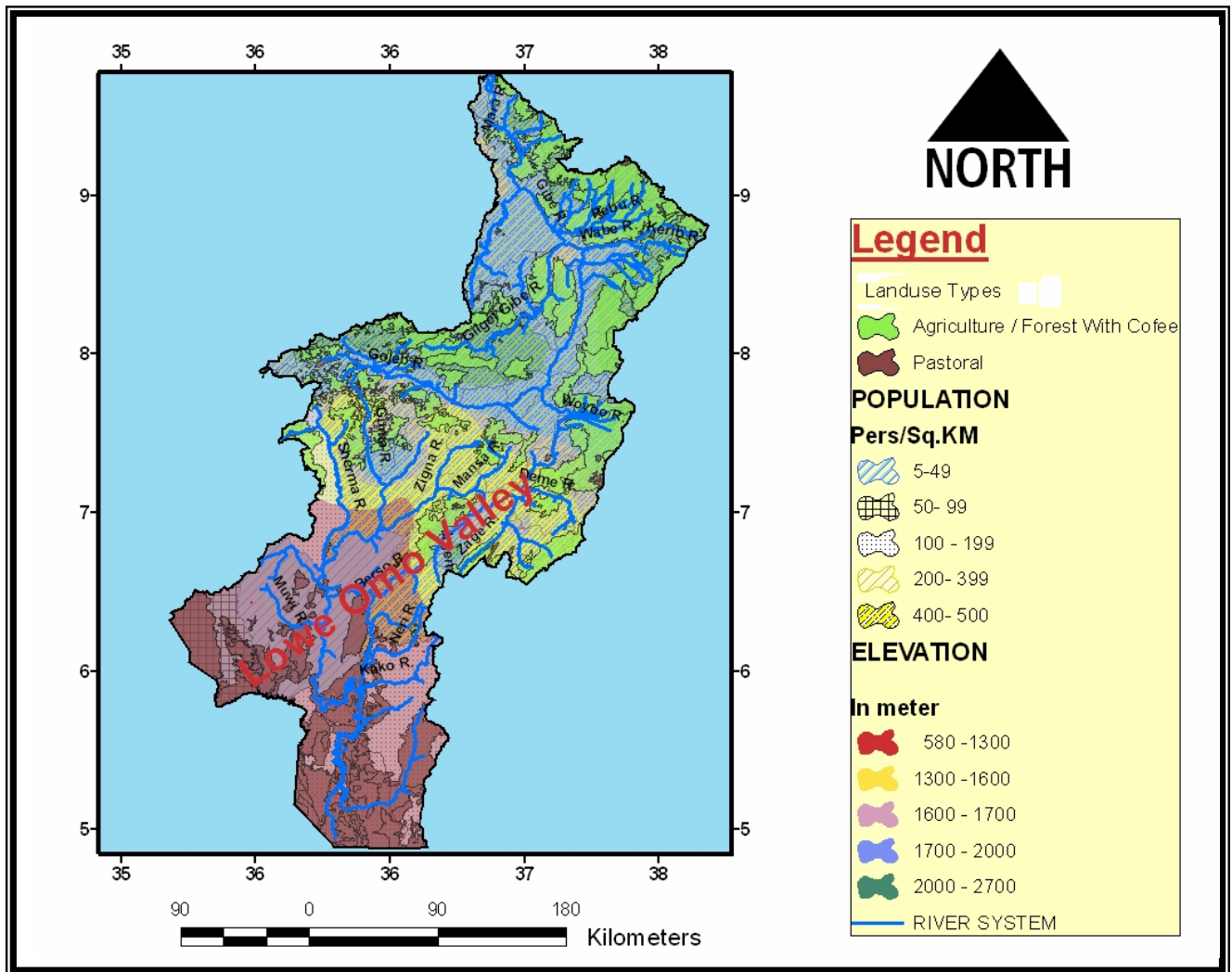


Figure 3.2 Physiographic and Land use System of Omo-gibe Basin

As the map above shown as the highlands are characterized by step slops with volcanic origin of soils, relatively fertile, and favored by humid and sub humid type of climate with sufficient rainfall for seasons of cropping. The western highlands are known as one of the remaining large forest area in Ethiopia. The lowland parts of the area are also characterized by relatively gentle slop and high and low temperature and rainfall respectively. As a whole, almost 38 percent of the lowlands have slops of less than 2 percent, and 2 to 10 percent of slop falls in the flat and the highlands regions respectively.

Another feature of the basin is the remoteness and inaccessibility. Especially, to the extreme south to border of Kenya and the Lake Turkana, the area is largely isolated from the development. Any of the rivers within the basin rises at altitude over 2000m to Lake Turkana at altitude of 420m.

The main drainage system is defined by three principal rivers, which rise from the plateau in the northern part of the basin, and flows to the south, a distance of 608 kms. These are:

- ✚ The great river Gibe running from the north the upper part of the basin south to Soddo, and from the eastern watershed to the Gibe river.
- ✚ Rise from the highland area along Bonga to Gilgel Gibe and to the south of Gojeb river gorge.
- ✚ And to the south of Gojeb are the catchments of many rivers drain from the region of high rainfall that flow through out the year (North West end and eastern side to the Omo river system, and the lower part.

In terms of surface water resource potential, the basin is the seconded largest contained a mean annual flow of 17.6 Bm<sup>3</sup> of water. (See summery table 3.1).The water resource of the basin is higher and still under utilized. More over, except the awash and Omo-gibe river basin, all of the river basins are Transboundary in nature with more than 75 percent of which water flow to neighboring countries.



### 3.4 Climatic Features

Climatologically, rainfall is the major element that shows the spatial and temporal variability. The water volume of the basin mentioned above is produced from rainfall governed by the seasonal migration of ITCZ and the associated atmospheric circulation. The topographical variation also plays a vital role in determining the spatial extent of both rainfall and temperature in amount and distributions. The climate of the basin ranges from semi-arid in the lowest Omo-valley to humid in the north and northeasterly highlands on bases of elevation above mean sea level of the areas. Climatic variations are a function largely of land surface altitude. Rainfall within the basin has strong seasonal and elevational variability. The primary wet season extends from April to October, July and September is the wettest months particularly in the upper north part of the basin. Isohyetal maps and rainfall patterns for the basin were prepared based on annual mean rainfall data collected and processed from 90 meteorological gauge stations for ten years in the period of 1997-2006. Figure 3.3 shows the mean annual Isohyetal map of the basin.

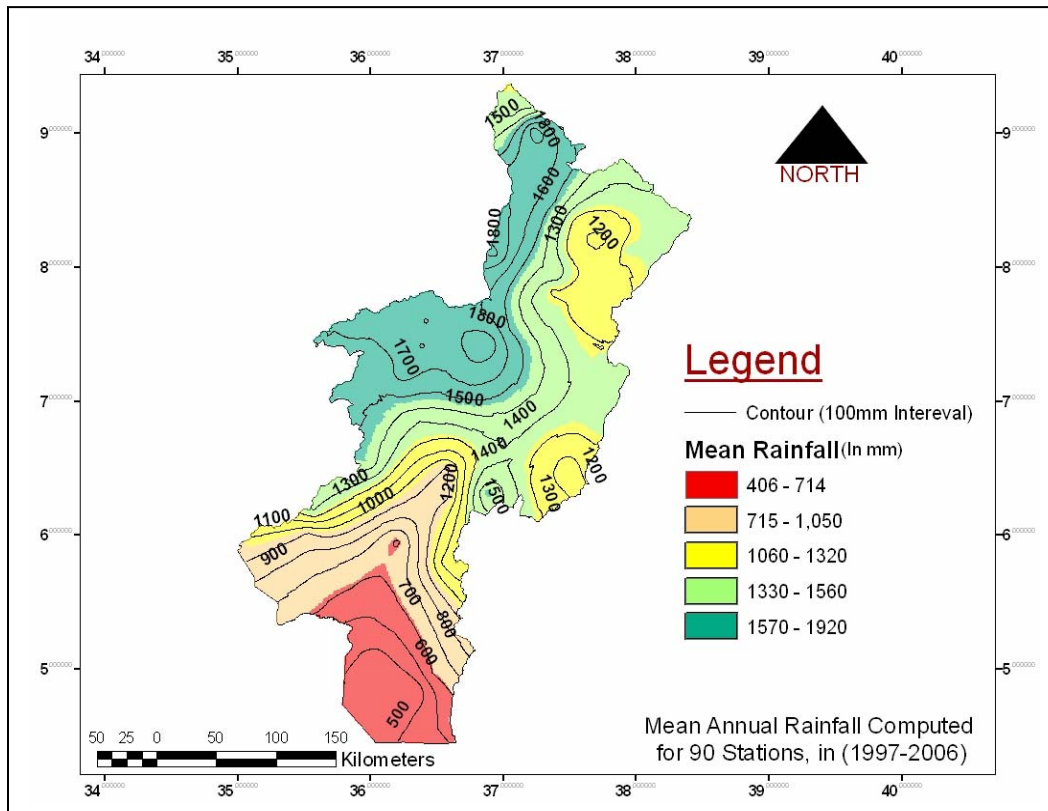


Figure 3.3 Long Year Mean Annual Rainfall of Omo-Gibe Basin

The Climatologically mean annual rainfall distribution of the basin shows a considerable spatial variation due to the complicated nature of the terrain (Refer the relief map of the basin). Over the highland area the mean annual rainfall between successive contour lines is 1749 mm and over the lowland regions it reaches as low as 600 mm. The amount and distribution of the rainfall decrease from north and east to the south of the Omo river valley floor.

The annual mean rainfall for some selected areas located in the north and western highlands in the basin are, with over 1800mm near Baco, Abelti, Maji,Algae, Shishinda, Whish Wish, Tibe,Assendabo, Dedo and Dimtu. In the North eastern highlands the rainfall is below the long year average but some places like Areka, sawla, Jinka and bulki have more than 1500mm.The central lowlands Chida, Hamer, SilaMago and the southern extreme lowland areas Bume,Ginimonere and Fejel have rainfall 1370mm and below 600mm respectively.

The mean annual temperature in the basin varies from less than 17.5°C in the highland to the west, to over 29. °c to the south with respect of the altitudinal variations. The major factor affecting the average daily sunshine hours on the basin is the cloud cover. The Average monthly minimum temperature during dray (winter) season ranges from 10 °c at the north and northeastern highlands to 14.2 °Cat the central and southern lowlands. The, Average monthly maximum temperature during the rainy (summer) months ranges from about 22 °C in the highland and more than 30 °C near and at the valley of Omo-river. For most of the year, maximum temperature is occurring around April and a minimum in July and August.

### **3.5 Socio-economic and Population Profile**

The administrative structure of the basin is divided by regional states, zonal and Wereda level. Most of zones of SNNP's are found within the basin with poor range of service and infrastructure development. As shown by field observations, the social service (health, school, market, tourism, energy, etc) are a product of under development of infrastructures (transport service) and lack of local administrative centers.

In general, all the agricultural production of the basin is rainfed, occupying over 3.1 million hectare of land from the total 38.9 percent of cultivable land. The majority of the highland area is covered by forest, with an estimated 9000, 000 hectare. Most of the remainder central lowlands and the Omo valley, generally on alluvial soils with low topographic relief, are occupied by a mix of grassland, bush lands and shrub lands.

The basin also contains major resource for irrigation (100km<sup>2</sup>).livestock (all types 16.7 million), fishing (69 fish species of which 21 considered commercially important), and tourism in the Omo and Mago National parks is the dominant activity in the lower omo sub-basin. The local heritages also have historic attractions as well as importance for the study of earlier hominids.

Except the lower Omo where the dominant mode of agriculture is pastoralist, mixing farming in the highlands and dominantly live stock production in the lowlands is common feature in the basin the general trend of the settlement is very dense in the high lands and sparse in lowland.

According to the report (2002) of Central Statistical authority, the population of the basin is estimated over 7 million. This population is not uniformly distributed. The lower basin represent approximately 51 percent of the basin area but only 5 percent of population. The vast majority of people live in the highlands where North Omo and Jimma zone are the most populated, with 26.7 percent and 23 percent of the basin population respectively. The least population zones in the basin are southern Omo and Maji with 4.1 percent and 1.3 percent respectively.

The ethnic groups living in the basin belongs to all four language families found in Ethiopia and includes most of languages in Omotic families. Agro-pastoralist live primarily in the lower basin whose ways of life is a combination of agriculture and livestock herding while the hunter- gatherers are small groups living in tower omo-valley towards the Kenya boarder. Summary of Socio economic, population, topographic and climatic characteristics and water resource potential of the study area is displayed in Table 3.1.

Table 3.1 Summary of Basin Description

| Characteristics                          | Descriptions         |  |
|--|----------------------|--|
| Topography                               | Source               | Northern ,Central and western highlands  |
|  | Flow Of Direction    | South to lake Turkana  |
|  | Highest Point        | Mount Gauge 3400 masl  |
|  | Lowest Point         | Lake Turkana 420 masl  |
| Climate                                  | Temperature (0c)     |  |
|  | Max.                 | 17.5   |
|  | Min                  | 29.0   |
|  | Rainfall(mm)         |  |
|  | Max                  | 1590   |
|  | Min                  | 500  |
|  | Average              | 1260   |
| Evaporation(mm)                          | 1600                 |  |
| Water resource Potential in Bm3          | Surface              | 16.6   |
|  | ground               | 1.90   |
|  | Annual volume        | 17.96  |
| Socio-economic, and Population (In'000') | Cultivable land      | 3.1 million hectares   |
|  | Irrigable area       | 13,000 hectares  |
|  | Land use             | About 63 percent of the land is covered by forest and farm land.Over 1.5 million hectare (i.e. 20 percent of the basin) is covered by grass land |
|  | Farming system       | Small-scale peasant agriculture, Private/Commercial agriculture, Missionary-sponsored development, and agro –pastoralist.                        |
|  | Population (In'000') |  |
|  | In 2002(.CSA)        | 11300  |
|  | Growth Rate (%)      | 2.9  |
|  | Density(p/km2)       | 81.5   |

(Source: derived from the respective master Plan studies and EGS report.)

# CHAPTER FOUR

## 4. Materials and Methods

### 4.1 Data Type and Source

#### (a) Data Types

In conducting this study some primary data sources from field observation and with the basic gauging and satellite rainfall data, much of secondary data resources including published and unpublished materials, books, journals, articles, reports, and electronic web sites, which are written on the subject matter of this study, were collected. Photographing, mapping, and tap recording are incorporated as supplement techniques to rich the finding.

Decadal (ten-daily) rainfall data from Gauge stations and RFE image derived from MetoSat thermal infrared imagery (TIR) CCD data at decadal basis are the basic secondary datasets used through out the study.

**Rain Gauges Station Data** – is a ground data. This dataset consists of decadal total rainfall from 90 stations over the Omo-Gibe basin. The data set ranges between 2000-2006. Of this data, only Selected years: - 2000(dry), 2003 (Normal), 2006 (wet) are taken for the purpose of comparing decadal, monthly and annual climatology of gauge with that of RFE obtained from the satellite data. The selections of the years are based on the past synoptic features of the observed rainfall-analogue trained. (NMA, 2006)

**Satellite Data**– Archived imageries of the CCD Data derived from MetoSat Thermal Infra red (TIR) at 2.5 km resolution and at  $-40^{\circ}\text{C}$  temperature threshold value for over all Ethiopia. These images are processed and converted into RFE using with GIS scripts (WinDisp, IDRIS and ILWIS software). Thus, for each selected year, 36 decadal RFE imageries and a total of 108 imageries for the three selected years were used. This later adjusted for the analysis based on geographical bounded location of the Omo-gibe basin.

A decade is defined as roughly one third of a month. These are:

Dekad-1: The first 1-10 days in the month.

Dekad-2: 11-20 days

Dekad-3: 21-days to end of the Months.

For this paper the decadal rainfall data of both gauging and satellite were combined into monthly, seasonal and yearly totals.

**Geographic Dataset-** were collected and stored in the digital database of GIS environment, in which used to prepare the description of the study area and relevant geo-processing works. Topographic map of the study area at 1:250,000 scales is scanned and digitized for major features like boundary, physiographic and Landuse status of study area. Downloading of GPS collected data for some stations are also integrated with the existing stations used in the Analysis.

**Field Observations:** - The field trip was arranged and carried out for 16 days from 17 May 2007. The first trip was from Addis to Bonga, Mizane-teferi and Maji and the second the trip from Bonga, Soddo to Jinka.

*The major return attained from the field includes:-*

- ✚ Observation and identification of Meteorological stations with associated basin characteristics. GPS data are also taken for some meteorological stations and reference points visited in the field.
- ✚ Observation and description of the basin that have demarcated influenced with good and poor rainfall distributions, including the Identification of the watershed system and its association with topographical and rainfall (Distribution and amount)
- ✚ The field investigation tasks were constituted an important understanding to the researcher in the way how rainfall is associated with the nature of basin characteristics (over all basin physical characteristics, social and economic practices)

## (b) Data Sources

For the first and second dataset, decadal rainfall of gauging stations and satellite data were obtained both from archived NMA Remote sensing unit and TAMSAT group at the University of Reading, UK; website database.

The base Maps, digital attribute and spatial data of the study area are available in NMA, Ministry of Water Resources, Ethiopian Mapping Agency, Agriculture and Rural development bureaus, Flood Early Warning offices and Aid agencies which are closest resource to the study Data from field observations, including official documents and reports, and relevant Internet Websites were the source of information.

## 4.2 Methodology

For the purpose of discussing the rainfall estimation processes, verification and analysis appropriate softwares and large database was assigned to accommodate the serious of CCD and RFE images and gauge data at EXCEL format. The Methods considered in interpolating and extraction of rainfall values from the satellite images, and comparing with the gauge observation include the following:

- I. Delineation of climatologically zones having the similar rainfall characteristics (HRR). Thus, dividing the Omo-Gibe basin into zones of homogeneous rainfall characteristics is the first step done in the data processing activities.
- II. TAMSAT methodology of rainfall estimation technique is selected and used to explain the process of rainfall estimation and further for comparing and characterization with the raingauge data of the same period and regions. TAMSAT is developed by the reading university in UK, for tropical Africa (Milford and Dugdall, 1989) is employed based upon the basic assumptions that in tropics most of the rains comes of the convective clouds and also assumes simple linear relationship between the “CCD” and “Rainfall(RF)” which is given as:

$$RR = a * CCD + b \quad , \text{ if } CCD > 0, \text{ Then } RR=0$$

Where 'a' and 'b' are constants determined by regression comparison of CCD values in hour with top temperature below defined threshold temperature (THT) to that of the rainfall from raingauge data. The RFE image for a decade is prepared using automatic rainfall estimation module of ILWIS application to cover the same study area at the same resolution of CCD data that have produced from MetoSat -TIR image. At last, Extraction of RFE values have been carried out for each pixel and delineated HRR at average decadal base using WinDisp Software V.4.0/5.1. For all image analysis of executed by WinDisp, the results of the extraction is stored in ASCII format further processed by Excel format for a given decadal basis.

The method TAMSAT is used to select because the technique is entirely pre-calibrated with historic of rainfall data that divides Africa into a number of zones at -40-0C threshold temperature. The method has the advantage of operational simplicity and is in wide use in many parts.

III. Quantitative analysis and mapping the rainfall using Geostatistical kriging approach are the basic methods applied for verifying and characterizing the estimations .some of statistical formulas used were presented below.

a) Descriptive statistics:- is the method used to produce general and simple description of the RFE and Gauge values in terms of Ratio, percentage, computation of Arithmetic Means (AM), standard deviation (Sd), and coefficient of Variation (Cv).

a.1. 
$$AM = \frac{\sum X_i}{N}$$
 Where,  $X_i$  =RFE and Gauge Value

- *With the respective estimated and actual gauge data of rainfall mean values of decadal, monthly and seasonal were characterized and compared in the selected years for HRR within the Basin. The results from the above operation is illustrated by graphs, table and mapping.*



a.2 
$$Sd = \sqrt{\frac{\sum (X_i - \bar{X})^2}{N}}$$
 - The standard deviation is here for measuring the dispersion of the existing rainfall values around the mean.

a.3 
$$Cv = \frac{Sd}{\bar{X}}$$
 - Is computed as a percentage of the mean to indicate the variability having between RFE and gauge measurements.

## b) Validation methods (Correlation and Bias)

- Correlation

b.1 
$$r = \frac{Sd_{xy}}{Sd_x * Sd_y}$$
 Where, Sd = Standard Deviation  
r = Correlation  
x,y = RFE and Gauge Value

- The correlation evaluation were used to measure the degree of closeness of the relationship between for RFE and Gauge values for the respective HRR

- Bias

b.2 
$$BIAS = \frac{1}{N} \left[ \sum_{i=1}^n (x_i - y_i) \right]$$
 - The positive bias indicated that the RFE value exceeds the observed value on the average, while the negative bias corresponds to under estimating the observed value on the average

The bias indicates the average direction of the deviation from the observed rainfall dataset. But it can not reflect the magnitude of the error. The Mean absolute error is indicated the error

- Coefficients of Quartile Deviation

b.3 
$$Coff.Q = \frac{Q_3 - Q_1}{Q_3 + Q_1}$$
 Where, Q = Estimated and Gauge rainfall Value

The result of quartile value explain, the smaller the value of coefficient of quartile is the larger the uniformity between the observed gauge and estimated rainfall.

**c) Geostatistical Kriging methods and mapping** were applied and characterized how Satellite based rainfall measurements are related with ground gauging depending on their relative locations.

**d) Software**

There are various images processing software developed, which assist for rainfall extraction from remotely sensed imageries. Among such software, ILWIS v.3.3 and WinDisp c 4.0/V.5.1, and ArcGIS9.1 spatial and Geostatistical tools were used for data processing, anglicizing and interpretation purpose

#### **4.2.1 Schematic Flow-Chart**

According to the steps put on the flow chart below in figure 4.1, the first step is to decide and display the type of data that need to use in the analysis. Therefore, the input data in this study is Gauge Rainfall from existing meteorological stations and satellite TIR image which put on view with a raster dataset. In the second step, the new information RFE and GIS data are derived from the input datasets. Based on the analytical and automated software processing system, the values of rainfall at HRR region for the periods the have been calculated and presented as layers.

Thirdly, the input datasets are further analyzed using statistical and spatial interpretation methods according to the values of attributes within each dataset that have describe the accuracy and difference of estimation. The final results have been presented specifying the scientifically examined application of the satellite-based rainfall estimation technique and the observed characteristics of the value of datasets. This is found to be a very good supplement for the need of rainfall information with the required spatial extent within the basin.

**(c) Schematic Flow-Chart of Assessment Methodology**

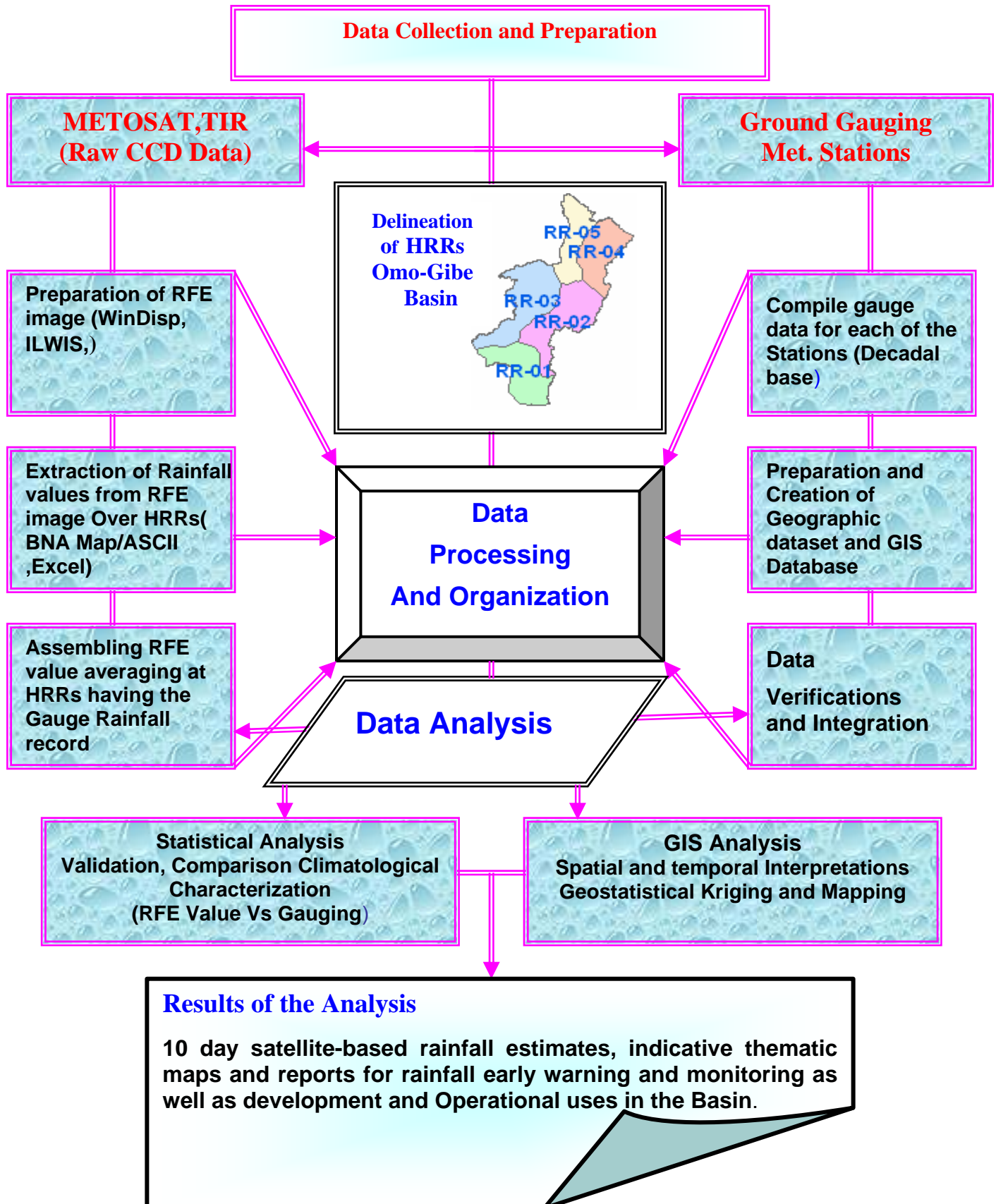


**Figure 4.1 Schematic Flow Chart: Steps in the Analysis and the General Study**

# CHAPTER FIVE

## 5. Data Processing and Analysis

### 5.2 Data Processing

#### 5.2.1 Input Dataset Format

In order to identify the basic objectives of the analysis and to create a database that help to solve the problem of the study, the data processing activities is drawn in two type of procedure. These are:

- I. Identifying and arranging the layers and the attributes required for each feature dataset. Processing of the data on each of the dataset has done based on that the layers are required further during the rainfall analysis. This involved in digitizing of study area boundary, delineation of HRR, and associated physiographic features
- II. And conversion of the MetoSat TIR – CCD images into (RFE) using ILWIS based on decadal format, setting the value extraction processes and analyzing steps and finally exported the result to ArcGIS environment with appropriate format and coordinate system.

Table 5.1 Data format Generated from Different Sources for the Analysis

| N | Type of Dataset | Format | Descriptions of feature                                     |
|---|-----------------|--------|---|
| 1 | Point           | vector | Dekadal Rainfall Value of meteorological gauging stations   |
| 2 | Line            | vector | Contour lines, Drainage system                              |
| 3 | Polygon         | vector | Study area and Wereda boundary, HRR, Relief and land cover  |
| 4 | Polygon         | raster | RFE image exported from WinDisp to ArcGIS- supported format |

### 5.1.2 Extent of Data Records

The extent of available stations data collected in the Omo Gibe basin was 122 in numbers. However, over 32 gauge station, the records of the available data required in the analysis are not found adequate and disused. Therefore, only 90 meteorological gauge stations is selected and used in the processing procedure. These stations have almost 95 percent sufficient rainfall records for the year 2000/ 2003/2006, and were very useful considerably for processing and interpretation purposes. The list of the data stations is given in Annex-A. The station distribution network in the northern and western highlands area of the basin is densely situated than the eastern and central areas.

In The southern and southeastern part of the basin, the gauge station distributions have not been found evenly distributed. However, according to WMO (1994) conventional requirement of station distribution standards, the resolution requirements for point measurement (gauging station) based on elevation categories are given as follow

- I. In mountainous area above 2000 meters the maximum resolution required is less than 20 km<sup>2</sup>.
- II In area 1500-2000 meter, is required a resolution of 20 - 40 km<sup>2</sup>
- III. In the area below 1500 meter, above 40 km<sup>2</sup> resolution is required according to expansions of the area.

It is also cited that the use of satellite- based techniques to measure areal rainfall in the tropical Africa recommended when the raingauge spacing resolution is less than about 40 km.( (WMO, 1988a)).It is therefore, in the study area of omo-gibe basin, the spacing of the selected gauging station considered for the analysis are fulfilled 85 percent of the requirements.

### 5.1.3 Homogeneous Rainfall Regions (HRR)

#### 5.1.3.1 Selection and Delineation

Rainfall distribution is characterized by great spatial variations. There are different climatologically regions having different characteristics within the basin. Thus, before the construction of HRRs, two independent criteria were used to divide the rainfall stations into zones.

- I. The rainfall stations were first divided into the rainfall seasonality and spatial coherence by using 1974-2004 climatologically mean rainfall data.(See Annex-B)
- II. Topographical correlation using elevation Data also carried out in the selection of similarly characterized stations.

Finally those stations having similar mean rainfall value correlated with elevation are clustered and form the HRRs for extraction of quantitative values RFE. Table 5.2 indicate the statistical summery for the classified Regions with the long year mean and elevation data.

Table 5.2 Statistical Summery for Classified HRRs

| HRR | No. of Stations Used | Area (km <sup>2</sup> ) | Elevation (masl) | Mean RF 1974-2004 | Std.Deviation |
|-----|----------------------|-------------------------|------------------|-------------------|---------------|
| 1   | 7                    | 13612.5                 | 500-900          | 823.8             | 123.4         |
| 2   | 18                   | 22161.5                 | 900-2300         | 1458.2            | 273.2         |
| 3   | 19                   | 22421.1                 | 1000-2200        | 1583.2            | 199.8         |
|     | 16                   | 12676.2                 | 1200-2000        | 1324.7            | 219.7         |
| 5   | 31                   | 8384.2                  | 1500-2500        | 1682.4.           | 355.6         |

The mean annual rainfall of the basin is 1297.5 mm with the standard deviation of 332.95.The deviations of the classified region from the mean is also very small. More over, as table 5.3 shows, the mean correlation coefficients for stations both within each

regions and with stations with every proposed regions. The cross correlation between all the stations for the maximum rainfall peak months of March, April, July and August was calculated.

Table-5.3 Mean cross-correlation between stations within and with stations in the other region.

| <b>Correlation Results</b> |              |              |              |              |              |
|----------------------------|--------------|--------------|--------------|--------------|--------------|
| <b>REGIONS</b>             | <b>HRR-5</b> | <b>HRR-4</b> | <b>HRR-3</b> | <b>HRR-2</b> | <b>HRR-1</b> |
| <b>HRR-5</b>               | <b>0.864</b> | <b>0.676</b> | <b>0.424</b> | <b>0.333</b> | <b>0.172</b> |
| <b>HRR-4</b>               | <b>0.676</b> | <b>0.401</b> | <b>0.374</b> | <b>0.422</b> | <b>0.116</b> |
| <b>HRR-3</b>               | <b>0.404</b> | <b>0.354</b> | <b>0.333</b> | <b>0.323</b> | <b>0.254</b> |
| <b>HRR-2</b>               | <b>0.283</b> | <b>0.422</b> | <b>0.323</b> | <b>0.168</b> | <b>0.113</b> |
| <b>HRR-1</b>               | <b>0.172</b> | <b>0.116</b> | <b>0.254</b> | <b>0.111</b> | <b>0.117</b> |

The table is used to confirm that the mountainous area in the north to low relief and escarpment around Gibe and Omo river valley and plateau in central and southern area of the basin have different in their rainfall distributions. The correlation result indicate that, for example, the mean of the cross-correlation between HRR-5 and HRR-2 would be the mean of the cross correlation between every station in HRR-5 and HRR-2.

Although inter station correlation was not particularly high in most regions, the results were found to generally satisfactory considering the purpose and current level. Based on the above criteria, the geographical proximity of the stations was used to divide the stations into five groups. In areas where the correlation produced unsatisfactory is resulted due to the station with extremely short records. Throughout this study these groups are referred as Homogeneous Rainfall Region (HRR) within the basin. The validity of the methodology is also tested by comparing the raingauge data with RFE

data for one of the region. Figure 5.1 indicates the geographical position of the classified HRRS within the study area, Omo-gibe basin.

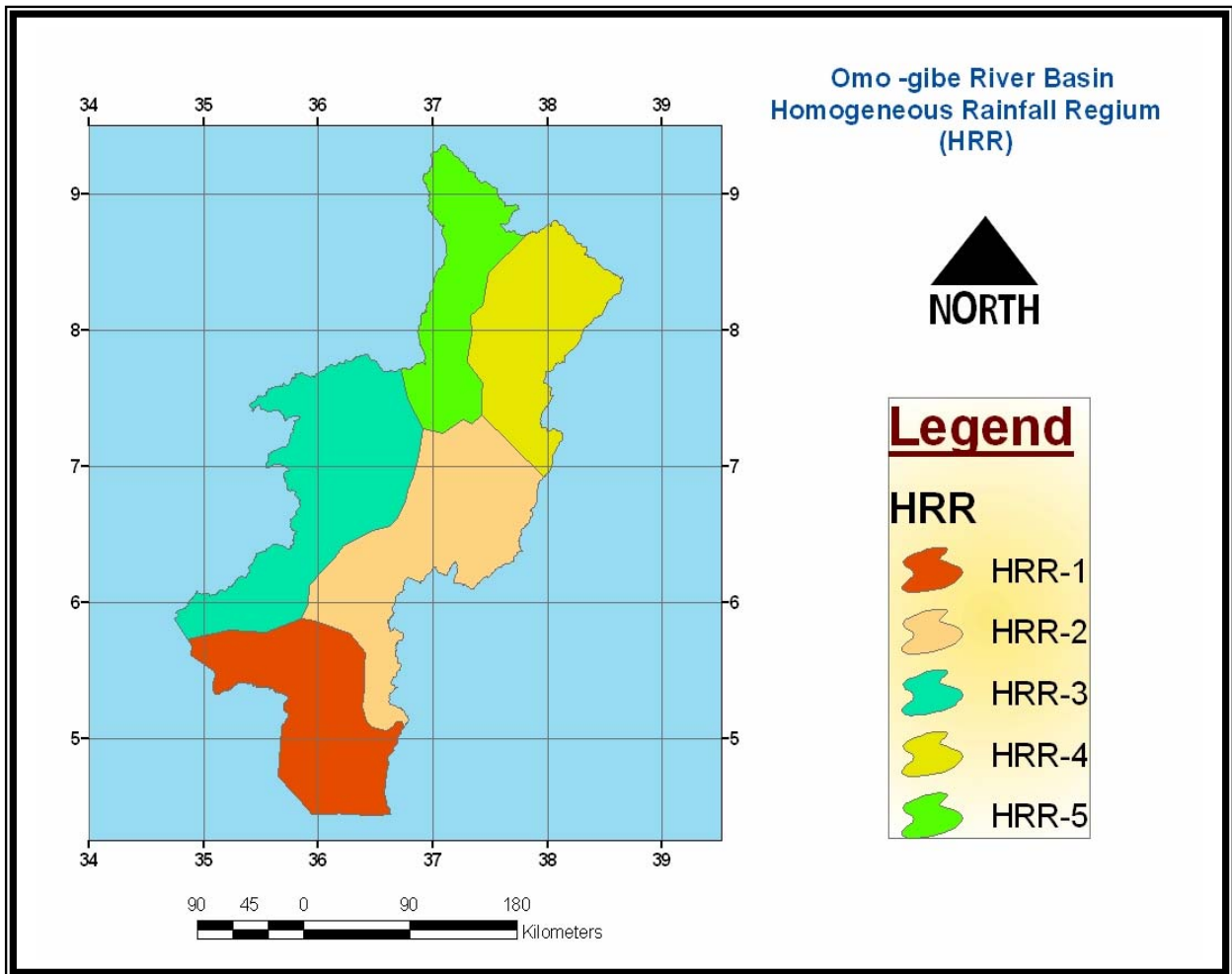


Figure 5.1 Homogeneous Rainfall Regions of OMO-Gibe Basin

For all of the groups except HRR-2 and HRR-1 the internal variability of a rainfall within a given group is reasonably coherent.(See table 5.3). This analysis was used to confirm the similarity of the rainfall over the delineated regions and further would help to assess the qualitative and quantitative RFE values derived from MetoSat-TIR, CCD data. It is therefore, the rainfall values are extracted based on the spatial average of these regions containing the rain gauges observation for the same period.



### 5.1.4 Processing of Gauge Rainfall Data

Since the gauge observation and satellite data are not at the same location, it is often necessary to adjust their representation in the same period and spatial extent for interpretations and comparison.

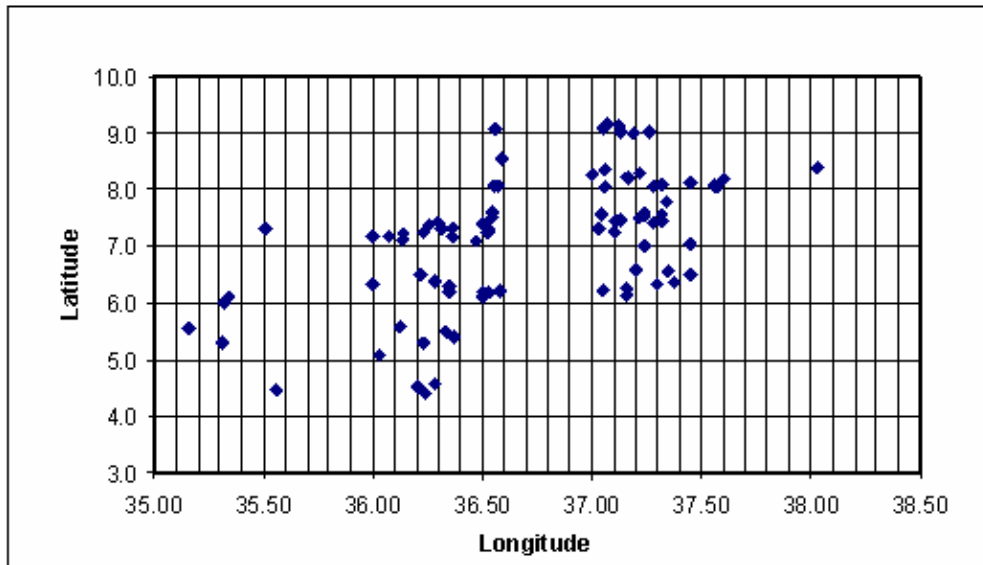


Figure 5.2 Map of Geographic Distribution of Stations

Evaluating the geographic distribution (as in figure 5.2) of stations and the statistical quantities were significant during the gauge data processing task. These patterns are also used as the basis of analysis in the comparison of RFE and gauge records. The gauge dataset consists of decadal total rainfall from 90 stations over the study area. Before proceeding for analysis, the collected data were checked in two ways: qualitatively and by performing diagnostic statistics and graphical computations on the measured gauge records. These are:

- I. Visual analysis of tabular data and Graphs
- II. Inspection of gauged data value with the classification of rainfall regime in Ethiopia, and with the study area as well.
- III. Inter -station correlation analysis.
- IV Determination of rainfall with Altitude
- V. Mapping station locations

The rainfall measurements taken at the station are processed at monthly, seasonal and annual base are used to interpolate in Kriging over the HRR within the basin. Ten years data from 1997 to 2006 is also computed to show the Mean Annual Rainfall over the target of HRR. The reliability of measurements has also tested by statistical parameters according to the summery table below.

Table 5.4 Profile of Mean Rainfall Distributions and Annual Variability

| Regions | ALYM(1997-2006) |       |      | 2000   |      |     | 2003   |      |     | 2006   |      |     |
|---------|-----------------|-------|------|--------|------|-----|--------|------|-----|--------|------|-----|
|         | Mean            | Sd    | Cv   | Mean   | Sd   | Cv  | Mean   | Sd   | Cv  | Mean   | Sd   | Cv  |
| HRR-1   | 585.6           | 178.9 | 30.6 | 230.1  | 12.3 | 5.3 | 277.2  | 19.2 | 6.9 | 710.0  | 23.8 | 3.4 |
| HRR-2   | 1276.2          | 264.2 | 20.7 | 943.0  | 18.0 | 1.9 | 1043.3 | 24.9 | 2.4 | 1255.1 | 26.4 | 2.1 |
| HRR-3   | 1590.5          | 277.4 | 17.4 | 1175.5 | 34.3 | 2.9 | 1374.0 | 42.5 | 3.1 | 1710.3 | 50.9 | 3.0 |
| HRR-4   | 1303.7          | 115.9 | 8.9  | 1265.0 | 55.0 | 4.3 | 1472.2 | 50.6 | 3.4 | 1509.4 | 27.3 | 1.8 |
| HRR-5   | 1674.8          | 201.9 | 12.1 | 1330.9 | 41.6 | 3.1 | 1396.7 | 40.7 | 2.9 | 1431.4 | 35.5 | 2.5 |

The table above illustrate that the rainfall variations as well as the spatial differences within the river basin. The mean annual rainfall amount of the study area is about 1286.2 with coefficient of variation 33.3 percent. The coefficient of variation with smaller values indicated that the rainfall is less variable and more consistent. In regard to spatial variability, the highest mean annual values are occurred in the HRR-5 and HRR-3, both in northwest and eastern highlands which are experiencing better rainfall distribution. In general the profile shown in the table 5.4 can give us an understanding that the inter-annual variability is one of the most important indicators of the reliability of the rainfall as the base for the interpretation of RFE data in the next section.

### 5.1.5 Building RFE Image from MetoSat -TIR raw DATA

RFE image is derived using the methodology by detecting cold cloud in each thermal infrared image and then converting these detections into rainfall estimate. The Methods, by default, create CCD based rainfall estimates for ten-daily periods for each pixel. The CCD images further can be used to produce RFE based on threshold temperature and regression parameters which are taken typically for a given decade and pixel. It is

explained that the TMSAT rainfall estimates method is pre-calibrated for tropical Africa, it is therefore, all the criteria and parameters assigned were also used in the Omo-Gibe basin for which this study is carried out. The parameters used for the processing of estimated rainfall were:

- IV. The optimum CCD threshold temperature  $-40^{\circ}\text{C}$ , which distinguished rainy day from non rainy day for an area (typically about 25 degree square but depend on topography) for each decade in the month.
- V. Using this threshold temperature, the simple algorithms of linear regression ( $RR = a + \text{CCD} * b$ ) between CCD (In hours) and gauge rainfall amount is calculated. The value of “a” and” b “are calculated using decadal totals and decadal CCD values for each pixel containing the gauge data.

In the data processing task, only the decadal monthly CCD TIR image at  $-40^{\circ}\text{C}$  THT for the month of August, 2006 at single 25 degree square pixel size over the HRR-5 is selected and verified in determining the value of the parameters “a” and” b” using TAMSAT’s Methodology as shown in the figure 5.3.

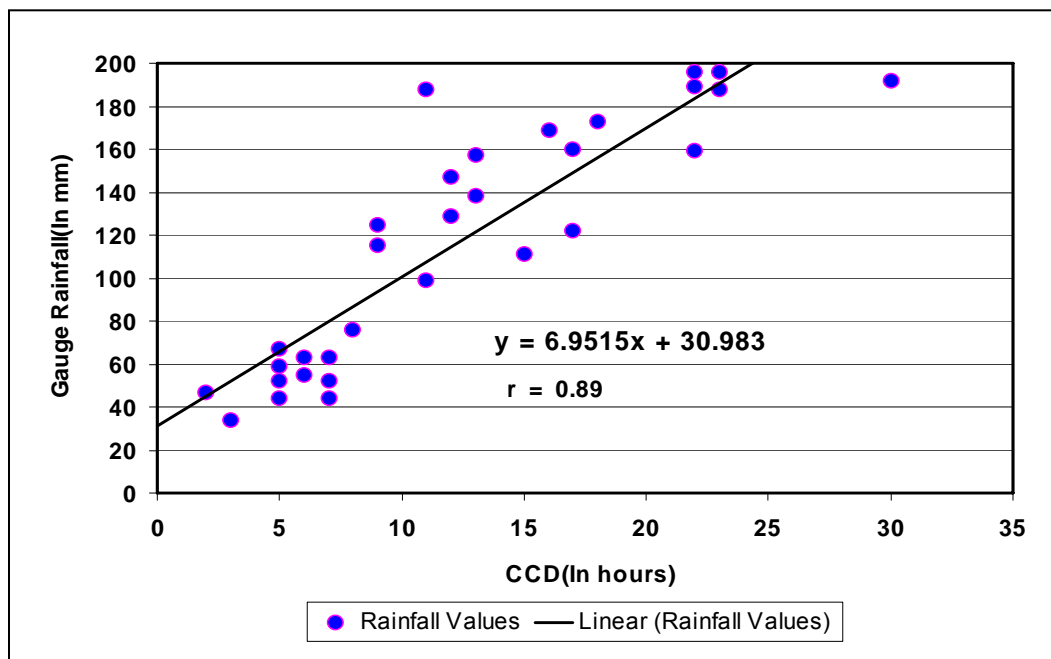


Figure 5.3 Average gauge values against CCD hour at 25 degree square pixel size.

As the figure above illustrated that the rainfall estimation is positively correlated and over the month areas within the regression lines received on average more than 30 mm or more. Thus, the area outside the line receiving more than 30 mm indicated areas with above average rainfall. In the case, the value of “a” and “b” are therefore 30.98 and 6.95 respectively.

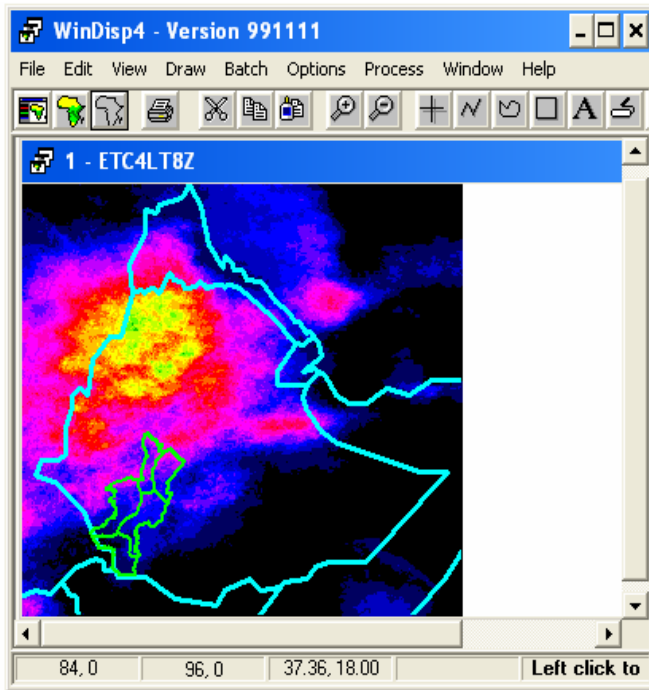
### 5.1.6 RFE Image and Value Extraction Process

#### (a) RFE

As discussed in the above section, RFE imagery is an automated (computer-generated) processed product which used MetoSat infrared data (MetoSat Rainfall Estimation), rain gauge reports from the defined zone. The steps of producing estimates of RFE image is basically started from the process of determination of rain from the CCD data which is already discussed earlier in the literature and it's Approach in TAMSAT methodology. In the process producing the RFE image, there are various methods of Versioned algorithms depending on the satellite, resolution and network of gauging data.

The RFE images used for the purpose of this study are the output of the process that prepared earlier from CCD image in TAMSAT approach and It is presented in the form of raster format with the same region and resolution of the raw CCD data, by using automated ILWIS and WinDisp software interface.

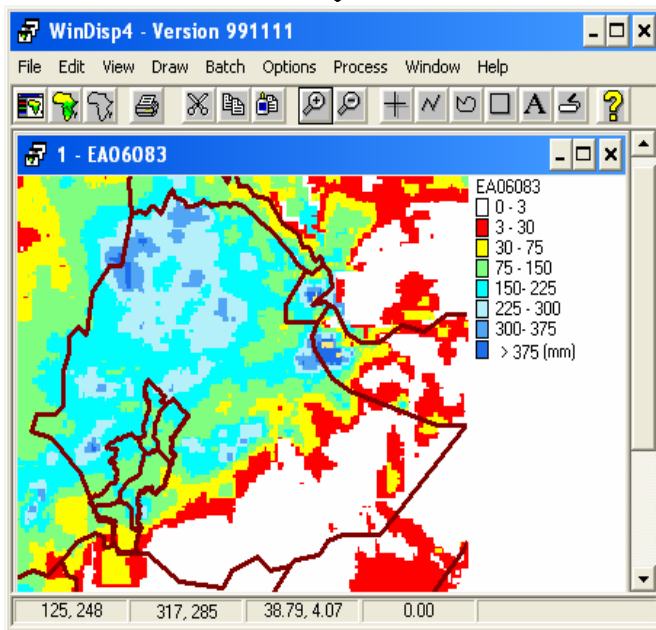
ILWIS and WinDisp have several nice features and viewer options that are useful in preparing RFE map and extraction of the values of each pixel falling within a certain geographical area. In this process, the estimated rainfall values were extracted based on averaged pixel value for each HRRs within the basin and this result for each decade in the selected years. The figure 5.4 below shows the WinDisp software processing steps for rainfall value extraction for decades and for each of HRRS.



✚ *MetoSat –TIR CCD image  
At -40 0c THT*

*For 3<sup>rd</sup> decade August, 2006*

✚ *The color and legends are adjusted using the options of the software, accurately representing the different rainfall value on the map*



✚ *RFE Image Derived from CCD*

*For 3<sup>rd</sup> decade August, 2006*

Figure 5.4 The Raw MetoSat-TIR CCD and Processed RFE Image

(The value (counts), given  $t$  is the TIR channel, relate to temperature ( $T$ ). The lower the counts, the lower the brightness temperature of the feature exercises.)

**(b) RFE Values**

In the previous section only the RFE images are prepared for the required periods in the study area. However, the quantitative value of rainfall at required geographic unit of HRR within Omo-Gibe was the next process determined by creating it in automated statistical extraction process.

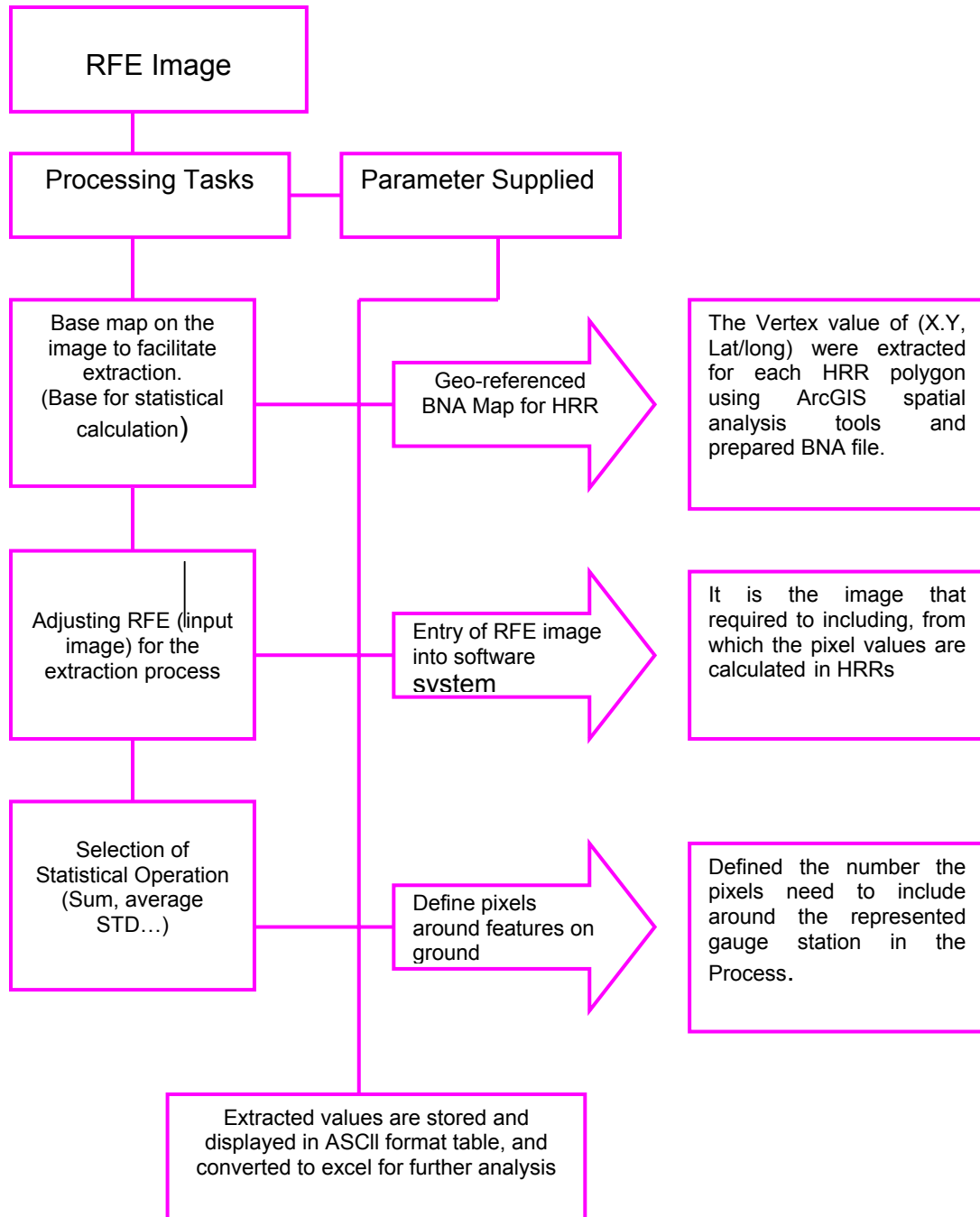


Figure 5.5 Steps in the Processing of RFE Value Extraction

From the Decadal RFE product, estimated values are calculated and extracted averaging each pixel value to HRR within the basin. These data are then compiled at EXCEL format Compared with the corresponding raingauge observations and further processed at monthly seasonal and annual basis. In order to extract quantitative estimate of rainfall for each HRR and periods, all pixel counts were statistically executed using automated processing system of Satellite Enhanced Data interpolation (SEDI) method of WinDisp V.4.0 software applying the following procedure outlined below.

### **(c) Overview of Geostatistical Kriging**

“Geostatistical Analyst builds a bridge between statistics and GIS”(Grimes,D.I.F.,1999)

One of the essential features of Geostatistics considered in this study is a Kriging methods used to generate a continuous surface map for gauge data from a point station, and to predict the exact value of their distribution to (unknown) unmeasured location in the study area. Later, the map would be evaluated and compared with The RFE image obtained for the same period.

Ordinary Kriging is one of the simplest interpolation techniques, is built on the assumption things that are close to one another are more alike than those farther away, and this is quantified as spatial autocorrelation. The method have the empirical *semivariograms model* which can explore the relationships across the data set, and the *Cross Validation dialog box* function gives an idea of view how the predicted value at unknown location is distributed very well. The relation with farther locations can be also determined by *search neighborhoods method* (i.e. searching for the value of the closest cell and to assign a value to output cell). The searching will be performed using the *variable search radius* used for calculating the value of interpolated cell which is specified based on the number of measured points within the maximum radius. These help to relate farther measured location to be used in each prediction and computational speed.

Kriging can accommodate estimation for both point and areal targets. In Geostatistical parlance estimation areas are known as “blocks”, hence you will see Kriging estimation of areal average amounts described as *block (ordinary) Kriging*. The reason is that the satellite provides information on a pixel basis, so by using block Kriging we provide estimates of rainfall on the same geographical support.

The general mathematical formula of interpolation using Kriging method formed as a weighted sum of the data:

$$P_i = \sum_{i=1}^N W_u R_i$$

Where

$P_{i=}$  is the prediction location

$R_{i=}$  is the mean annual Rainfall in millimeter at the  $i_{th}$  location (Station)

$W_{u=}$  is weights to be assigned for the measured value at the  $i_{th}$  location (Station)

Regarding The RFE image, the WinDisp software has option to export the image to ERDAS and ArcGIS supported format called -image ".LAN" format with the same geo-referenced coordinate system containing the basin Geographical boundary at BNA file and the data itself. There is nothing done in ERDAS, but GIS Arc Map is enabled to display the image format and used to delineate active rainfall areas by reclassification using spatial analyst function, In such case, the values of the rainfall is assigned based on the color table and legend defined on the map during RFE image processing system. Each color defined on the legend map is represented the extracted rainfall value at an average over HRRS and the basin at all

The value of the RFE exported to ArcGIS ArcMap would be determined based on the defined and edited **color table** and legend **of map** in during WinDisp image processing activity. Henceforward, the images are organized and reclassified using spatial analyst function and the value of the rainfall on the legend are assigned by adopting the color table which defined when the image is prepared earlier. Some times this method may not give good result because of the color combination of the computer system



requirement. And this is therefore the limitations. However, Super VGA (800 x 600) or higher resolution with 256 colors is recommended for which the color is assigned and exported in another format from WinDisp. The figure below is constructed based on the methods mentioned above.

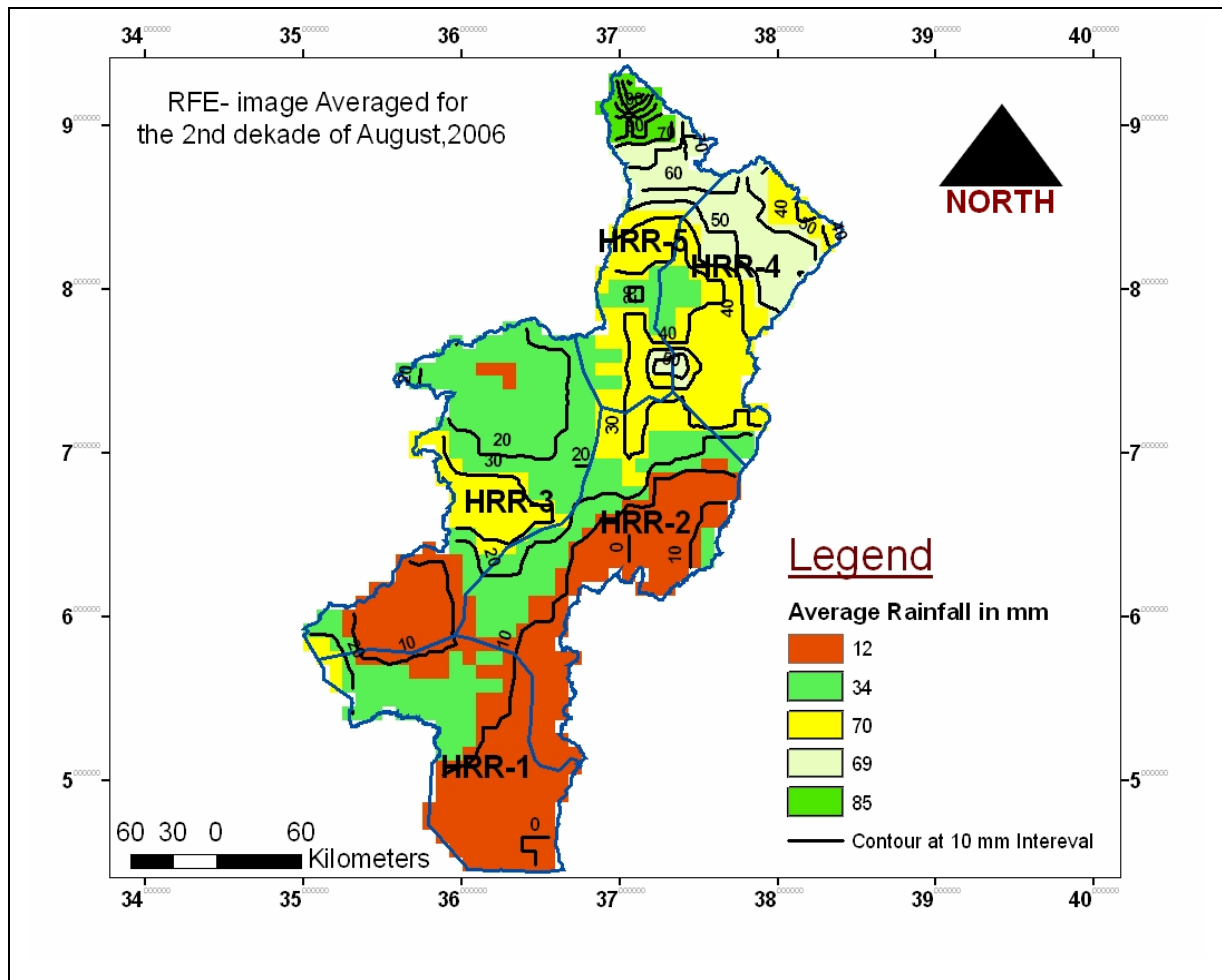


Figure 5.6 Map of RFE image Average for rainfall 2<sup>nd</sup> decade of August, 2006

All average value of decadal, monthly, seasonal and annual RFE images which are 78 in number were exported to GIS environment for mapping compare with the map showing the gauge value interpolated using GIS, Geostatistical Ordinary Kriging method. Hence, the decadal average map of August shown in Figure 5.6 is illustrated the gauge value at 10 mm contour interval overlaid on the decadal RFE value for the HRRs within the basin

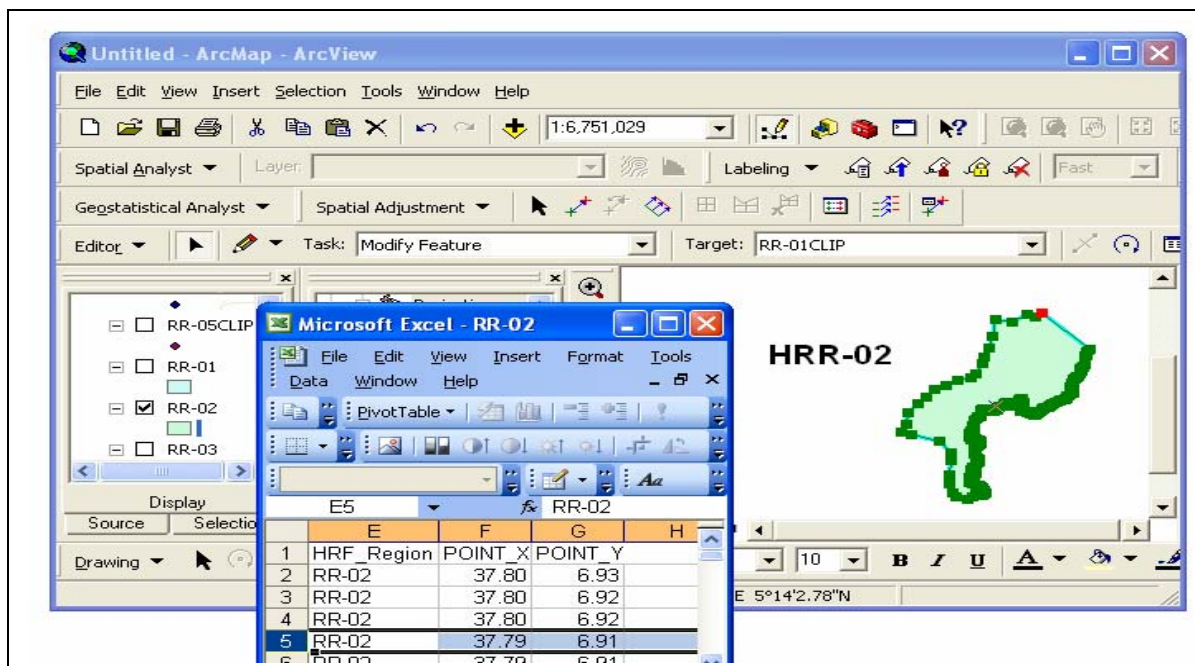


Figure 5.7 Extraction of VERTEX for HRRs (ArcMap: Spat. Analysis Tools)

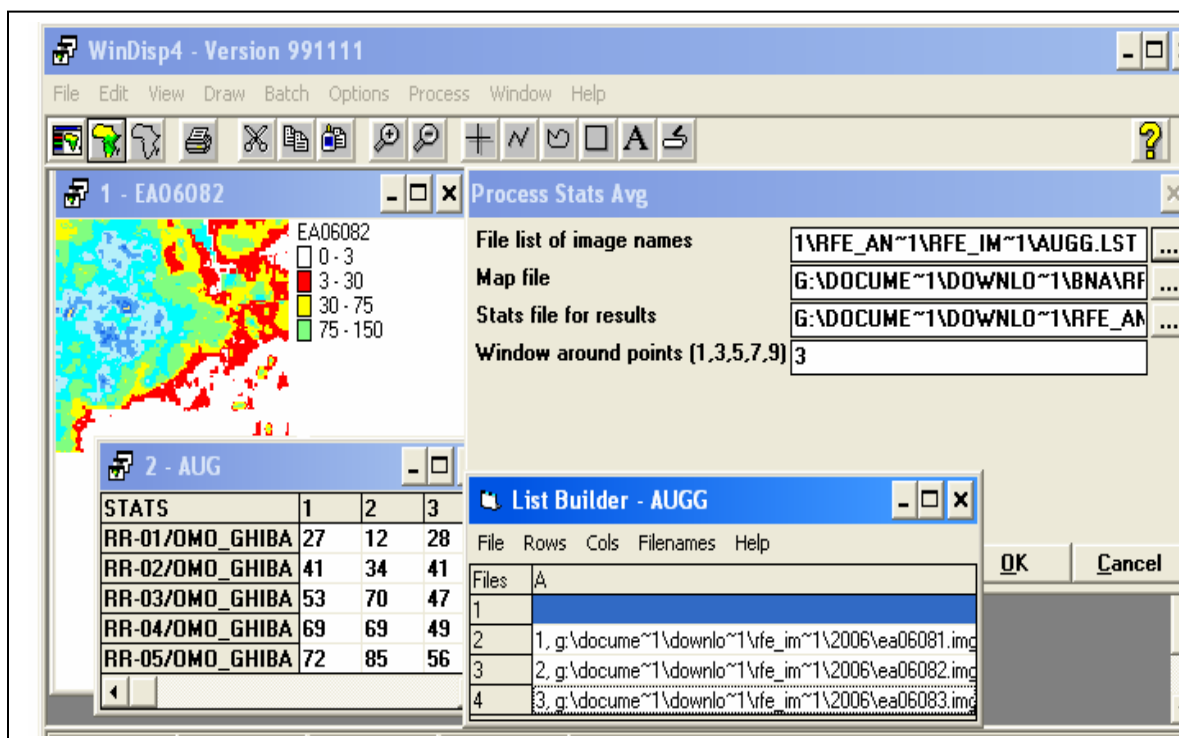


Figure 5.8 Sample View of Value extracted at ASCII file from RFE image ( for 2<sup>nd</sup> deked of August,2006)

Based on the process above, the spatial statistics for each RHH are extracted at a decadal base from the series of 108 RFE images and the results are stored in a tabular ASCII file. For averaging the values, all pixels covered by a single HRR are selected and supplied into the system of pixel parameter setting. The decadal ASCII files are then consolidated into a number of monthly EXCEL files. To ensure that the data at ASCII format is matched with the exact image and Period, the files are stored by default containing the original data and the extracted value. For the distorted pixels and polygon having values outside the limits, -9999 is replaced

The extracted statistical Values obtained are:

- I. Average - Mean rainfall value for each decade in the months
- II. Standard deviation - Standard deviation from the RFE value
- III. Coverage - Percentage of the basin that has maximum rainfall within a given period and places.
- IV. Sum - Total rainfall at monthly, seasonal and annual basis
- V. Maps – Rainfall surface maps for basin and HRRs area showing average rainfall values for assigned periods.

## CHAPTER SIX

### 6. Results and Discussion

#### 6.1 Evaluation and Interpretations

##### 6.1.1 Performance of Value Extracted from RFE

The estimates and extraction of RFE Values of a region should not be an end by itself. It is also important that some evaluation of the estimates be made and it is extremely desirable that this evaluation should be quantitative rather than just anecdotal. There are three reasons:

- I. There is a need to identify any area or time periods for periods for which the estimation algorithm is inappropriate.
- II. There is also a need to identify areas where the under and over estimated situations of rainfall should be modified.
- III. There is a need to demonstrate the accuracy and reliability of the estimation process to interested end users and –makers

Ideally, it must be evaluate and compare the performance of satellite rainfall estimates with an independent set of data, which can be regarded as ground truth. Unfortunately such ground truth rarely if ever exists. In this part of discussion, the evaluation process is basically depend on to comparism of the mean gauge value in a HRRS with the mean satellite estimate for the same regions containing the gauges. It is possible to calculate the error associated with a gauge as an estimator of pixel rainfall by the mathematical technique of Kriging. However this is a somewhat complicated process and requires a reasonable density of rain gauges to give useful results, which means it may not always be feasible

Climatologically, statistics offer a convenient and practical approach to compare estimation for time series of rainfall fields. In order to assess the accuracy of the satellite estimates, it is necessary to compare them with raingauge data. In this case, in fact, the

satellite estimates represent the real average while the gage values the rainfall at point any where in the vicinity of the pixel. Of course, in any literature and research output these difficulties are often arises, but does not found the method established the relationship between area and point rainfall. Instead, statistical parameters and Geostatistical kriging approaches are applied to quantify errors in order to determine the performance of the estimates. (Dutarter.et.al, 1993).

In the determination process of ‘overestimation and underestimation’ the threshold percentage below 33.8 percent is not convenient to agree with the gauge record over that specifically assigned similar climatic zone. (Tufa Dinku, 1994)

## **6.1.2 Validation and Accuracy**

### **6.1.2.1 Bias indicator**

#### **(a) Decadal Profile**

In this study, the performance of overestimate and underestimate, for RFE values were determined using Quantitative evaluation of the bias based on the equation-(b.2)In computation of the bias, all 90 gauge stations are used and all the dataset were converted to the spatial resolution of HRR where the boundaries of the Regional Classification described in the previous section. The derivation of bias was made bearing the difference of the values of RFE with the corresponding rainfall at an average rainfall value for all HRR and for all decadal, monthly seasonal bases in the respective 2000, 2003 and 2006. In determining the bias indicator graphical method were used discriminating just between over and under estimation conditions of the estimated rainfall values.

In the bias analysis, the bias indicators explain only the performance of the satellite during the estimation process that is whether the value is over overestimated or not. The bar graphs displayed in figure 6.1 to 6.3) were prepared to show the level of the bias for the estimated rainfall value. The positive bias are indicators in which the estimated values are exceed the gauge value on the average and is said to be over estimated, with a negative bias corresponds to under estimating the observed value on

the average. The indicators do not reflect the magnitude of the error but the mean absolute error can show the magnitude of error but not the direction. When interpreting the result of such analysis, the smaller the value of the bias and closer to “0” is the better the performance of the estimation and closer to measured Gauge value. Several conclusions were drawn from the inspection of consecutive figures below for the validation of the selected periods.

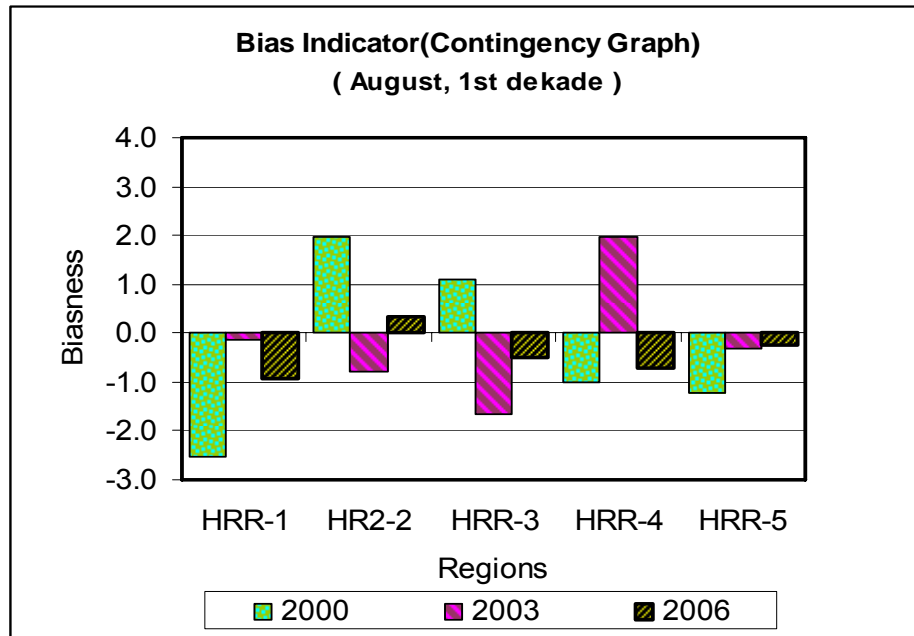


Figure 6.1 Bias Indicator for 1<sup>st</sup> Decade August, 2000/2003/2006

In figure 6.1, the first decade of August in each of selected three years is chosen for Validation of estimated rainfall. The decade is in the main rainy season for over all the basin and it is the month in which maximum rain fall is recorded in the three selected years. The figure emphasized that about 73.5 percent of estimated rainfall from the satellite is under estimated, of which. 89.2 percent is closer to the observed gauge values in each HRR. In particular, for HRR-1 and HRR-6 in the whole three year and HRR-2 in 2003, HRR-3 in 2003 and 2006, HRR-4 in 2000 and 2006 the estimated value was below the observed gauge rainfall. However, estimated satellite values are reasonably closer to observed measurements from the gauge except HRR-1. In the other side, HRR-2 in 2000 and 2006, HRR-3 in 2000 and HRR-4 in 2003 have shown the estimates were exceeded the observed gauge value.

## (b) Monthly Profile

The month considered for validating the estimated rainfall performance was April which is the second rainy season within the study area particularly in the central and southern lowland regions and in the eastern periphery. This month is also having better rainfall and experienced in the range of maximum records in all selected year. This month is selected to show the evaluation of estimated rainfall value as the same method discussed earlier.

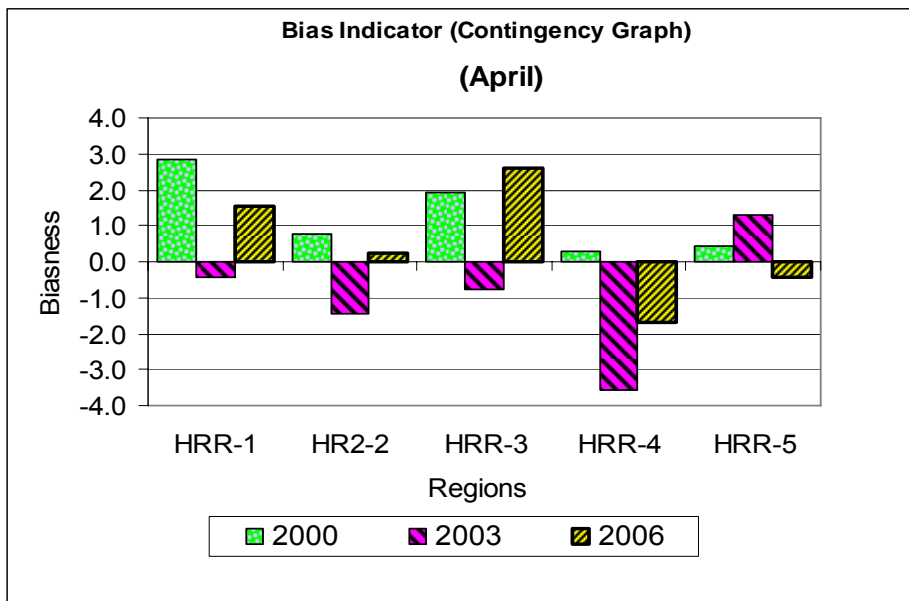


Figure 6.2 Bias Indicators for the Month April, 2000/2003/2006

Figure.6.2 is also illustrated that in all HRR-1 to HRR-3, and in HRR-4 of 2003 and 2006, as well as in 2006 at region HRR-5, the estimated rainfall was below the gauge record. In the remaining period 66.3 percent of the rainfall estimates in the regions indicated were overestimated. The rainfall estimates in 2003 and 2001 at region HRR-1 and HRR-4 were much underestimated. This may be resulted from the quality of the image and automated extraction process or the interruption of receiving system. The overall performance of the evaluation, whether it has positive and negative effect, the bias indicator is manifested in the range of 0 and -1. So that, it indicate that the rainfall estimated is nearly agreed with the observed gauge values.

### (C) Seasonal Profile

Kiremet season is a period selected for evaluation of the estimated rainfall over the assigned HRRs.( Figure 6.3 ).As it has been displayed in the figure, the rainfall estimated for HRR-1 and HRR-4 were exaggeratedly underestimated. This may be true for the reasons explained for the same thing seen in the above monthly validation profile. Over all performance of the season 60 percent of underestimation is below the observed value. In such case the seasonal profile also observed that still the rainfall estimates are closer to observed gauge value.

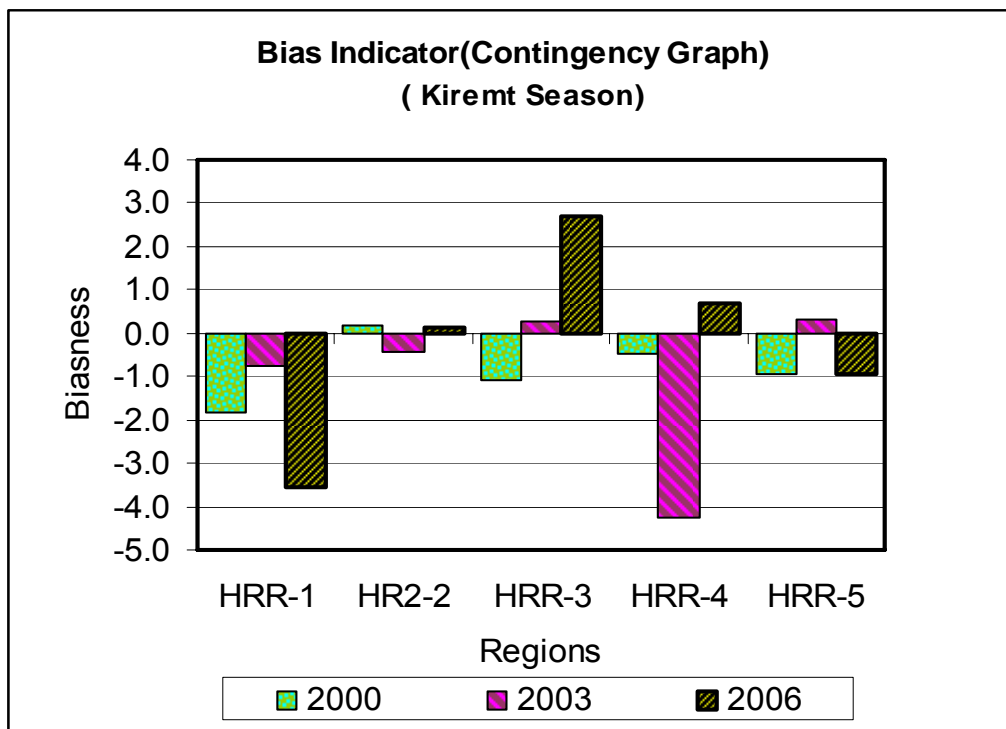


Figure 6.3 Bias Indicator for Kiremet season, 2000/2003/2006

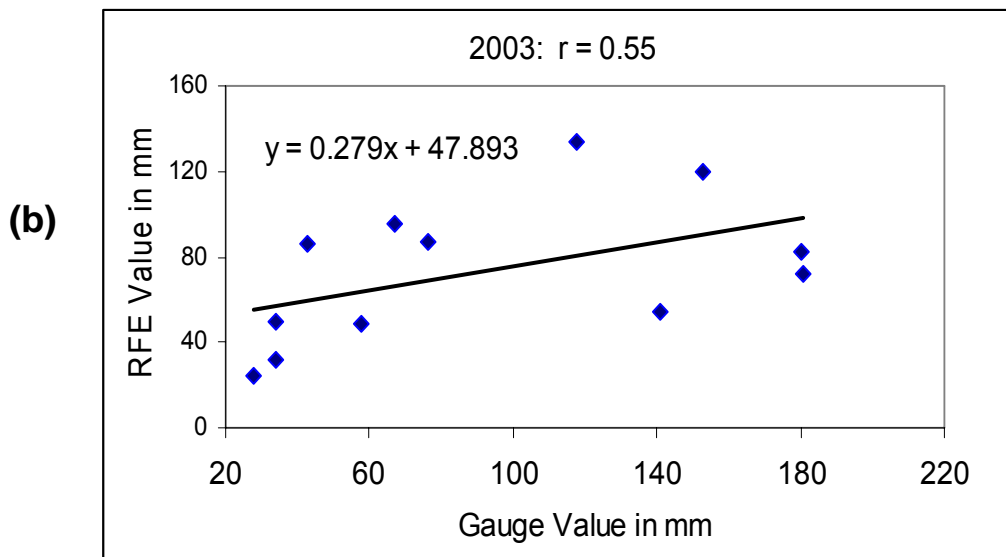
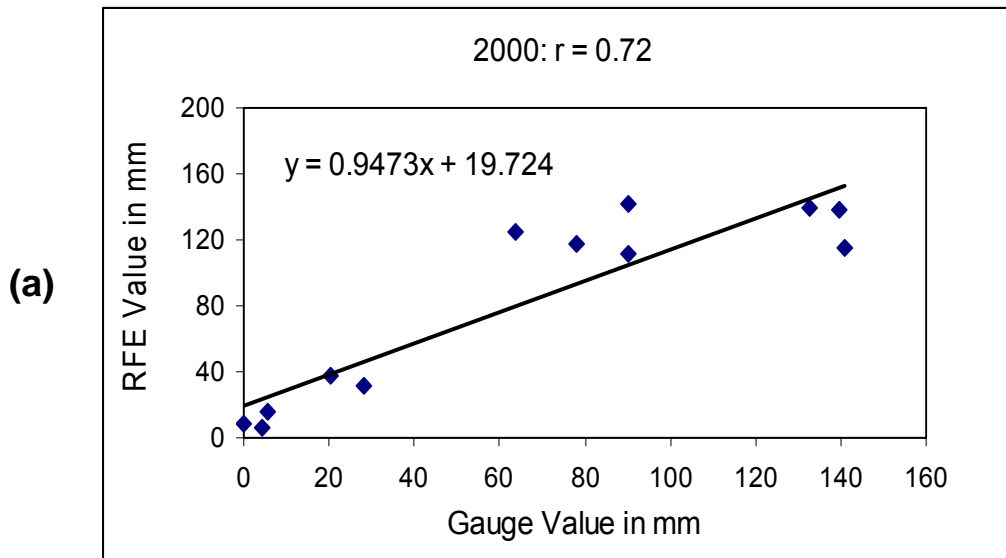
In general, the bias indicator which is shown exaggerated over and underestimation in some period and years are arises mainly due to local climatic conditions (Orographic cloud) and other interacting weather system. There are also another factors that fluctuate the performance of the estimations in all period, this fluctuations are particularly observed within a seasons which are governed by temporal and spatial behavior of rainfall.



## 6.1.2.2 Validation using Correlation and Quartile Deviation

### (a) Correlation Analysis

According to the report of (FAO,2000), validation of Satellite estimated rainfall data of sudan-darfur was done based on correlation analysis of annual rainfall averaged over long time and defined area. The result showed that such statistical method is useful tool for evaluation of the performance for estimated rainfall values. In this study, correlation analysis of estimated rainfall against gauge values have been made only for those purposely selected dry (2000), normal (2003) and wet (2006). (Figure.6.4 (a,b&c).



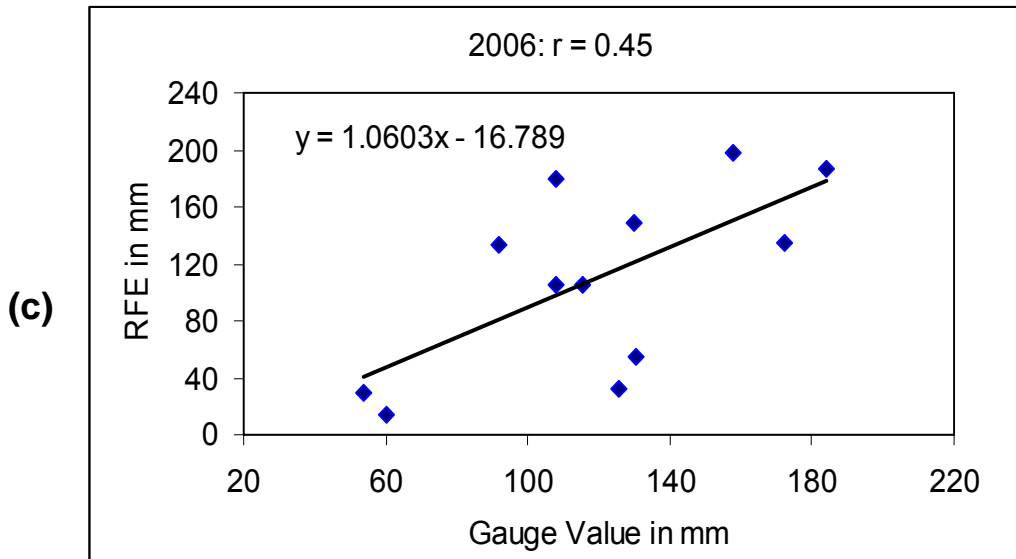


Figure 6.4 Plot of RFE Value Against Gauge :(a) 2000,(b) 2003 and (c) 2006

In the above three plots, if we look at the regression line and the associated data points, the data points which are confined closely to the regression line are the better relationship showing between the estimated and the gauge. The result of correlation indicate that for the dry-2000 is the highest (0.72) while 0.55 and 0.45 for normal (2003), and (wet) 2006 years respectively. In terms of their relation, all the three plots in figure 6.4 have shown a good performance and representation. However, because of over and underestimation, the correlated values are lower for 2003 and 2006.

Hence, the equation tells us that for each annual averaged new record of rainfall, there is an increase of the estimated rainfall (Y) by about (x) mm of the slop of the regression line for each year. In this analysis only the performance of the estimated rainfall with the gauge data is evaluated. The accuracy and reliability would be reviewed by statistical methods of coefficient of quartile deviations in the following section.

### (b) Quartile Deviation

Quartile deviation is one of the statistical methods applied to validate the estimated value of rainfall. The method verifies the uniformity and difference for the serious of the estimated rainfall and the corresponding gauge data for the same time and the same place of HRRs. As it is described in the previous validating method, the accuracy of the RFE value were better both over the time and the HRRs. Beside the determination of the performance, quartile deviation is a suitable statistical parameter to view the

difference, uniformity and level of the accuracy of the two variables. (See equation b.3). The average rainfall of the months March, April, July and August in 2003 have been taken and processed in the way required for calculating the quartile deviation as put on view in table 6.1

Table 6.1 Data Table for Quartile of Coefficient for Selected Months based on 2003 RFE and Gauge record.

| RFE                |       |       |       |        |
|--------------------|-------|-------|-------|--------|
| Regions            | MARCH | APRIL | JULY  | AUGUST |
| HRR-1              | 28    | 41    | 29    | 63     |
| HRR-2              | 35    | 166   | 102   | 63     |
| HRR-3              | 54    | 172   | 134   | 67     |
| HRR-4              | 39    | 160   | 203   | 114    |
| HRR-5              | 55    | 166   | 231   | 143    |
| Gauge              |       |       |       |        |
| Regions            | MARCH | APRIL | JULY  | AUGUST |
| HRR-1              | 18.8  | 52.8  | 14.7  | 16.2   |
| HRR-2              | 33.0  | 132.0 | 111.7 | 117.8  |
| HRR-3              | 57.8  | 143.1 | 153.7 | 139.2  |
| HRR-4              | 23.8  | 128.9 | 203.3 | 210.5  |
| HRR-5              | 26.7  | 119.1 | 210.4 | 223.9  |
| RESULT             |       |       |       |        |
|                    | March | April | July  | August |
| Estimated Rainfall | 0.40  | 0.02  | 0.33  | 0.29   |
| Gauge Rainfall     | 0.16  | 0.05  | 0.29  | 0.28   |

During the analysis, It was necessary to convert the absolute measures of quartile deviation ( $(Q_3-Q_1)/2$ ) to coefficient of quartile deviation ( $(Q_3-Q_1)/(Q_1+Q_3)$ ). Thus, if the result of the deviation is larger, it is therefore explained that there would be high variability and smaller uniformity independently within the estimated and gauge data series. These later compared among the two variables and determine that the level of accuracy between and within each estimated and gauge data. The result in table 6.1 illustrates that the coefficient of quartile value 0.40 and 0.16 for estimated rainfall and gauge are not found in uniform mode when they are compared during March. In the remaining months they are almost similar and so it is good agreement.

In general, the difference that have observed in the estimation were very less when compared to the raingauge records. The coefficient of quartile deviation in both dataset in April and August has small value different from the other months. This difference shows that only the variability within the data itself. But when the values are compared with estimated and gauge, it shows the more the convenience and consistency of the two datasets.

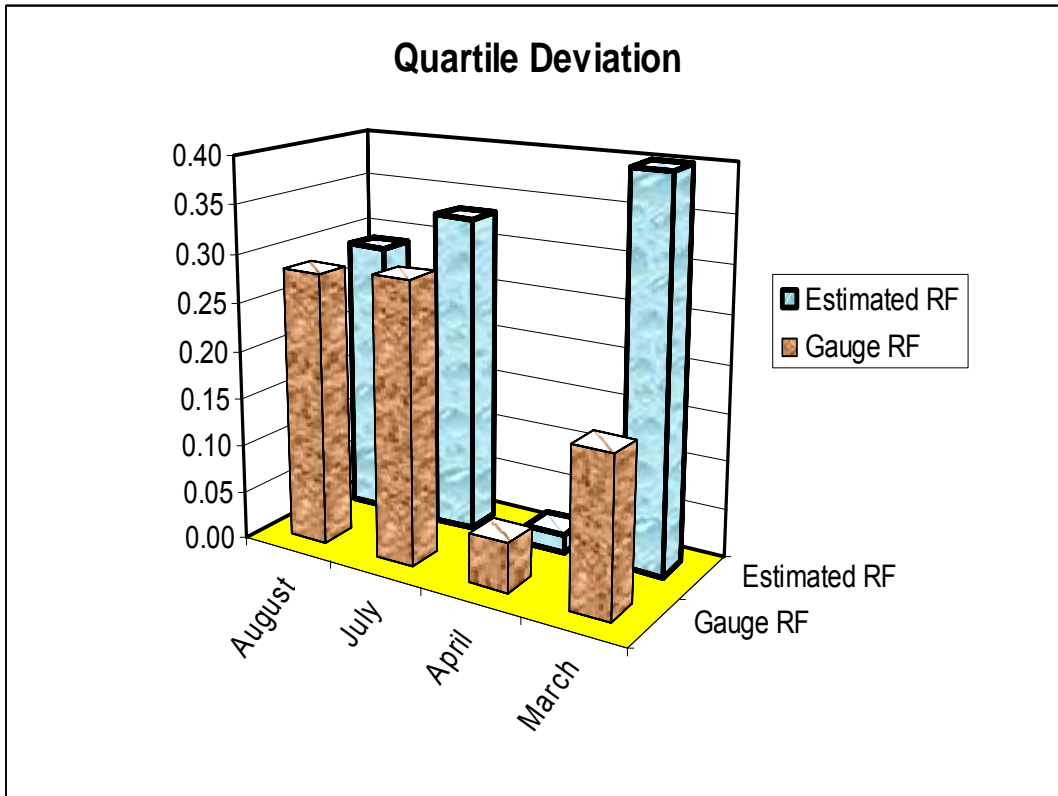
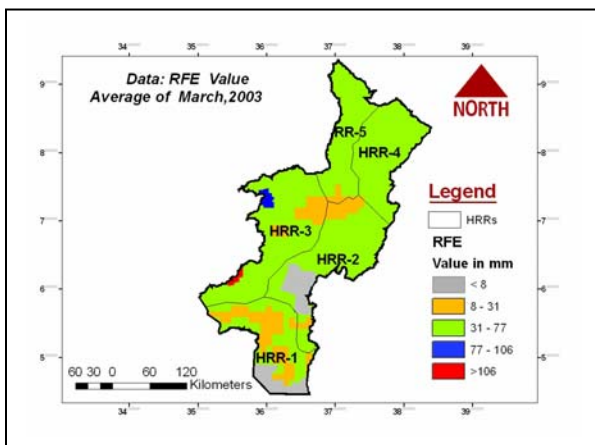


Figure 6.5 Graph of Validation for estimated and gauge recorded rainfall. (Using quartile deviation, MAJA, 2003)

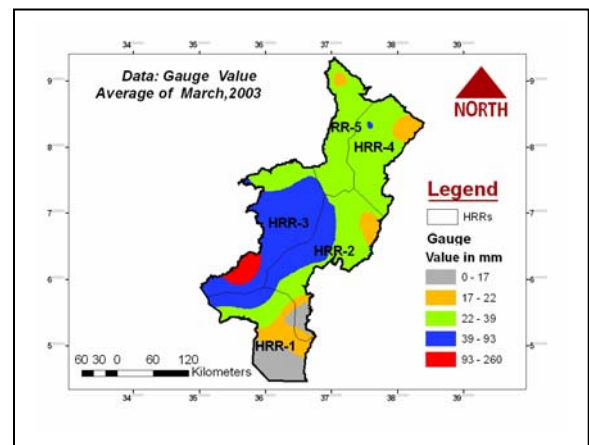
The result of the deviation shows that for the selected months both the uniformity of the data within estimated and gauge rainfall value are explained very well. However, as viewed in figure 6.5, over estimated rainfall in March is highly variable. The same to in the month April the underestimated rainfall shows small variability compared to gauge value. These situations were also observed in validating the performance of the estimated rainfall for the same months.

### 6.1.2.3 Rainfall Surface Map (filled contour Pattern)

Another method applied for validating the estimated rainfall was based on the surface map showing the rainfall distribution and the value on the map for both RFE and Gauge record as it is discussed in section 5.1.7(b). In order to distinguishing and evaluate the difference and similarity of estimated rainfall and gauge rainfall distribution on the surface map, the month of March and August, 2003 were selected. As it is shown in figure 6.5, the estimated rainfall value for March was identified underestimated and August is almost in agreement.

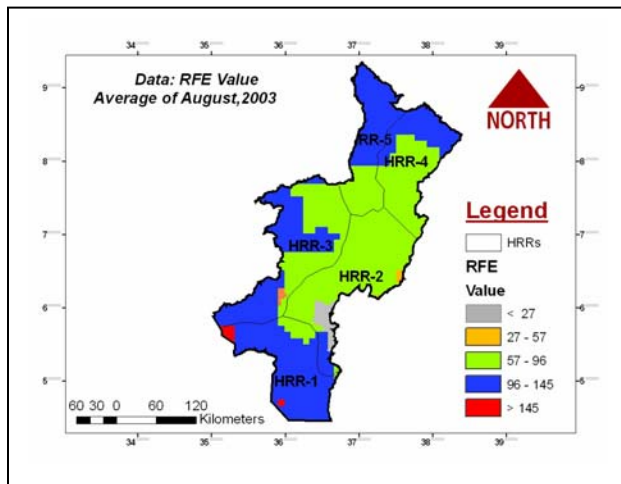


(a) RFE

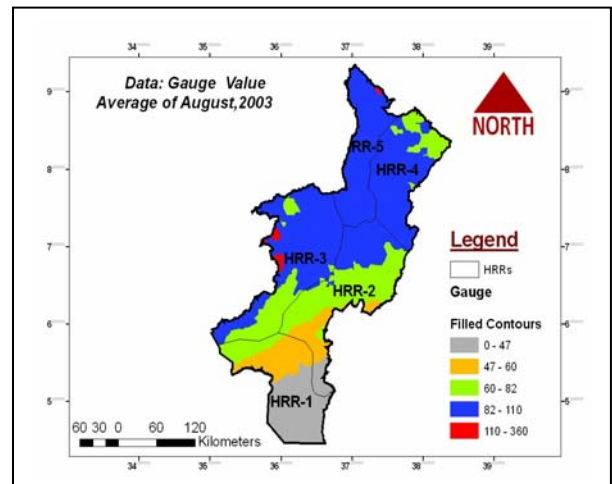


(b) Gauge

Figure 6.6 Monthly Rainfall Map for March over Omo-Gibe basin



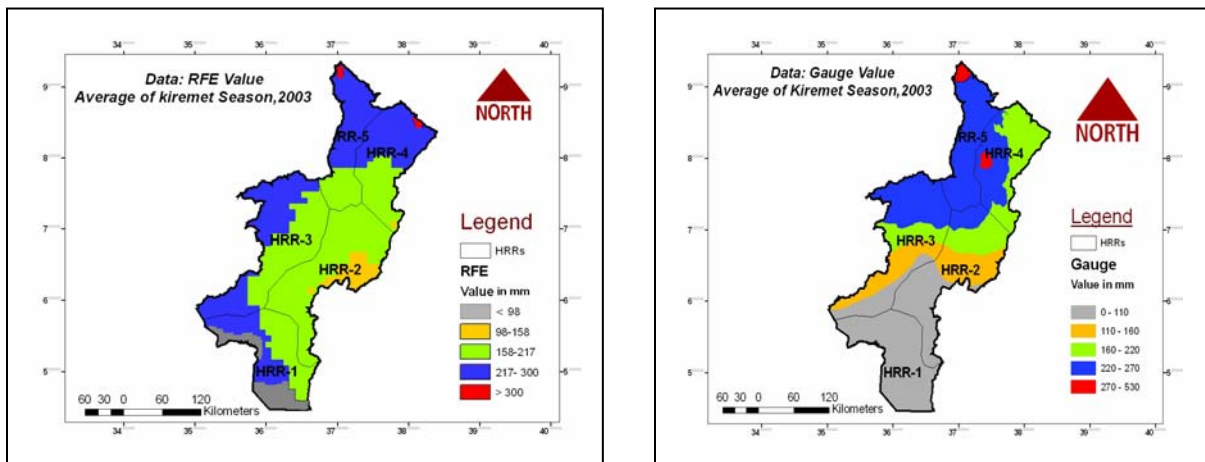
(a) RFE



(b) Gauge

Figure 6.7 Monthly Rainfall Map for August over Omo-Gibe basin

In the Figures 6.7, (a) and (b) it is shown that the RFE and gauge filled contour map are different. This situation was also observed in bias indicator and quartile deviation for the same month that was underestimated. In Figure 6.7. it shows that the estimated rainfall in august was relatively in agreement with the raingauge record, particularly in the south HRR-1 an HRR-2. The Average seasonal estimated rainfall for kiremet, 2003 which is shown on the map were also nearly closer in the north, northwestern and southeastern area.



(a) RFE

(b) Gauge

Figure 6.8 Seasonal Rainfall Map for Kiremet in 2003 over Omo-Gibe basin

## 6.2 Climatological Characterization of RFE Vs Gauge Values

### 6.2.1 Rainfall Regime of Omo-Gibe Basin

For the discussions of this section, it should be important to know the climatology of the rainfall characterized over the basin. Rainfall is one of the main components in defining the basin characteristics. In Ethiopia there are three major rainfall regimes A, B and C. and are indicated in Figure 6.8. (Bekele, 1993 and NMA, 1996).

Area under Region A are characterized by bimodal-I having three distinct seasons Kiremet, Bega and Belg, Region B is a mono-modal type which have one long rainy

season throughout the year. Region C is the second bimodal-II type dominated by double peak in April/march and July/august.

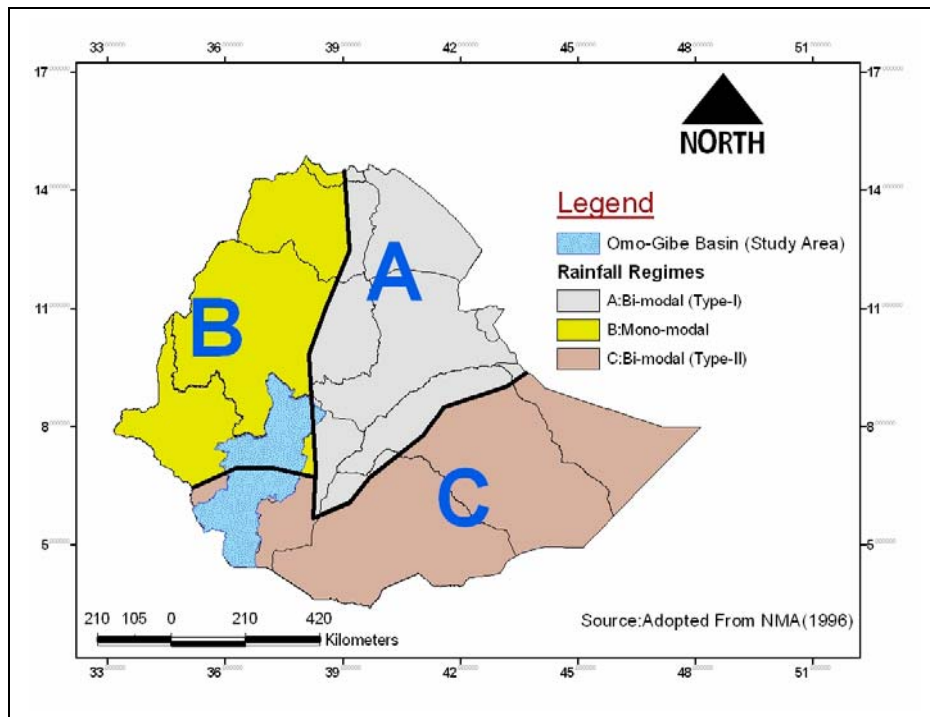


Figure 6.9 Rainfall Regimes in Ethiopia

With refer to the figure above, the rainfall of the basin is characterized by all types, but the two rainfall regimes B (in north, northwest) and C (in central and southern) are the dominant type. Most of HRR-5 and HRR-4 are found within type B while the central and southern in type C. Statistical analysis for the estimated rainfall ad gauge records were made at the monthly, seasonal and yearly level and it is characterized both in temporal and spatial scale.

Meteorologically, the seasons in Ethiopia are generally classified into three main groups:

- I. Belg Season (small rainy season) -- February to May
- II. Kiremet Season(main rainy season) -- June to September
- III. Bega (Dry season) -- October- to January

## 6.2.2 Results from Temporal Characterization

Among the tools the approach of rainfall characterization over time and geographical unit is useful in carrying out a comparative assessment and understanding of the satellite based estimated rainfall as a signal for climatic condition of the study area. The rainfall characteristics over the basin is highly variable from month to month, seasonally and annually. To show this variability, the average value of estimated rainfall and gauge records were calculated for each period in the year 2000/2003/2006.

### 6.2.2.1 Decadal Pattern and Trend of Rainfall

The decadal time series analysis can provide great opportunity for detecting, describing and to identify the onward and backward tendency of the variability of the estimated rainfall over the study area. By using this method, the decadal RFE value and gauge data from all 90 stations for the selected three years were processed and used to characterize the climatology of estimated rainfall data as shown in figure 6.11. more over, The Decadal estimated rainfall in years and at HRRs level with the gauge record has put on show in Annex-D and Annex-E respectively

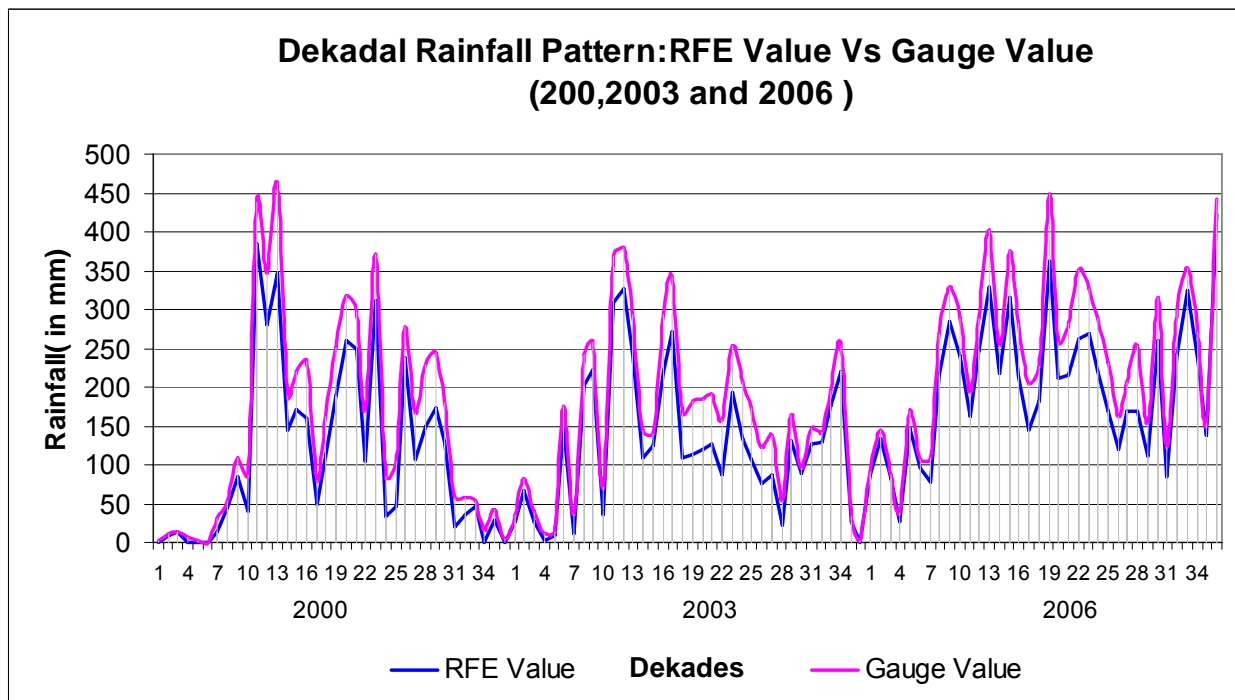


Figure 6.10 Plots of Rainfall Pattern And Characterization for RFE value (Using Pattern analysis, decadal in2000/2003/2006)



The plot in Figure 6.10 shows that the RFE value is nearly follow the shape of the seasonal cycle and represented well in all three years except for those exaggeratedly below and underestimated, The rainfall regime type B and C are truly propagated through out the three years, in which, estimated decadal rainfall followed the gauge rainfall pattern and the occurrence of the peak rainfall time over the study area. In the graph, the bi-modal type C rainfall, double peaks of rainfall characteristics are also represented by estimated rainfall during the third decade march up to first decade august. Compared to the rainfall pattern of gauge value, both the overestimated and underestimated rainfall was reflected on the graph. In some decades such as the first march and September in 2003, first and third decade of august in 2003, and from august to first decade of October the estimated values are mismatched with he existing pattern of lines of the gauge value. This also observed during validating the RFE values using the bias indicator in the previous section.

In general the graph is a good indicator of the agreements between the estimated value and the in order to determine the performance of the RFE value. The exaggerated underestimated rainfall in August of Kiremet season also viewed on the graph. The gap shown between the two lines are the errors shows the error between the estimated and the gauge value

### **6.2.2.2 Monthly and Seasonal Profile**

The result obtained from this analysis confirms that satellite estimated rainfall Value is subsequent to the year to year and inter-annual variability within the basin. Even though the values of RFE for some decades is under and overestimated the, but it can be seen that the amount and distribution is in agreement with the corresponding gauge record and the climate system over the basin. The monthly rainfall distributions records of the two dataset is annexed, (See Annex F&G)

For the whole basin, the estimated rainfall is also closely represented the rainfall regime characterized by type B and C with similar peaks During April and July, in particular, the monthly average estimated rainfall for 2003 and 2006 were closely associated with variation seen within the month and the seasons in the gauge data

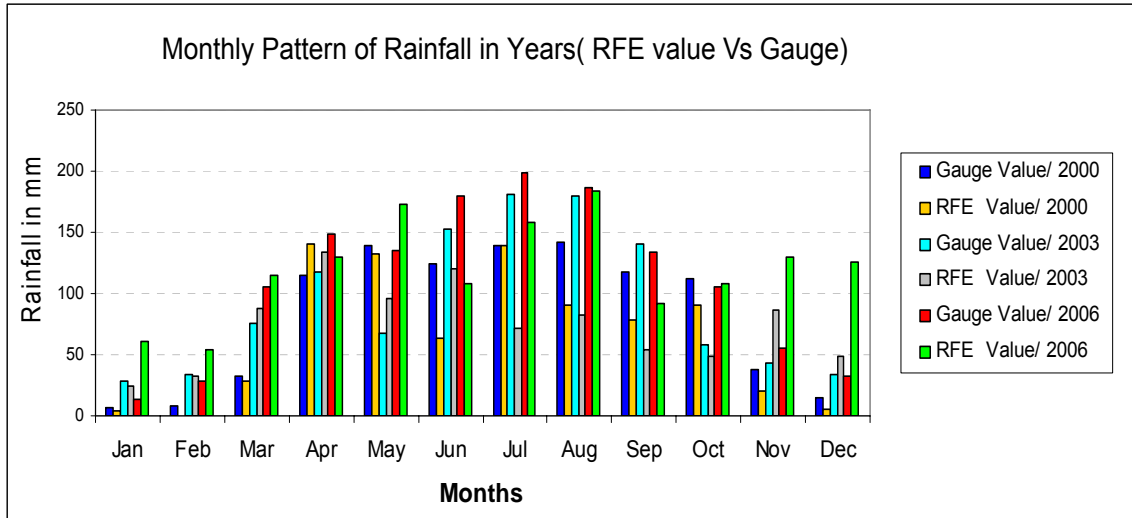


Figure 6.11 Average Monthly Rainfall Profile

As it can be inferred from the above Graph, April to September the estimated rainfall is performed well both by amount and distribution at the same pattern of the normal climatic conditions. On both rainfall data the maximum average amount of rain, above 150 mm, has been observed during the month July in Kiremet season. But, during this month the estimated rainfall in 2003 was not agreed and much below, because it was underestimated. This situation was discussed in the previous section 6.5 while validating the performance of the RFE value. In particular in 2003 for the same month in Kiremet the RFE values did not harmonized with the gauge record and not replicate the characteristics of the season. In the other side, it was found that the temporal comparism of RFE Value for April was agreed continuously with the rain gauge record in the range of 100-150 mm in all years. Bega is, in fact, dry season but there is some places particularly in the southern lowland and periphery area of the basin getting small rain up to 50mm. The detail of the monthly statistical data is presented in Annex -F & G.

### 6.2.2.3 Maximum Rainfall Profile

The other significant feature that can be compared and characterized the RFE value and the gauge record were the maximum rainfall existed in each dataset and commonly applied to characterize extreme condition like flood and also presents basis for studying rainfall depth and pattern between the maximum rainfall and physical

basin. Summery statistics of the monthly maximum rainfall are presented in table 6.2 for each year.

Table 6.2 Maximum Rainfall Profile for RFE and Gauge Value

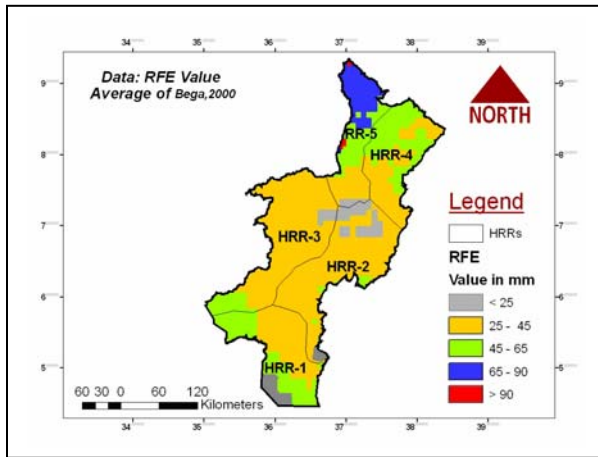
| Year | Gage Record |       |      | Estimated Rainfall |     |      |
|------|-------------|-------|------|--------------------|-----|------|
|      | Month       | MAX   | HRRs | Month              | MAX | HRRs |
| 2000 | Aug.        | 223.9 | 5    | May                | 232 | 5    |
| 2003 | July        | 287.4 | 5    | July               | 211 | 5    |
| 2006 | Aug.        | 307.5 | 5    | Aug.               | 283 | 2    |

The table above reveals that most of maximum monthly estimated rainfall exhibited, during August and July at which the seasonal rainfall peak is apparent for most of northern and central region within the basin. The value of the maximum rainfall estimated is also close but more interesting is that such most of the Maximum values are occurred in upstream of HRR-5 where the highest topography and the heaviest rainfall are observed. Most of the big tributaries also originate from this upstream region. In addition to this, the recent devastated flood that occurred and lost the life of the downstream at Omorate and Dasenech in the basin were the result of this effect.

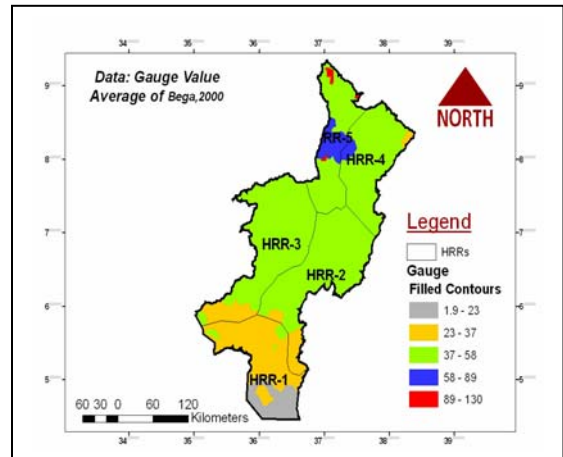
#### 6.2.3.4 Rainfall Surface Map on Temporal Overview

As it was mentioned about the climate and rainfall regime of the study area earlier, in general, the rainfall is decreasing from north, west and northeastern highlands towards the Omo river valley and the southern low land areas. Thus, Bega season of dry (2000), Belg season of normal(2003) and Kiremet season of wet (2006)years are selected and generated rainfall maps to show the representation of RFE Value with respect with the rainfall climatology of the rains within the basin. Hence, it would be possible to distinguish the errors and relevance of the RFE value in two ways as follow.

- I. To examine the performance of RFE value in terms of characterizing the seasonal temporal variability
- II. To show the difference of maps compared to RFE that exhibited over and under estimation.
- III.



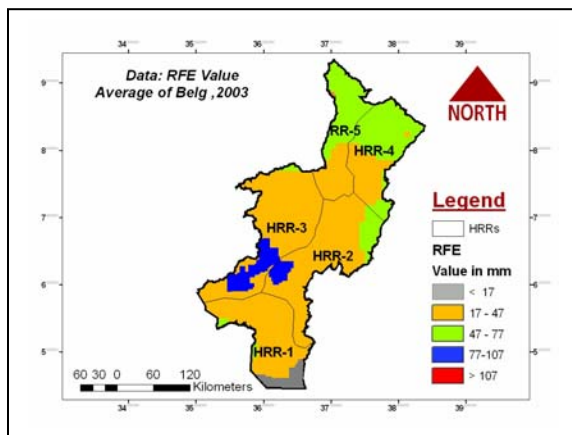
(a) RFE



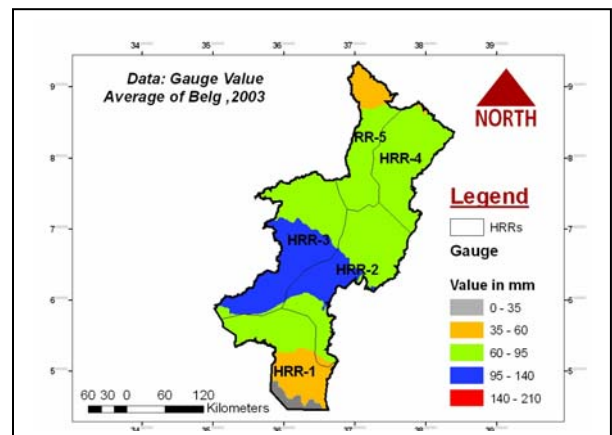
(b) Gauge

Figure 6.12 Rainfall Map for Bega Season:2000

Result from map of Bega rainfall (figure 6.11, a & b) shows that on both maps the rainfall is generally decreasing north to south direction. In such case the performance is better but could not show the places in the central and southern lowland where Bega is their season for getting high rainfall compared to the other. In fact this situation also did not observed on the map of the seen from gauge value. There is also overestimation seen on the RFE value in the north and eastern side compared to the gauge maps.



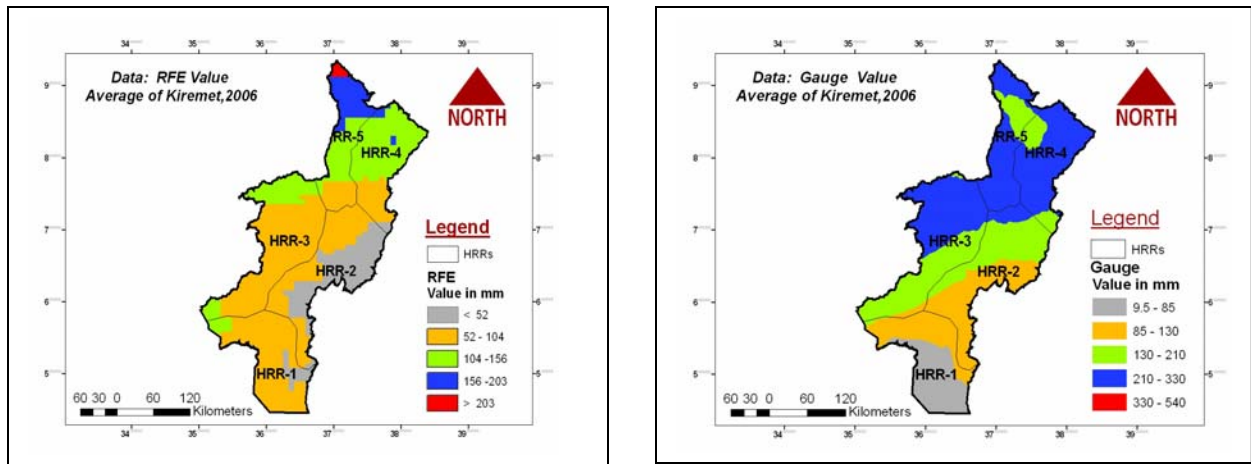
(a) RFE



(b) Gauge

Figure 6.13 Rainfall Map for Belg Season: 2003

Belg season, in 2003, the rainfall seasonality and extents are explained better. In particular in the northern half of the places the RFE and Gauge values are in agreement. But in the southern western side the RFE is shown underestimate situations.



(a) RFE

(b) Gauge

Figure 6.14 Rainfall Map for Kiremet Season: 2006

In the figure 6.13, the rainfall maps shows that the seasonality of The RFE value is better illustrated, however, in most places in the south west the extent of the rainfall values did not agreed, because of the bias that disused in previous sections and local conditions

As a whole, the effect of RFE value on the temporal variability of the basin is more ore less explained with those of the limitations of bias and based on the satellite image quality and processing procedure, the estimated rainfall also mentioned the dry, normal and wet situations of the years in there selected seasonal distribution of rainfall maps

## 6.2.4 Results From Spatial Characterization

This study has shown that the spatial variability of the rainfall during the year is more pronounced in seasonal cycle and a reasonable agreement on large scale. Thus, the statistical computations and the rainfall maps are general generated based on the averaged annual values of RFE processed from 36 decadal images of each year and the corresponding gauge records of the same period.

### 6.2.3.1 Seasonal Profile of Spatial Pattern of RFE value. .

Average seasonal rainfall for the RFE and gauge value is calculated, at HRRS level for all three selected years .The results are also shown in Figure 8,(a) and (b) for both dataset independently.

(a) Based on RFE Value

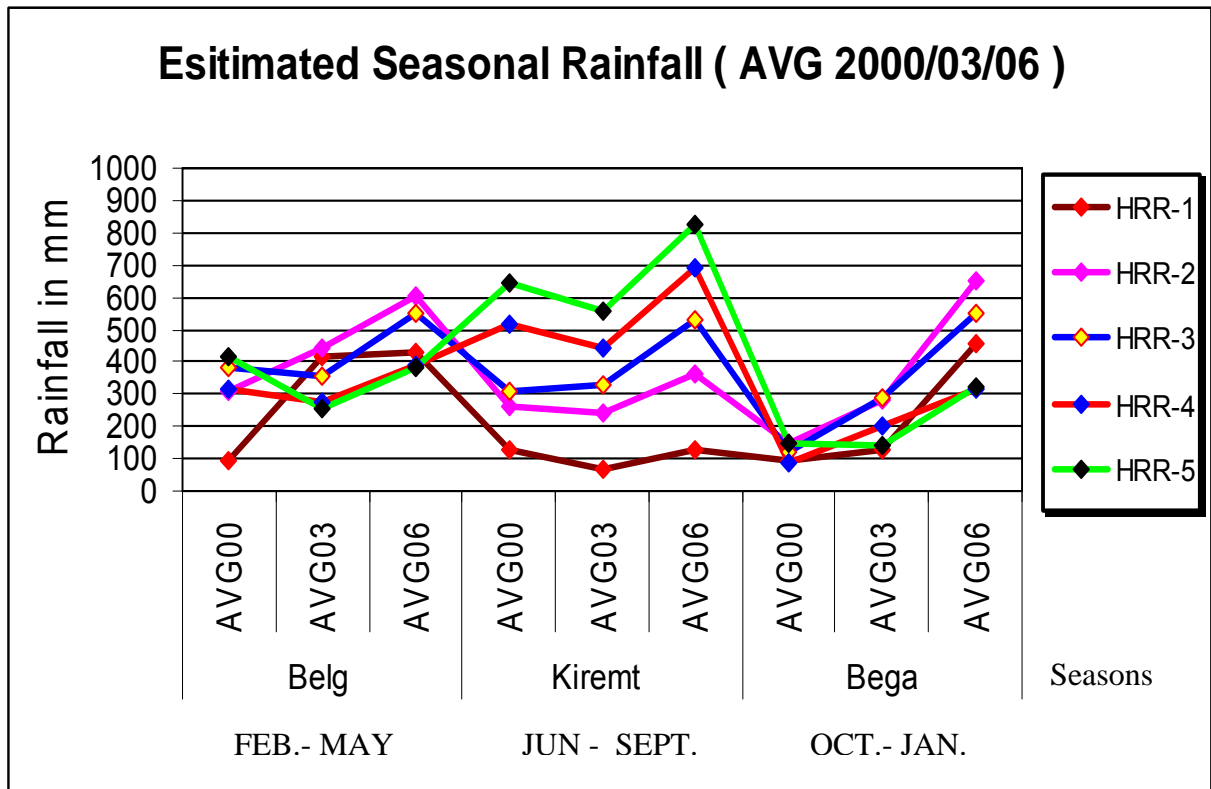


Figure 6.15.(a). Plots of Spatial Pattern of RFE Value on Seasonal Basis

The estimated rainfall has shown us the seasonality of the rainfall both by amount and distribution almost at the same pattern of the distribution of the rainfall over the basin. The peak rainfall time in Belg and Kiremet is also indicated in better way. For example, the low land of Omo Valley in HRR-1 and most central and southern parts of HRR-2 and HRR-3 Kiremet is not their season and do not get rain during this period. Instead, these regions get rain during Bega season. These situations can be also clearly observed in the graph. During Belg 2003, rainfall was good in most of HRRs.

The best performance for estimated rainfall is in Belg 2000 and 2003 which is matched with the correlation results done for the period. Interestingly, the average rainfall estimated for 2006 was 800mm for HRR-5 which is decreasing to the south HRR-1 to about 100 mm. In Kiremet 2006, most part of the northwest and eastern highlands in HRR-5 and HRR-4, and upstream of Gibe and Gojeb River were attained much rain amounting above 600 mm. This was the cause for over flow of Omo-river and flooding

that severely affect the downstream lowland resident. This situation can be also observed from the Figure 6.15(b) below. In this case, we can suggest that the satellite based rainfall estimation is an essential loom for getting rainfall information.

(b) Based on Gauge Value

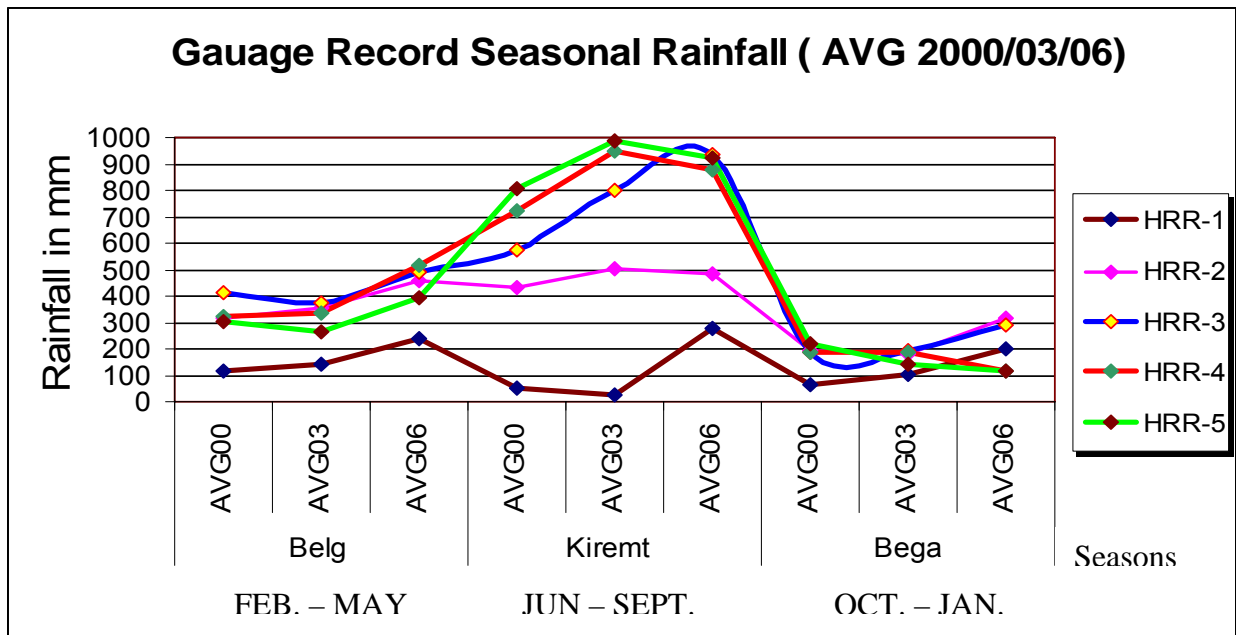


Figure 6.15.(b). Plots of Spatial Pattern of RFE Value on Seasonal Basis

Compared to Gauge values, the over and underestimated situation are observed in areas where receive the highest rainfall in the north (HRR-5) and (HRR-4) during Belg and kiremet in 2006. In addition, a positive spatial correlation viewed in table 6.3 between the RFE and gauge values describes the agreement over HRRs among all years but there is important difference in amount.

Table 6.3 Correlation results of average Annual RFE Value Vs Gauge record

|       | YEARS | R1   | R2   | R3   | R4   | R5   | r       |
|-------|-------|------|------|------|------|------|---------|
| RFE   | 2000  | 317  | 713  | 814  | 921  | 1208 | 0.93633 |
|       | 2003  | 612  | 973  | 973  | 915  | 953  | 0.89851 |
|       | 2006  | 1011 | 1614 | 1635 | 1400 | 1530 | 0.84618 |
| Gauge | 2000  | 230  | 943  | 1176 | 1265 | 1331 |         |
|       | 2003  | 277  | 1043 | 1374 | 1472 | 1397 |         |
|       | 2006  | 710  | 1255 | 1710 | 1509 | 1431 |         |

### 6.2.3.2 Rainfall Surface Map on Spatial Overview

Each of 36 decadal series of RFE imagers for the selected years were averaged and the values are extracted based on annual basis indicated in table 6.4. Consequently, average annual rainfall maps are generated using geostatistical ordinary kriging as shown in Figure 6.16(a,b&c) below. The main purposes of these maps are to compare the average estimated rainfall and gauge values in each of the dry, normal and wet years, and that matches the spatial structure of the background rainfall climatology within the basin.

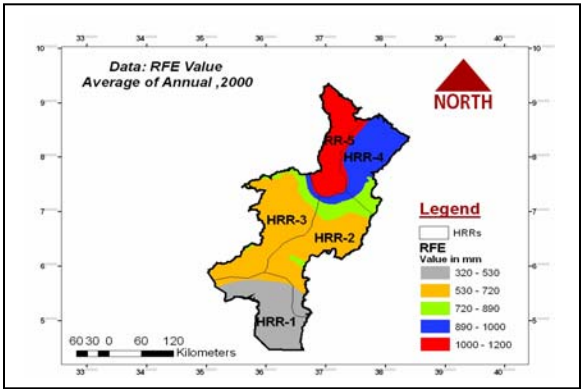
Table 6.4 Average Annual rainfall of Estimated and Gauge Values

| Rainfall  | YEARS | REGIONS |        |        |        |        | Basin Average |
|-----------|-------|---------|--------|--------|--------|--------|---------------|
|           |       | HRR-1   | HRR-2  | HRR-3  | HRR-4  | HRR-5  |               |
| Estimated | 2000  | 317.0   | 713.0  | 814.0  | 921.0  | 1208.0 | 794.6         |
|           | 2003  | 612.0   | 973.0  | 973.0  | 915.0  | 953.0  | 885.2         |
|           | 2006  | 1011.0  | 1614.0 | 1635.0 | 1400.0 | 1530.0 | 1438.0        |
| Gauge     | 2000  | 230.1   | 943.0  | 1175.5 | 1265.0 | 1330.9 | 988.9         |
|           | 2003  | 277.2   | 1043.3 | 1374.0 | 1472.2 | 1396.7 | 1112.7        |
|           | 2006  | 710.0   | 1255.1 | 1710.3 | 1509.4 | 1431.4 | 1323.3        |

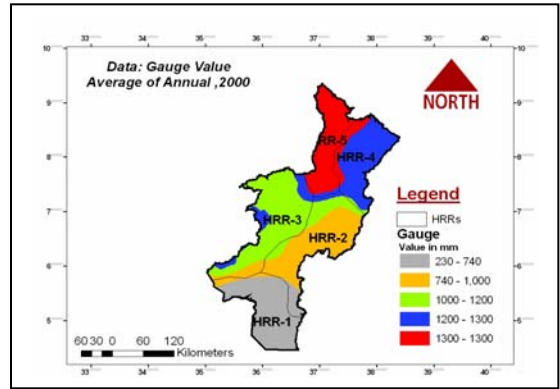
The annual average surface rainfall map is shown for each year in Figure 6.16 and the Statistical parameters are listed in Table 6.4. The rainfall estimated for region HRR-1 has been clearly indicated on the maps with very low rainfall in all three years. But as we discussed it earlier, this region is getting rain during Bega season. On the contrary, the regions in north and eastern highlands in HRR-5 and HRR-4 are received much rain during those periods. The rainfall map of 2000 has also shows the closeness of the estimated and gauge value particularly over the HRR-5 and HRR-4. Likewise, the correlation (0.93) with the estimated rainfall in 2000 was higher than 2000 and 2006.

The annual average estimated rainfall in 2003 and 2006(Figure 6.16.c and e ) is widely show similar distributions over HRR- 2, HRR-2 and southern part of HRR-3 and this is therefore not well represented the rainfall characteristics compared to the rainfall map of the gauge in the same period.(Figure 6.16.d and f).

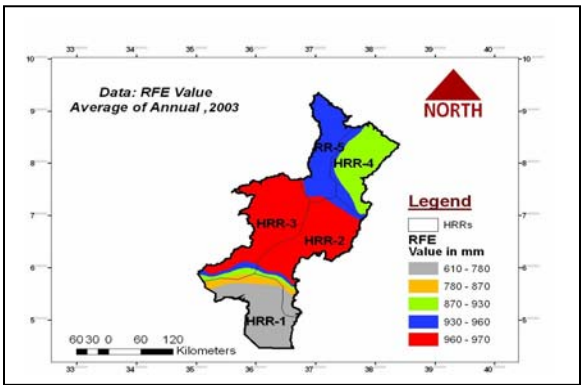




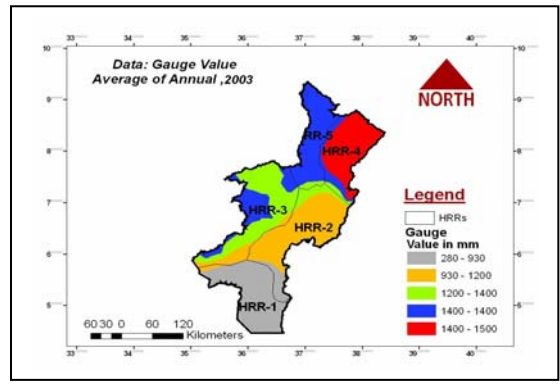
(a) RFE: Average Annual 2000



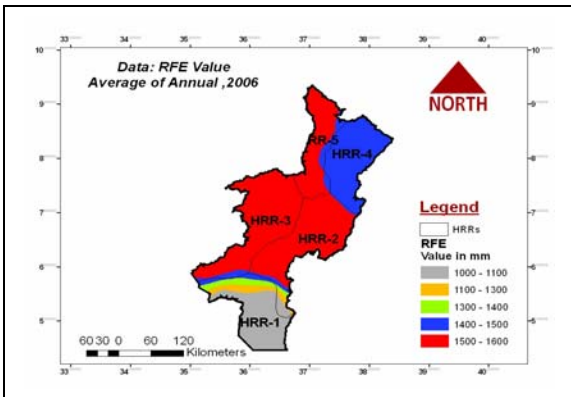
(b) Gauge: Average Annual 2000



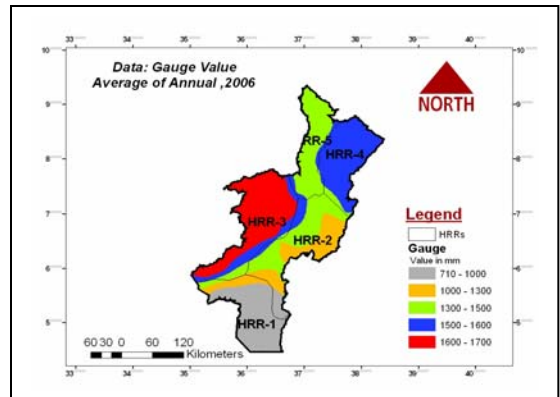
(c) RFE: Average Annual 2003



(d) Gauge: Average Annual 2003



(e) RFE: Average Annual 2006



(f) Gauge: Average Annual 2006

Figure 6.16 Rainfall Map: Average Annual 2000/2003/2006

The average mean annual rainfall computed from the estimated value is also represented the dry, normal and wet situations of the year 200, 2003 and 2006 respectively. As shown from Figure 6.16 and Table 6.4, the estimated rainfall was highest by amount and distributions in the year 2006 which is in the same manner to

gauge records. In addition, the best performance of the estimated rainfall is explained that the standard deviation of the rainfall calculated from average annual rainfall was very small for each year in the whole basin. Except 2000 which has a best performance in the estimation, deviation is highest when calculated from each HRRs of 2000 and 2003.

### **6.3 Advantage and Disadvantage of Using Satellite Data for Rainfall Estimation**

In the previous discussions what the results realized is indicate, with out any doubt, the use of satellite based rainfall estimation has been found to be a good supplement to the conventional data source for different applications. In fact, the satellite source data is useful and advantageous providing continuous, large area coverage and real time estimating of rainfall, but also this study has identified its own advantage and disadvantage as follow

#### **(a) Advantage**

- ✚ The satellite data used for rainfall estimation purpose has very good coverage of the country including the study area at 25 km<sup>2</sup>. Data is also acquired on near real-time basis and it could be acquired continuously for areas where there are no surface observations or where there is some social unrest or other similar problem.
- ✚ The Data is easily handled and processed using automated processing system. The digital data obtained from the process could be easily imported into a GIS system for digital analysis.
- ✚ Once the system is established, it is economical and requires much less input than to manage a net work of surface rainfall station covering the whole country.
- ✚ It is highly secured and protected compared to the gage network that frequently interrupted because of intervention of local problems

## (b) Disadvantage

- ✚ In most case it requires dense Ground gauge measurements to compare and evaluate the estimated rainfall.
- ✚ The accuracy of the methods can not be easily verified as well as that of conventional methods.
- ✚ It requires high capacity of processing machine and system because of the enormous volume of image and data processing activity.
- ✚ Less cost-benefit, the prices of the data do not cover both the cost of processed data and the satellite system at all.
- ✚ The Satellite system gives areal average rainfall that one can not obtain the amount of rainfall falling at a particular point.

In addition, while the procedures used in the TAMSAT and the evaluation and characterization of the estimated rainfall have been discussed in detail, yet, the TAMSAT method has also some technical limitations. These are:

- ✚ The method is applicable to convective rainfall regions. And it is poor when applied to frontal rainfall, ad with Orographic rainfall. Therefore, the very complex topography of the study area do not considered.
- ✚ The method require the background of the rainfall climatology of the area and dense net work of stations for verifying the performance of the estimated value, but this situation was one of the difficulty because of small number of station in the basin, in particular in remote southern area.
- ✚ Spatial variation of rainfall: The method estimates rainfall using the cloud top temperature without looking beneath the cloud. However, the intensity of rainfall may show spatial variation beneath the cloud and thus the technique does not consider the actual spatial variation of rainfall intensity

beneath the cloud. Thus, the technique is useful for getting average rainfall over an extended area and period of time rather than detail information over small area and short period of time.

- ✚ Contamination by Low clouds: In some places and times low clouds produce rainfall and in that case the approach that assumes rain occurs only from convective cloud, fails to work. When there is rain from low cloud, the technique says no rain.
- ✚ Some of the MetoSat –TIR images are not clearly visible and difficult to process it further. In such case there is no way to correct it.

# CHAPTER SEVEN

## 7. Conclusion and Recommendations

### 7.1 Conclusion

Satellite based methods of rainfall estimation has a great value for monitoring areal rainfall. This would definitely help for rainfall monitoring for relevant applications such as drought assessment, flood monitoring and early warning system are the major one. The use of such technologies can be particularly useful in the risk assessment, mitigation and preparedness phases of disaster management.

The main objective of this study was to produce RFE image from MetoSat- (TIR) CCD and further to make validation and characterization of extracted estimated values compared to the gauge record over the study area.

In the study, the basis of the rainfall estimation technique was TAMSAT which has a long history in Africa, and used routinely in many national meteorological offices to provide operational data. NMA of Ethiopia has been also used such method since 1991. The assumption of the methods that discussed under study most of the rain comes from convective cloud, and then they can therefore be recognized in the TIR satellite imagery by their cloud tops at a THT-40 °c. The cumulated hours with this low temperature the CCD is related with observed characteristics and rainfall on ground finally represented as an image and then using automated processing software the estimated rainfall RFE image and extracted values were obtained.

The strength of the method including its ability to give a real time estimates over the study area was investigated using comparism and climatologically characterization of the estimated value with the gauge record at temporal and spatial perspective. In order to compare the gauge (point measurement) with estimated value (areal averages) over each HRRS was necessary to bring all measurements to the same spatial scale. In this regard,

all the input data were processed and converted to the spatial extent of HRRs rather than to the whole Omo-gibe basin which is too coarse to represent the rainfall estimations.

The analysis carried in this work has been found to be applicable in getting the rainfall and its performance was better and representative when it is compared with the corresponding gauge values and climatology of the study area. Although most of the estimates are better, the disadvantages also need to have attention or other methods to correct the gap. For example, in particular the effect of topography, the source of the rainfall from frontal effect, the variation of THT from month to month was not considered in the TAMSAT methods.

The advantage of using quantitative evaluations and Kriging were also helpful in order to see some bias of over and under estimation of the rainfall during the periods and over HRRs. In general digest, the main points identified from the result of the study are highlighted as follow.

- The performance using bias indicator revealed that the estimated rainfall in the first decade of August underestimated for HRR-1 in 2000, but it was better in the remaining years and regions. In 2000, the correlation result against the gauge record was higher (0.92) compared to the selected years. During April, HRR-1 was overestimated in 2000 while HRR-4 underestimated in 2006. During kiremet both HRR-1 and HRR-4 exaggeratedly underestimated in 200 and 2006 respectively.
- The temporal variability of the estimated rainfall was highly explained in the south and east area. The spatial pattern of the rainfall climatology is totally explained in better way especially for Kiremet season. However, there was tendency of overestimation in HRR-5 and HRR-4, over the north and eastern highlands in the basin.
- The maximum rainfall values and the occurrence of peak month were also very close compared to gauge records.

- The estimated rainfall was well characterized and represents the climatology of the area in seasonal variability than the annual. Except in the south, estimated value has shown the seasonality in better performance.
- The correlation of rainfall estimated increased during small rainy and dry period and decrease in Kiremet season. In particular, the seasonal and annual climatic characteristics of the study area were defined better, except in the central and southern regions made the performance poor due to less gauge network for comparism

In the TAMSAT method, the researcher suggest that when describing the estimated value compared to climatologically ,it would be more better to characterize using periods of ‘above-average”, ”below-average”, or “normal” over defined area like for HRRs used in this study. Furthermore, as far as the satellite data and gauge data network is available. The TAMSAT methodology of estimating rainfall from MetoSat –TIR imagery is a good proxy of rainfall in the study area and in all Ethiopia too.

### ***Limitation of the work***

- Comparism of other rainfall estimation methods and thequinqes against TAMSAT approach has not been carried out.
- The gauge and CCD agreement with respect to the prevailing weather system have not been examined.
- The merging of satellite estimates and gauge records has not been mapped.

## 7.2 Recommendations for Future Studies.

Basically, reliability of rainfall forecasts or associated events are depends on the availability of rainfall information. For instance, in the case of floods, rainfall forecast is indispensable. Their accuracy is not sufficient yet. Further refinements are required. Although the accuracy of satellite-based rainfall product is not fully clarified and need to be further study, but such a source of rainfall data could be still of some help for ungauged and inaccessible areas.

The following future study are recommended so that the result obtained from this work can be used in the operational work ,or other relevant academic or development research institutions in Ethiopia.

- The estimate of the rainfall is found to be good performance to explain the climatology of the study area. Hence, this work should be extended to other drought prone area and to all over the country at large. It is also recommended that the work is very useful in providing information of the rainfall in time and space. Efficient, appropriate and effective communication system among the major stakeholders and collaborators should be also necessary with respect to agricultural planning, flood and drought early warning system.
- To analysis the comparism and characterization, average of all gauge and RFE value was used for given period and HRRs. but it would have been better to see for more periods and very small area that contain representing gauge truly. This also another task which needs to make further study and improve the reliability of the data, and thereby the output result.
- Improved use of satellite data involves collaboration with the satellite data researcher and producer to insure that practical information is extracted from the data. Establishing standards for data coding system, data format, as well as developing national strategies for satellite data collection and processing is fundamental.



- Due to time limitation, the opportunities and constraints are not analyzed in-depth. Further investigation is needed to promote the implementation of rainfall estimation approach.
- With regard to the data processing, particularly on the one derived from TIR- image, the development of other model is important for verifying the present data quality as well as to account for the changes on the image taking place over time.
- This study has demonstrated the possibility of evaluating and characterizing of estimated values through use of spatial data transfer system in and interoperable GIS environment and mapping. However, the datasets were not arranged on proper justification with respect to the application it is intended to use. Thus, it should be appropriate to use spatial data modeling compatible to verify the mapping task in good way.
- In the study, the absence of standards related to data format, selection of statistical parameters, and coding the data format system, software manipulation have been recognized as the main constraint, which has contributed to most of the problems. So it is also need to be Justify and designing of standard database from different sets are compatible to the required software.

## References

- Admasu Gebeyehu,1989.Regional flood frequency Analysis. Technical Report. Royal Institute of Technology Stockholm, Sweden.
- Arkin, P.A. and P.E. Ardanuy 1989. Estimating climatic-scale precipitation from space: a review. *J. Climate*, 2, 1229-38.
- Arkin, P. A., and B. N. Meisner, 1987: The relationship between large-scale convective rainfall and cold cloud over the Western Hemisphere during 1982-84. *Monthly weather review*.ams, 115, 51-74
- Bekel,F 1993: Probability of Drought Occurrence under Different Events ,Addis Ababa, Ethiopia: NMA
- Dugudal G, 1994. Satellite-derived Rainfall estimates over Africa: their validation and use in monitoring climate change. In global precipitation and climate change, proceeding of Global Environmental metering, Amsterdam, November 1994.
- Dutarter,P.Coudert.,J.M and Delponi.G.1993.Evolution in the use of satellite data for the location and development of Ground water. Article in advanced space research.102,300-567
- Engman E.T and Gurney.1991. *Remote sensing in hydrology*. Current operational application of remote sensing in hydrology, WMO no.884, 1999.
- EUMETSAT (2000), meteorological data user conference Proceeding. Germany. , Belgium 07th May, 2000
- EUMETSAT (1997a), satellite-derived Rainfall estimates over Africa: their validation and use in monitoring climate change. Proceeding of meteorological data user conference. Brussels, Belgium 29th September 1997.

- Fekadu Negash, 2004, Paper Presentation on integrated water resource management and planning through basin development for sustainable development .MoWR, September 2004.Addis Ababa.
- Food and agricultural organization (FAO), 2000: *Review of Seasonal rainfall over Sudan*. A report of Darfure relieve rehabilitation assistance program, 2000 No.45, 34-89.
- Gissila, T., Black, E., Grimes, D., and Slingo, J. (2004). Seasonal forecasting of the Ethiopian summer rains. *International Journal of Climatology*, 24, 1345-1358
- Griffiths C.G, 1971. The variation with height of the top brightness of precipitating convective cloud. Report of WMO technical report, N0 .237/2000, Switzerland, zananghug. April 2000.
- Grimes D.I.F.1992, Application of Satellite based Rainfall estimates to hydrology. Proceeding of WMO workshop, Niamey, April 1992.
- Grimes,D.I.F.,1999.Optimal areal rainfall estimation using raingauge and satellite data.Proceeding of EUMETSAT in meteorological data user conference.2000.
- Hallikainen.M.,1984:Satellite microwave radiometry of snow cover :Proceeding of the 18<sup>th</sup> international symposium on remote sensing of environment ,1-5 October, Paris
- Herman S.B., Hallikainen.M., and Tayor.B.N.,1997:A comparison of two satellite rainfall estimates technique over tropics. *Journal of applied Meteorology*, 20 .120-178.
- Houghton and Taylor, 1973/1975/1988.The accuracy of estimates of areal mean rainfall .In proceeding results of research representative and experimental basins Wellington, international association of hydrology science publication No.93. p 203-218.
- Hulme. M., (1992.) A 1951-80 Global land precipitation climatology for the evaluation General Circulation Models. *Climate Dynamics*, 7, 57-72.
- Kavvas,M.L and Z.chen.1989: the radar based short term prediction of the time-space evolution of rain fields. In: precipitation and forecasting. Operational hydrology report .46. WMO.V.No.887.

- Kidder S. Q., and T. H. Vonder Haar, 1995: *Satellite Meteorology: An Introduction*. Academic Press, 466 pp
- Kidder S.Q .and T.H Vonder Haar 1997. Tropical oceanic precipitation frequency from microwave data. Atmospheric Science paper No.248, Department of atmospheric science Colorado state university,
- Malczewski, Jacek (1999). GIS and Multicriteria Decision Analysis. New York: John Wiley & Sons, Inc*
- Milford J.R& Dugudal, 1986.Rainfall estimation over the Sahel using METOSAT thermal infrared Data. Proceeding of Regional WMO Conference, Rome, Italy, 2-6 December 1985.
- Milford J.R. and Dugdale G., 1989: Estimation of rainfall using geostationary satellite data. In Application of remote sensing in agriculture. Proc. 48th Easter School in Agri. Sci. Univ. Nottingham. April, 1989. Butterworth, London.
- Ministry of Water Resource (MoWR), 1996.Master plan study. *Executive summery Report*. Omo-Gibe river basin integrated development master plan study. Addis Ababa
- NMA (Long Range Forecast Group), 1990.Seasonal out look of Kiremet. NMA. Mimeo. Addis Ababa, Ethiopia. NMA
- NMA 1996: Climate and agro-climatic resource of Ethiopia. National Meteorological Service, Ethiopia. Meteorological research. report serious Vol.1,1-137
- Ortolani A. "Satellite rainfall assimilation to improve the quantitative precipitation forecasting" Proc. Of The 2001 EUMETSAT Meteorological Satellite Data Users' Conference, EUMETSAT 2001,pp.453-460
- Organization for economic co-operation and Development (OECD), 1984-1988).*Satellite Remote Sensing and the Sahel*, Western Africa Regional research groups, Annual report, May 1988.Abuja, Nigeria.
- Simpson, J., R.F. Adler and G.R. North 1988. A proposed Tropical Rainfall Measuring Mission. *Bull. Amer. Meteor. Soc.*, 69, 279-295

- Tesfay Haile 1987, 1987. A case study of Seasonal forecasts in Ethiopia. In WMO RAI(Africa) *Seminar on modern Weather forecasting(Part II)*,30 December 4,1987. Addis Ababa, Ethiopia.
- Yitaktu Tesfatsion, 1999. Rainfall calibration for Ethiopia. NMA, internal report. Addis Ababa, Ethiopia
- Tufa Dinku, 1994. The use of smaller calibration zones for better rainfall estimation over Ethiopia. Paper presented at a workshop on Evaluation of Precipitation by Satellite, 1- December 1994, Niamey, Niger
- Turk, F. J., G. D. Rohaly, and P. Arkin, 1997. Utilization of satellite-derived tropical rainfall for analysis and assimilation into a numerical weather prediction model. *Presented on 9th Conference Hurricanes and Tropical Meteorology*. AMS.
- Tuker M.R .1997.satelite Derived rain storm distributions an aid to forecasting African armyworm out breaks .Weather report. American meteorological association. April /august. No. 23-27, 1997.
- UNICA/WMO international conference on water resources management and policy in drought prone areas. *International workshop proceeding*, Addis Ababa 18-22 march.1996
- Vicente. G.A R.A Schofield and W.P Menzale, 1998.the operational GEOSs infrared-estimation technique. Bulletin of American Meteorological society, No.69, 1998.
- Workineh Degefu, 1987. Some aspects of meteorological drought in Ethiopia. pp 23- In, *Drought and Hunger in Africa: denying famine a future*, M.H. Glantz (ed.). Cambridge University Press.457 pp.
- World meteorological organization (WMO), 1988a: *Application of satellite data for estimation of precipitation*. Technical report to the commission for hydrology No.26,WMO/TD- No.300,Geneva.
- World meteorological organization (WMO), 1994.In remote sensing for hydrology Progress and prospect, operational report.No.36.WMO No.7

## ANNEXES

### 1. Annex-A : List of Meteorological Stations in Omo-Gibe Basin

| NO | RR | Sta_Name      | HRR | Lat_Y | Long_x | Lat_Yd | Long_XD | Elevation | LYM_10Y |
|----|----|---------------|-----|-------|--------|--------|---------|-----------|---------|
| 1  | 1  | Bume          | R1  | 5.29  | 35.31  | 5.48   | 35.52   | 680       | 750.0   |
| 2  | 2  | Dimeka        | R1  | 4.58  | 36.28  | 4.97   | 36.47   | 827       | 750.8   |
| 3  | 3  | Fejel         | R1  | 4.39  | 36.24  | 4.65   | 36.40   | 600       | 575.7   |
| 4  | 4  | Ginimonere    | R1  | 4.47  | 35.56  | 4.78   | 35.93   | 600       | 460.0   |
| 5  | 5  | Hamer bena    | R1  | 5.30  | 36.23  | 5.50   | 36.38   | 850       | 780.2   |
| 6  | 6  | Omorate       | R1  | 4.50  | 36.20  | 4.83   | 36.33   | 575       | 325.8   |
| 7  | 7  | Turmi         | R1  | 5.06  | 36.03  | 5.10   | 36.05   | 670       | 457.0   |
| 8  | 1  | Kaka          | R2  | 5.41  | 36.37  | 5.68   | 36.62   | 900       | 1200.8  |
| 9  | 2  | Jinka         | R2  | 5.48  | 36.33  | 5.80   | 36.55   | 1290      | 1290.0  |
| 10 | 3  | SilaMago      | R2  | 5.57  | 36.12  | 5.95   | 36.20   | 700       | 600.0   |
| 11 | 4  | Beto          | R2  | 6.10  | 36.50  | 6.17   | 36.83   | 1555      | 1500.0  |
| 12 | 5  | Dara Malo     | R2  | 6.13  | 37.16  | 6.22   | 37.27   | 1500      | 1300.0  |
| 13 | 6  | Laska basketo | R2  | 6.18  | 36.35  | 6.30   | 36.58   | 1400      | 900.0   |
| 14 | 7  | Bulki(Mindre) | R2  | 6.19  | 36.50  | 6.32   | 36.83   | 2300      | 1560.0  |
| 15 | 8  | Sawula        | R2  | 6.19  | 36.53  | 6.32   | 36.88   | 1472      | 1643.8  |
| 16 | 9  | Zenga         | R2  | 6.21  | 36.58  | 6.35   | 36.97   | 1480      | 1523.6  |
| 17 | 10 | Malanaha      | R2  | 6.23  | 37.05  | 6.38   | 37.08   | 1560      | 1400.0  |
| 18 | 11 | Morka         | R2  | 6.26  | 37.16  | 6.43   | 37.27   | 1600      | 1211.6  |
| 19 | 12 | Wib Hamer     | R2  | 6.30  | 36.35  | 6.50   | 36.58   | 1365      | 893.7   |
| 20 | 13 | Dinke         | R2  | 6.32  | 37.30  | 6.53   | 37.50   | 1470      | 1100.1  |
| 21 | 14 | Gessuba       | R2  | 6.35  | 37.38  | 6.58   | 37.63   | 1650      | 1296.4  |
| 22 | 15 | Wolaita Sodo  | R2  | 6.51  | 37.45  | 6.85   | 37.75   | 1700      | 1376.6  |
| 23 | 16 | Bele          | R2  | 6.55  | 37.35  | 6.92   | 37.58   | 1655      | 1324.8  |
| 24 | 17 | Tercha        | R2  | 6.58  | 37.20  | 6.97   | 37.33   | 1641      | 1435.5  |
| 25 | 18 | Sekoru        | R2  | 7.00  | 37.24  | 7.00   | 37.40   | 1645      | 1414.0  |
| 26 | 1  | Adiya Kaka    | R3  | 7.17  | 36.36  | 7.28   | 36.60   | 1726      | 1726.0  |
| 27 | 2  | Aman          | R3  | 7.10  | 36.47  | 7.17   | 36.78   | 1450      | 1770.2  |
| 28 | 3  | Beta Woshi    | R3  | 7.42  | 36.30  | 7.70   | 36.50   | 2100      | 1690.4  |
| 29 | 4  | Bonga         | R3  | 7.23  | 36.14  | 7.38   | 36.23   | 1747      | 1850.7  |
| 30 | 5  | Bulki         | R3  | 6.32  | 36.00  | 6.53   | 36.00   | 1230      | 1607.0  |
| 31 | 6  | Chena         | R3  | 7.32  | 35.51  | 7.53   | 35.85   | 1971      | 1732.0  |
| 32 | 7  | Chida         | R3  | 6.38  | 36.28  | 6.63   | 36.47   | 1221      | 1260.3  |
| 33 | 8  | Gibe Farm     | R3  | 7.31  | 36.31  | 7.52   | 36.52   | 1723      | 1739.4  |
| 34 | 9  | Gimbichu      | R3  | 7.31  | 36.36  | 7.52   | 36.60   | 2001      | 1801.1  |
| 35 | 10 | Goga Kemise   | R3  | 7.25  | 36.23  | 7.42   | 36.38   | 1624      | 1632.5  |
| 36 | 12 | Kerise        | R3  | 7.13  | 36.14  | 7.22   | 36.23   | 1472      | 1825.4  |
| 37 | 13 | Kulu          | R3  | 6.00  | 35.32  | 6.00   | 35.53   | 926       | 900.0   |
| 38 | 14 | Maji          | R3  | 6.11  | 35.34  | 6.18   | 35.57   | 933       | 1480.9  |
| 39 | 15 | Mardur        | R3  | 5.54  | 35.16  | 5.90   | 35.27   | 991       | 1000.3  |
| 40 | 16 | Sankura       | R3  | 6.51  | 36.22  | 6.85   | 36.37   | 1962      | 1370.2  |
| 41 | 17 | SekaChekorsa  | R3  | 7.36  | 36.25  | 7.60   | 36.42   | 2107      | 1862.7  |

| NO | RR_N0 | Sta_Name        | HRR | Lat_Y | Long_x | Lat_YD | Long_XD | Elevation | ARF_LYM |
|----|-------|-----------------|-----|-------|--------|--------|---------|-----------|---------|
| 42 | 18    | Wushwush        | R3  | 7.17  | 36.07  | 7.28   | 36.12   | 1501      | 1580.4  |
| 43 | 19    | Yanfa           | R3  | 7.18  | 36.00  | 7.30   | 36.00   | 1670      | 1577.5  |
| 44 | 1     | Areka IAR       | R4  | 7.04  | 37.45  | 7.07   | 37.75   | 1983      | 1370.0  |
| 45 | 2     | Babu            | R4  | 8.10  | 37.32  | 8.17   | 37.53   | 1628      | 1250.4  |
| 46 | 3     | Bege            | R4  | 8.18  | 37.60  | 8.30   | 38.00   | 2200      | 1300.4  |
| 47 | 4     | Bilambilo       | R4  | 8.09  | 37.32  | 8.15   | 37.53   | 1620      | 1205.6  |
| 48 | 5     | Bombe Edget     | R4  | 7.80  | 37.34  | 8.33   | 37.57   | 1723      | 1180.6  |
| 49 | 6     | Dembi           | R4  | 7.50  | 37.22  | 7.83   | 37.37   | 1650      | 1213.2  |
| 50 | 7     | Deri (K.Gebeya) | R4  | 8.07  | 37.28  | 8.12   | 37.47   | 1626      | 1290.5  |
| 51 | 8     | Dilela          | R4  | 8.37  | 38.03  | 8.62   | 38.05   | 2334      | 1425.3  |
| 52 | 9     | Fugo Ieka       | R4  | 7.56  | 37.32  | 7.93   | 37.53   | 1900      | 1325.3  |
| 53 | 10    | Gecha School    | R4  | 7.58  | 37.24  | 7.97   | 37.40   | 1670      | 1523.1  |
| 54 | 11    | Gunchire        | R4  | 8.03  | 37.57  | 8.05   | 37.95   | 2700      | 1300.0  |
| 55 | 12    | Imdiber         | R4  | 8.08  | 37.56  | 8.13   | 37.93   | 1838      | 1379.1  |
| 56 | 13    | Saja            | R4  | 7.43  | 37.28  | 7.72   | 37.47   | 1950      | 1387.4  |
| 57 | 14    | Tinishu Miti    | R4  | 7.55  | 37.24  | 7.92   | 37.40   | 1945      | 1453.2  |
| 58 | 15    | Welkite         | R4  | 8.13  | 37.45  | 8.22   | 37.75   | 1809      | 1145.4  |
| 59 | 16    | Yaya otena      | R4  | 7.45  | 37.32  | 7.75   | 37.53   | 1545      | 1110.0  |
| 60 | 1     | Aba             | R5  | 7.51  | 36.54  | 7.85   | 36.90   | 1983      | 1723.4  |
| 61 | 2     | Abelti          | R5  | 7.31  | 36.52  | 7.52   | 36.87   | 2096      | 1825.6  |
| 62 | 3     | Alge            | R5  | 8.36  | 37.06  | 8.60   | 37.10   | 1648      | 1806.7  |
| 63 | 4     | Ambuye          | R5  | 7.59  | 36.54  | 7.98   | 36.90   | 1796      | 1789.1  |
| 64 | 5     | Ano             | R5  | 9.07  | 36.56  | 9.12   | 36.93   | 1789      | 1420.8  |
| 65 | 6     | Assendabo       | R5  | 7.45  | 37.13  | 7.75   | 37.22   | 2046      | 1344.6  |
| 66 | 7     | Baco            | R5  | 9.07  | 37.05  | 9.12   | 37.08   | 1908      | 1353.5  |
| 67 | 8     | BARO(y-hurum)   | R5  | 7.58  | 36.54  | 7.97   | 36.90   | 1795      | 1723.8  |
| 68 | 9     | Bechi           | R5  | 8.06  | 36.55  | 8.10   | 36.92   | 2000      | 1926.3  |
| 69 | 10    | Bido            | R5  | 7.57  | 37.04  | 7.95   | 37.07   | 1956      | 1622.2  |
| 70 | 11    | Bilboshe        | R5  | 8.54  | 36.59  | 8.90   | 36.98   | 1630      | 1500.0  |
| 71 | 12    | Boneya          | R5  | 7.32  | 37.03  | 7.53   | 37.05   | 1946      | 1560.3  |
| 72 | 13    | Botar Bacho     | R5  | 8.22  | 37.16  | 8.37   | 37.27   | 1780      | 1623.3  |
| 73 | 14    | Busa            | R5  | 7.24  | 36.52  | 7.40   | 36.87   | 1970      | 1825.0  |
| 74 | 15    | Debena          | R5  | 7.40  | 36.50  | 7.67   | 36.83   | 1923      | 1670.9  |
| 75 | 16    | Dedo            | R5  | 7.30  | 36.52  | 7.50   | 36.87   | 2100      | 1776.4  |
| 76 | 17    | Dedo Gordomo    | R5  | 7.27  | 37.10  | 7.45   | 37.17   | 2000      | 1570.0  |
| 77 | 18    | Dimtu           | R5  | 8.06  | 36.55  | 8.10   | 36.92   | 2046      | 2000.0  |
| 78 | 19    | Ejaji           | R5  | 9.00  | 37.19  | 9.00   | 37.32   | 1900      | 1826.7  |
| 79 | 20    | Ermichi         | R5  | 7.26  | 36.53  | 7.43   | 36.88   | 2270      | 1995.2  |
| 80 | 21    | Fede            | R5  | 8.20  | 37.17  | 8.33   | 37.28   | 1786      | 1623.9  |
| 81 | 22    | Gedo            | R5  | 9.03  | 37.26  | 9.05   | 37.43   | 2210      | 1547.9  |
| 82 | 23    | Gibe            | R5  | 7.45  | 37.11  | 7.75   | 37.18   | 1978      | 1460.1  |
| 83 | 24    | Guben           | R5  | 9.12  | 37.12  | 9.20   | 37.20   | 1908      | 1320.0  |
| 84 | 25    | Ifabia          | R5  | 9.16  | 37.07  | 9.27   | 37.12   | 1999      | 1333.4  |
| 85 | 26    | Jimma           | R5  | 7.40  | 36.50  | 7.67   | 36.83   | 1911      | 1680.0  |
| 86 | 27    | Limu Seka       | R5  | 8.26  | 37.00  | 8.43   | 37.00   | 1770      | 1825.7  |
| 87 | 28    | Seyo            | R5  | 8.30  | 37.22  | 8.50   | 37.37   | 1970      | 1654.3  |
| 88 | 29    | Shedatura       | R5  | 8.04  | 37.06  | 8.07   | 37.10   | 1754      | 1655.5  |
| 89 | 30    | Shishinda       | R5  | 8.06  | 36.57  | 8.10   | 36.95   | 1700      | 1954.3  |
| 90 | 31    | Tibe            | R5  | 9.02  | 37.13  | 9.03   | 37.22   | 2002      | 1977.3  |

ARF\_LYM:Actual(Gauge )Rainfaal LonYear Mean(1997-2004)

## 2. Annex-B: Climatological Mean Annual Rainfall (1974-2004)

| No. | Stations     | Lat. | Long. | Alt.   | JAN  | FEB  | MAR   | APR   | MAY   | JUN   | JUL   | AUG   | SEP   | OCT   | NOV   | DEC  | BELEG  | KIREMT | BEGA  | ANNUAL |
|-----|--------------|------|-------|--------|------|------|-------|-------|-------|-------|-------|-------|-------|-------|-------|------|--------|--------|-------|--------|
| 1   | Abossa       | 8.0  | 38.7  | 1650.0 | 8.4  | 50.1 | 53.2  | 64.3  | 81.4  | 82.4  | 165.7 | 143.7 | 83.5  | 30.8  | 2.0   | 6.3  | 248.9  | 475.3  | 47.5  | 771.8  |
| 2   | Ardita Sito  | 7.1  | 39.0  | 2490.0 | 10.8 | 30.8 | 40.8  | 110.8 | 210.8 | 78.8  | 157.8 | 212.8 | 133.8 | 77.8  | 20.8  | 50.8 | 393.2  | 583.2  | 160.2 | 1136.6 |
| 3   | Areka        | 7.0  | 37.4  | 1750.0 | 40.8 | 54.3 | 87.7  | 138.6 | 179.2 | 147.4 | 199.7 | 218.4 | 167.1 | 97.6  | 27.1  | 16.8 | 459.8  | 732.6  | 182.3 | 1374.6 |
| 4   | Bacco(Shewa) | 9.1  | 37.1  | 1650.0 | 31.7 | 54.7 | 111.7 | 119.5 | 65.4  | 387.4 | 255.9 | 253.7 | 177.2 | 44.5  | 12.2  | 7.3  | 351.3  | 1074.2 | 95.7  | 1521.2 |
| 5   | Backo(Gamo)  | 5.8  | 36.6  | 2300.0 | 23.0 | 71.6 | 120.7 | 168.8 | 82.0  | 133.9 | 196.0 | 156.5 | 123.4 | 117.3 | 110.2 | 45.2 | 443.1  | 609.8  | 295.8 | 1348.7 |
| 6   | Belle        | 7.1  | 37.4  | 1200.0 | 32.2 | 39.0 | 86.1  | 119.4 | 140.3 | 165.3 | 201.6 | 196.4 | 156.7 | 90.0  | 40.0  | 19.8 | 384.9  | 719.9  | 182.0 | 1286.7 |
| 7   | Bonga        | 7.1  | 36.1  | 1650.0 | 42.0 | 78.7 | 123.9 | 184.1 | 222.6 | 203.7 | 216.3 | 217.6 | 197.3 | 141.7 | 74.0  | 55.4 | 609.4  | 834.8  | 313.1 | 1757.4 |
| 8   | Bulki        | 6.3  | 36.8  | 2600.0 | 54.7 | 56.9 | 99.5  | 104.1 | 302.3 | 308.7 | 402.0 | 174.3 | 208.7 | 99.9  | 8.7   | 27.7 | 562.8  | 1093.7 | 191.0 | 1847.5 |
| 10  | Chora        | 8.4  | 36.1  | 1930.0 | 21.2 | 39.1 | 84.8  | 101.3 | 183.9 | 239.5 | 242.0 | 262.4 | 241.7 | 142.4 | 33.9  | 41.7 | 409.2  | 985.5  | 239.2 | 1633.9 |
| 11  | Dimka        | 4.6  | 36.5  | 680.0  | 27.1 | 76.6 | 122.5 | 191.3 | 299.9 | 255.5 | 133.2 | 267.2 | 313.0 | 75.1  | 14.0  | 12.0 | 690.3  | 968.9  | 128.2 | 1787.4 |
| 12  | Durame       | 7.2  | 37.9  | 2085.0 | 28.5 | 58.8 | 93.5  | 116.4 | 154.5 | 100.0 | 127.4 | 162.1 | 128.8 | 79.4  | 26.1  | 13.4 | 423.1  | 518.2  | 147.5 | 1088.8 |
| 13  | Ejaji        | 9.0  | 37.3  | 1650.0 | 13.6 | 25.6 | 73.8  | 82.9  | 125.0 | 180.6 | 243.0 | 225.2 | 154.2 | 62.4  | 24.8  | 12.3 | 307.4  | 803.0  | 113.0 | 1223.4 |
| 14  | Erbora       | 5.2  | 36.4  | 1400.0 | 22.9 | 31.1 | 106.4 | 134.1 | 175.7 | 197.5 | 120.5 | 197.5 | 156.4 | 76.9  | 25.1  | 21.9 | 447.3  | 671.9  | 146.8 | 1266.0 |
| 15  | Gedo         | 9.0  | 37.5  | 2515.0 | 43.2 | 43.1 | 74.4  | 182.8 | 122.5 | 201.4 | 331.4 | 201.4 | 167.4 | 44.0  | 24.5  | 11.4 | 422.8  | 901.6  | 79.9  | 1404.3 |
| 16  | Gesuba       | 6.4  | 37.4  | 1650.0 | 27.9 | 52.4 | 87.1  | 146.7 | 153.7 | 102.4 | 152.2 | 145.8 | 130.4 | 65.1  | 40.5  | 40.2 | 439.8  | 530.7  | 173.7 | 1144.2 |
| 17  | Hosana       | 7.3  | 37.5  | 2200.0 | 30.9 | 56.5 | 95.0  | 123.3 | 147.4 | 128.9 | 159.7 | 186.7 | 163.0 | 63.3  | 14.0  | 27.0 | 422.3  | 638.2  | 135.1 | 1195.6 |
| 18  | Endibre      | 8.6  | 37.6  | 2000.0 | 19.8 | 39.6 | 85.2  | 72.1  | 107.3 | 155.8 | 244.9 | 251.9 | 146.9 | 45.2  | 11.3  | 10.0 | 304.2  | 799.5  | 86.2  | 1190.0 |
| 19  | Jimma        | 7.4  | 36.5  | 1667.0 | 40.4 | 53.3 | 94.0  | 140.0 | 164.9 | 214.3 | 211.9 | 213.2 | 185.2 | 87.7  | 56.3  | 34.3 | 452.3  | 824.6  | 218.8 | 1495.6 |
| 20  | Jinka        | 5.8  | 36.6  | 1430.0 | 55.5 | 77.3 | 55.3  | 47.4  | 288.7 | 257.5 | 123.0 | 256.0 | 127.0 | 53.5  | 11.5  | 7.5  | 468.7  | 763.5  | 128.0 | 1360.2 |
| 21  | Kersa        | 7.5  | 39.0  | 2700.0 | 73.2 | 65.1 | 67.4  | 52.9  | 111.5 | 303.6 | 222.6 | 103.4 | 73.6  | 129.6 | 17.6  | 6.3  | 296.9  | 703.2  | 226.7 | 1226.8 |
| 22  | Kolme        | 5.2  | 37.1  | 1200.0 | 25.8 | 51.3 | 101.2 | 154.9 | 126.2 | 244.8 | 22.0  | 26.4  | 53.2  | 112.4 | 76.7  | 30.0 | 433.6  | 346.3  | 244.9 | 1024.8 |
| 23  | Kumbi        | 8.1  | 37.3  | 1980.0 | 22.7 | 63.1 | 54.1  | 88.8  | 212.3 | 177.1 | 167.1 | 139.0 | 105.0 | 33.2  | 21.1  | 1.1  | 418.3  | 588.2  | 78.1  | 1084.6 |
| 24  | Morka        | 6.4  | 37.3  | 1100.0 | 17.4 | 23.7 | 16.7  | 22.5  | 245.7 | 134.2 | 254.2 | 67.3  | 97.1  | 55.1  | 73.1  | 4.2  | 308.6  | 552.8  | 149.8 | 1011.2 |
| 25  | Saja         | 7.6  | 37.2  | 2100.0 | 23.8 | 46.4 | 119.0 | 109.9 | 123.8 | 224.9 | 259.8 | 222.7 | 155.1 | 74.4  | 47.3  | 31.3 | 399.0  | 862.4  | 176.9 | 1438.4 |
| 26  | Sawla        | 6.2  | 36.5  | 1472.0 | 38.5 | 55.2 | 97.4  | 204.2 | 178.1 | 124.2 | 117.7 | 125.6 | 157.7 | 113.8 | 85.5  | 40.1 | 535.0  | 525.2  | 278.0 | 1338.1 |
| 27  | Sekoru       | 7.6  | 37.2  | 2100.0 | 30.2 | 44.7 | 93.8  | 98.4  | 173.4 | 230.2 | 230.1 | 238.8 | 174.9 | 62.2  | 14.2  | 23.7 | 410.4  | 873.9  | 130.3 | 1414.6 |
| 28  | Shishinda    | 8.1  | 36.6  | 1700.0 | 77.4 | 33.3 | 53.3  | 154.7 | 217.5 | 302.8 | 225.8 | 199.8 | 79.8  | 98.8  | 12.8  | 2.8  | 458.8  | 808.2  | 191.8 | 1458.8 |
| 29  | Soddo        | 6.5  | 37.5  | 1800.0 | 38.1 | 46.1 | 88.2  | 141.5 | 177.2 | 113.3 | 167.8 | 153.8 | 96.3  | 64.0  | 26.3  | 27.5 | 453.0  | 531.2  | 155.9 | 1140.1 |
| 30  | Tibe         | 9.0  | 37.2  | 1680.0 | 27.7 | 13.7 | 45.7  | 155.6 | 197.7 | 213.9 | 117.9 | 97.9  | 43.9  | 32.1  | 3.9   | 2.7  | 412.7  | 473.6  | 66.4  | 952.7  |
| 31  | Turmi        | 5.4  | 36.5  | 670.0  | 1.1  | 0.0  | 79.1  | 192.8 | 0.0   | 11.9  | 28.0  | 6.8   | 59.2  | 121.0 | 31.3  | 0.0  | 271.9  | 105.9  | 153.4 | 531.2  |
| 32  | Wajifo Farm  | 6.5  | 37.8  | 1240.0 | 21.6 | 10.3 | 63.1  | 158.0 | 159.8 | 225.6 | 236.7 | 206.2 | 62.4  | 164.4 | 48.3  | 16.7 | 391.2  | 730.9  | 251.0 | 1373.1 |
| 33  | Weito        | 5.4  | 37.0  | 650.0  | 6.3  | 13.8 | 50.7  | 116.7 | 106.6 | 32.3  | 22.8  | 28.5  | 24.4  | 60.1  | 40.8  | 15.5 | 287.8  | 108.0  | 122.6 | 518.4  |
| 34  | Welkite      | 8.3  | 37.8  | 1860.0 | 21.6 | 40.8 | 79.9  | 97.9  | 119.0 | 182.2 | 279.6 | 254.2 | 147.3 | 51.6  | 15.5  | 11.9 | 337.5  | 863.4  | 100.5 | 1301.4 |
| 35  | Woliso       | 8.3  | 37.6  | 2000.0 | 18.7 | 51.1 | 67.4  | 82.4  | 95.7  | 144.4 | 258.3 | 279.9 | 153.2 | 25.1  | 4.2   | 12.0 | 296.6  | 835.8  | 60.0  | 1192.3 |
| 36  | Wush Sush    | 7.2  | 36.1  | 1501.0 | 73.1 | 94.9 | 289.7 | 387.5 | 271.4 | 388.0 | 314.7 | 473.9 | 149.0 | 76.4  | 32.0  | 41.0 | 1043.5 | 1325.6 | 222.5 | 2591.6 |
|     | AVG          |      |       |        | 30.8 | 46.9 | 87.5  | 130.5 | 163.5 | 188.4 | 194.5 | 187.6 | 137.0 | 79.1  | 32.2  | 20.8 | 428.4  | 707.5  | 162.1 | 1298.1 |
|     | STD          |      |       |        | 18.3 | 20.7 | 43.3  | 62.6  | 68.2  | 87.5  | 83.4  | 86.7  | 58.4  | 34.9  | 25.6  | 15.3 | 142.5  | 252.3  | 68.2  | 370.8  |
|     | CV           |      |       |        | 0.6  | 0.4  | 0.5   | 0.5   | 0.4   | 0.5   | 0.4   | 0.5   | 0.4   | 0.4   | 0.8   | 0.7  | 0.3    | 0.4    | 0.4   | 0.3    |



### 3. Annex –C: Average Decadal Estimated Rainfall Value and Gauge Records in Years

| Data               | Decades     |           |           |           |           |           |           |           |           |           |           |           |           |           |           |           |           |           |           |
|--------------------|-------------|-----------|-----------|-----------|-----------|-----------|-----------|-----------|-----------|-----------|-----------|-----------|-----------|-----------|-----------|-----------|-----------|-----------|-----------|
|                    | Year        | 1         | 2         | 3         | 4         | 5         | 6         | 7         | 8         | 9         | 10        | 11        | 12        | 13        | 14        | 15        | 16        | 17        | 18        |
| Estimated Rainfall | <b>2000</b> | 0.0       | 1.8       | 2.6       | 0.0       | 0.2       | 0.0       | 2.6       | 8.8       | 16.8      | 8.2       | 77.0      | 55.8      | 69.4      | 29.0      | 34.4      | 31.8      | 9.8       | 22.2      |
|                    | <b>2003</b> | 5.2       | 13.4      | 5.4       | 0.6       | 1.8       | 29.8      | 2.4       | 40.4      | 44.4      | 7.2       | 61.6      | 65.2      | 48.8      | 21.8      | 24.8      | 44.0      | 54.2      | 21.6      |
|                    | <b>2006</b> | 17.4      | 26.6      | 16.4      | 5.4       | 29.2      | 19.0      | 15.6      | 43.0      | 56.8      | 48.2      | 32.6      | 49.2      | 65.8      | 43.6      | 63.0      | 42.8      | 29.0      | 36.4      |
| Gauge Records      | <b>2000</b> | 2.0       | 2.1       | 1.9       | 5.4       | 0.9       | 2.6       | 16.8      | 8.2       | 21.0      | 36.6      | 48.8      | 57.2      | 87.1      | 44.6      | 48.2      | 67.8      | 36.3      | 46.3      |
|                    | <b>2003</b> | 10.3      | 14.5      | 13.1      | 8.0       | 4.1       | 26.2      | 23.6      | 40.1      | 35.3      | 35.5      | 61.6      | 54.4      | 50.0      | 34.4      | 16.4      | 74.4      | 71.8      | 57.6      |
|                    | <b>2006</b> | 4.4       | 11.3      | 3.6       | 10.3      | 22.5      | 12.5      | 31.5      | 54.4      | 44.9      | 48.3      | 29.4      | 42.0      | 72.3      | 36.3      | 60.7      | 67.9      | 59.7      | 43.6      |
|                    |             | <b>19</b> | <b>20</b> | <b>21</b> | <b>22</b> | <b>23</b> | <b>24</b> | <b>25</b> | <b>26</b> | <b>27</b> | <b>28</b> | <b>29</b> | <b>30</b> | <b>31</b> | <b>32</b> | <b>33</b> | <b>34</b> | <b>35</b> | <b>36</b> |
|                    | <b>2000</b> | 38.0      | 52.0      | 49.8      | 21.0      | 62.2      | 6.8       | 9.4       | 47.4      | 21.4      | 29.6      | 34.8      | 25.8      | 3.8       | 7.2       | 9.2       | 0.2       | 5.6       | 0.0       |
|                    | <b>2003</b> | 22.6      | 24.0      | 25.4      | 17.2      | 38.6      | 26.6      | 21.4      | 15.2      | 17.4      | 4.4       | 26.4      | 18.0      | 25.2      | 25.8      | 35.2      | 43.8      | 5.4       | 0.0       |
|                    | <b>2006</b> | 72.6      | 42.2      | 43.2      | 52.4      | 54.0      | 44.2      | 33.8      | 24.2      | 33.8      | 33.8      | 22.4      | 51.8      | 17.0      | 48.6      | 64.8      | 47.2      | 27.4      | 84.6      |
|                    | <b>2000</b> | 61.3      | 50.6      | 48.6      | 65.4      | 56.2      | 49.2      | 53.0      | 38.8      | 53.2      | 64.7      | 57.9      | 42.3      | 33.8      | 19.6      | 6.4       | 9.9       | 11.3      | 3.9       |
|                    | <b>2003</b> | 69.7      | 63.9      | 63.3      | 72.8      | 61.4      | 73.5      | 66.3      | 45.7      | 50.5      | 30.7      | 32.9      | 4.8       | 21.2      | 13.1      | 20.6      | 34.8      | 5.8       | 3.2       |
|                    | <b>2006</b> | 84.8      | 47.7      | 66.8      | 89.9      | 55.6      | 68.4      | 62.4      | 42.1      | 37.3      | 83.4      | 40.4      | 55.7      | 36.8      | 58.0      | 29.4      | 34.3      | 15.5      | 19.6      |

❖ Photograph Taken During Field Visit



**Tonjo and Upper Gibe River; Tributary of Omo-Gibe River System.**  
Type B-rainfall regime (getting rainfall through out the year): HRR-5 and HRR-4



Rainfall Measuring Instrument at Station Bonga (EARO)



*Oho...Wawoo. Thanks for God. It's finished as its raining*